VOLUME 14 NO. 3/4

Special Issue

NEW ROLES OF GEOPHYSICAL METHODS IN EXPLORATION FOR WATER RESOURCES

Proceedings of the first Course of the International School of Applied Geophysics "Ettore Majorana" International Centre for Scientific Culture, Erice, Sicily, Italy, 15—26 April 1975

Edited by

D.S. PARASNIS and R. CASSINIS

Department of Applied Geophysics, University of Lulea, Lulea, Sweden
International School of Applied Geophysics, Milan, Italy

CONTENTS

Geoexploration, 14 (1976) 14 (1976) 155—156

Foreword

The International School of Applied Geophysics is a new one among the many others held under the sponsorship of the "Majorana Center", a well established and internationally known organization for post-graduate, high level summer schools and seminars in different fields of Science.

The topic for the first Course was selected after consultation with many distinguished Geophysicists.

The application of geophysical methods to the exploration, management and protection of groundwater is a very important subject especially considering the increasing economic value of water all around the world.

The multidisciplinary character of this approach is very clear, perhaps more than in the application of geophysical methods to the search for oil. A close cooperation is needed between geologists, hydrologists, geophysicists and hydraulic engineers.

While the main topic of the Course has been the study of the refinements of geophysical methods, an introduction was also made to the hydraulic parameters of the acquifers. On the other hand, at the end of the Course a session was dedicated to the problems of the management of the acquifers and a general discussion took place on the contribution of geophysical measurements to the determination of the hydraulic parameters to be inserted in the mathematical models, that are becoming a necessary tool for a correct management and protection of water resources.

As far as the bulk of the Course, geophysical exploration, is concerned a primary role has been played by the electrical methods. The importance of these techniques in groundwater surveys is comparable to the one of seismic reflection method in exploration for oil.

The measured physical parameter, the resistivity of the geological formations, is particularly related to the porosity and to the type of the fluid filling the pores.

The updated methods of field surveying and of interpretation of the measured data were discussed. The interpretation techniques require a good background in mathematics and in physics in order to correctly understand the possibility and the limitations of geophysical methods.

Another very interesting topic was the integration of different geophysical methods which, in underground water surveys, has a greater value than in oil exploration.

The seismic method (especially the refraction technique) is a very useful complement to electrical resistivity measurements in several geological cases.

Other methods used to give additional information are gravimetry, induced polarization (a relaxation method), electromagnetic techniques and the magnetotelluric method.

Especially the latter three methods are still in the experimental stage; their future developments were discussed as well as the results of theoretical studies

and field tests.

The need for testing the geophysical results by boreholes was particularly stressed and vertical measurements in the water wells were also discussed (logging techniques).

One lecture was dedicated to the geophysical exploration for hot groundwater and, generally, to the role of geophysical methods in geothermal surveys, while a report was presented on the nuclear techniques of tracers, especially in Karst areas.

Finally, a round table discussion was held on the use of remote sensing techniques for water resources. The role of remote sensing is in the operational stage to study the distribution of surface temperature of open water bodies (fresh water upwellings in Karst coastal areas) and to determine the sedimentation pattern at the mouths of rivers. Other problems, such as the forecast of the runoff, will be solved in the near future, especially by using artificial satellites as observation platforms.

On ground, remote sensing can be employed as an exploration tool to observe some surface indicators (moisture, vegetation, geology) indirectly related to the presence of underground water.

To the invited lectures several short presentations were added, some of which being by the students. The afternoon discussion sessions were an extremely useful complement to the lectures.

Owing to the limited space available and realizing also that a long delay in publishing could be of nuisance to an updated information, the Editors have decided to publish all the lectures in a summarized form, but following a logical sequence. An exception to this general rule is made for the seven papers published here in full since these have been considered as presenting new topics, original subjects or comprehensive reviews.

We hope that this work will be a good guide to a modern treatment of the subject.

R. Cassinis

Director of the International
School of Applied Geophysics

D.S. Parasnis

Editor of
Geoexploration

Geoexploration, 14 (1976) 157—178

THE AQUIFERS AND THEIR HYDRAULIC CHARACTERISTICS

MARCELLO BENEDINI
Water Research Institute of C.N.R., Rome (Italy)

ABSTRACT

Benedini, M., 1976. The aquifers and their hydraulic characteristics. Geoexploration, 14: 157—178.

The main aspects of aquifers are examined from the view point of hydraulic engineering, aiming to point out which are the parameters related to the exploitation and protection of underground water resources.

Mention is made of the permeability, upon which are based the calculations for water withdrawal, and to the storage coefficient necessary to evaluate the unsteady conditions. Non-linearities occurring in some typical soils are recalled as well as some characteristics of fractured aquifers.

The problem of protecting water from contamination refers to some peculiar parameters of the molecular dispersion mechanism, to be considered together with the hydraulic components. Some characteristics of the unsaturated aquifers are also included. In the conviction that the underground water resources are the basic and unique possibility for some regions, the future outlines of research in this field are emphasized.

INTRODUCTION

The rational exploitation of underground water resources became possible only in the middle of last century (Darcy, 1856) due primarily to some important scientific outcomes. In fact, after his experimental investigations, Darcy, a French engineer, was able to point out the proportionality between pressure difference and seepage velocity in a porous medium. Up to now further investigations, both in the field and in the laboratory with appropriate mathematical elaborations, have made it possible to suggest reliable criteria for the management of underground water resources (Muller-Feuga and Ruby, 1900; Todd, 1959; Irmay, 1964; Davis and De Wiest, 1967; Childs, 1969; De Wiest, 1969).

Similar to the other problems of fluid dynamics, the motion of underground water is characterized, first of all, by two terms, namely the *seepage velocity* $V\,[LT^{-1}]$ and the *gradient of pressure* $J\,[0]$, the specifications of which are shown in Fig.1.

Following the suggestions made by Darcy, the general fundamental equation of the dynamics of underground water can be written:

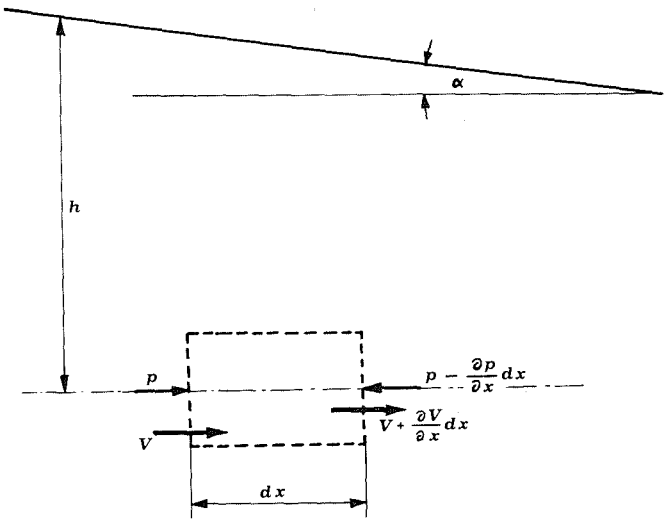

Fig. 1. Conditions for water motion: the dynamical equilibrium for the elementary fluid particle. The pressure is supposed hydrostatic ($p = \gamma h$, γ being the specific gravity of water). The hydraulic gradient J is referred to the slope of the piezometric line ($J = \text{tg}\alpha$).

$$\vec{V} = -K \overrightarrow{\text{grad}}\, h = K\vec{J} \tag{1}$$

or, in scalar form (in the x-direction):

$$V_x = -K \frac{\partial h}{\partial x}$$

in which the vectors $\vec{V}$ and $\overrightarrow{\text{grad}h} = \vec{J}$ may have a random orientation in space and therefore need not necessarily be parallel. The coefficient $K[\text{lt}^{-1}]$ therefore becomes a tensor and eq. 1 corresponds to the following scalar relations:

$$V_x = K_{xx}J_x + K_{xy}J_x + K_{xz}J_x$$

$$V_y = K_{yx}J_y + K_{yy}J_y + K_{yz}J_y$$

$$V_z = K_{zx}J_z + K_{zy}J_z + K_{zz}J_z$$

$K_{xx}, K_{xy}, \ldots K_{zz}$ being the nine tensor components referred to a cartesian space x, y, z.

The tensor K, known as *permeability* or *hydraulic conductivity*, is characterized by the aquifer's peculiarities. Moreover it varies from point to point within the aquifer and can be expressed as a function of the adopted coordinates:

$$K = K(x,y,z) \tag{2}$$

Several remarks can be made about the coefficient K, starting with its definition.

It is usual to distinguish between "standard permeability", K_s, and "field permeability", K_f, if the water flow is considered at the conventional temperature of 15.6°C (60°F) or at the effective in-field temperature.

To point out the difference between these two definitions, it is useful to recall the analogy existing between the Darcy equation and the equation of laminar flow in a pipe. In the latter case, assuming the x-axis to be parallel to the main direction of flow, the following relationship holds:

$$\vec{V} = -\frac{Cd^2 g}{\nu} \overrightarrow{\text{grad}h}$$

where C = shape coefficient of the pipe
g = acceleration due to gravity
d = pipe's diameter
ν = kinematic viscosity

From the above it is easy to find eq. 1, by putting

$$K = Cd^2 g/\nu \tag{3}$$

Eq. 3 shows the inverse proportionality of K_x with respect to the kinematic viscosity ν which is the only temperature-dependent term. Therefore it is easy to find:

$$\frac{K_s}{K_f} = \frac{\nu_f}{\nu_s}$$

where ν_s and ν_f are the kinematic viscosity of seeping liquid at 15.6°C and at the field temperature, respectively.

Eq. 3 allows another definition of the coefficient K.

If d is the average diameter of the empty cavities (apart from the numerical value of the shape coefficient C) in which the water flows, the relationship shows how the permeability depends both on the rock's geometry and on the liquid's characteristics. By putting:

$$\bar{k} = Cd^2 \tag{4}$$

it may be obtained

$$K = \frac{\bar{k}g}{\nu} \tag{5}$$

and the effects due to the liquid and solid matrix can be found.

The term $\bar{k}$ is generally called the *intrinsic permeability* [l^2]. Eq. 5 allows conversion from the "intrinsic permeability to the hydraulic conductivity. The foregoing formulations can also be used to define the units of measurement for the introduced terms (Paolillo, 1900). According to eq. 1 the per-

meability has the same dimensions as the velocity and in metric units is expressed in m sec^{-1} or better, since it involves generally very small quantities, in cm sec^{-1}. In British Units* it is expressed in gall day^{-1} ft^{-2}, being: 1 gall = $3.785 \cdot 10^{-3}$ m^3, 1 ft^2 = $9.29 \cdot 10^{-2}$ m^2, 1 day = 86,400 sec, the transformation is

1 gall day^{-1} $ft^{-2} \equiv 4.72$ cm sec^{-1}.

To measure the intrinsic permeability, especially in oil-fields, a unit called *darcy* is generally used which, starting from eq. 1 and using c.g.s. units, is equivalent to (Davis and De Wiest, 1967):

1 darcy = $0.987 \cdot 10^{-8}$ cm^2 = $1.062 \cdot 10^{-11}$ ft^2

From eq. 5, taking an average $\nu \cong 10^{-2}$ cm^2 sec^{-1} and $g = 981$ cm sec^{-1} (for water at 20°C) gives the result:

1 darcy $\cong 1 \cdot 10^{-3}$ cm sec^{-1}

As an order of magnitude, permeability is deemed "middle" from 10^{-3} to 10^{-1} cm sec^{-1}, "high" 10^{-1}—10 cm sec^{-1}, "very high" above 10 cm sec^{-1}, "low" from 10^{-3} to 10^{-7} cm sec^{-1}, while values below 10^{-7} cm sec^{-1} generally correspond to cases of impermeability.

THE TENSOR K

Recalling eq. 1, it is worthwhile to examine how the tensor K behaves in practical cases. If all the tensor's components differ from zero, the aquifer is called *anisotropic* and the permeability varies following the considered direction. Therefore, at every point of the aquifer there is one or more directions in which the permeability is greater than in any other (Fig. 2).

Strictly speaking this always happens, and after enlarging the picture at point P the permeability in the x-direction going through the cavity among the solid grains is greater than in the y-direction (Fig. 3).

However, these ideas must be modified when considering several grains lumped altogether where, neglecting local aspects having a smaller order of magnitude, the effect can be "statistically" considered even in every i- and j-direction (Irmay, 1955; Benedini et al., 1972).

Similar considerations hold for the dependence of K upon the local conditions. Since the size of solid particles in the aquifer is never constant — the small grains constantly fitting in the spaces left by the larger ones — the size of the empty cavities is tremendously varied and so the seeping velocity changes from point to point.

Thus in a microscopic picture, the aquifer is always *inhomogeneous* and the permeability also is a restricted function of the x-, y-, z-coordinates.

In contrast, if a larger portion of the aquifer is examined, "statistically" constant permeability values can be considered for large zones, and the aquifer can be seen as *homogeneous*.

---

*The system of British Units for measuring the permeability is called the Meinzer System.

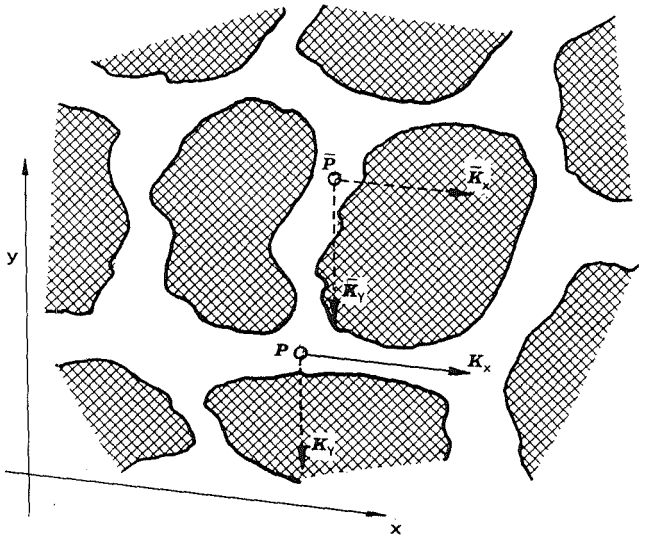

Fig. 2. Local aspect of permeability: in P and $\bar{P}$ different values can be expected (inhomogeneity). In P the permeability in the x-direction is greater than that in the y-direction.

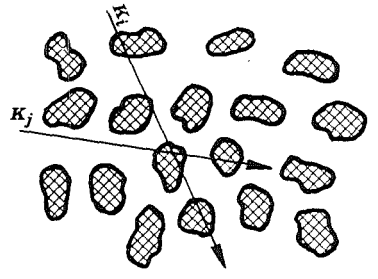

Fig. 3. Global-aspect of permeability: in an enlarged scale the permeability can be considered "statistically" independent of the direction.

From the above, the basic concepts of homogeneity and isotropy appear strictly related to the choice of an appropriate volume and a corresponding scale of representation: the larger the way in which the phenomena are examined, the more the detailed peculiarities disappear and the more the configuration becomes homogeneous and isotropic. Such a criterion leads to the adoption of the so-called *scale of homogeneity* which has been fruitfully applied in several practical situations (Louis, 1968).

Some attempts have also been made in the case of water-flows within a discrete set of fissures where large portions of the rocky matrix remain practically impervious. This approach appears the only possible one to treat the problems of water-flow in *fractured aquifers* (Figs. 4 and 5).

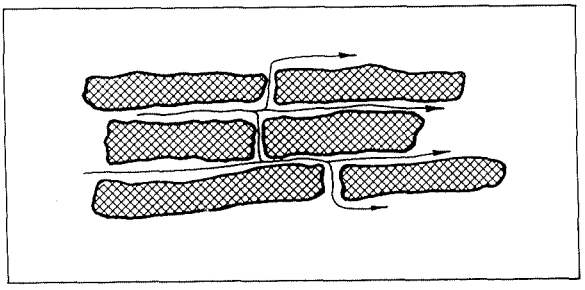

Fig. 4. Real behavior of a fractured aquifer.

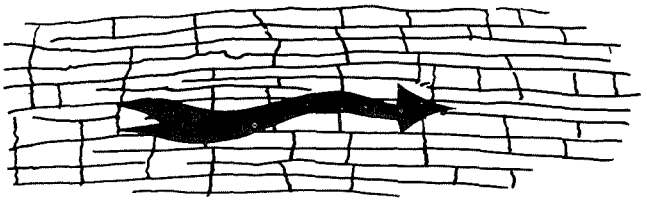

Fig. 5. The concept of "scale of homogeneity" applied to a fractured aquifer allows the problem of water seepage to be treated in the same way as in the case of porous aquifers.

The adoption of the scale of homogeneity has made it possible to extend to these aquifers the concept of permeability and, consequently, to apply all the mathematical relationships which have been so successful in sand or gravel aquifers (say in the *porous aquifers*), although a substantially different behaviour occurs.

In fact, even in the most irregular configuration in porous aquifers the size of sand or gravel grains does not prevent continuity among the empty cavities, so water can move from one point to another without any remarkable interruption of its flow. Therefore, the plot of an interpretation of the behaviour of scattered points, like the piezometric line over a predetermined path or the piezometric surface over an extended zone, can have a physical meaning because the continuity of the water particles causes a continuous variation of the represented property (apart, of course, from some error of interpolation).

Dealing with the water motion in fissures separated by large impervious blocks does not allow a similarly reliable interpretation, since the properties of two points are not necessarily related to the same field of motion, but, conversely, they can belong to different streams, separate from one another or connected through an indefinable and tortuous way. After "expanding" the scale of representation (i.e., assuming an appropriate scale of homogeneity), the interpretation of the aquifer's properties can be given in a general way neglecting both their small details and their real cause/effect ratios, which may have no physical meaning in the representation (Fig. 6).

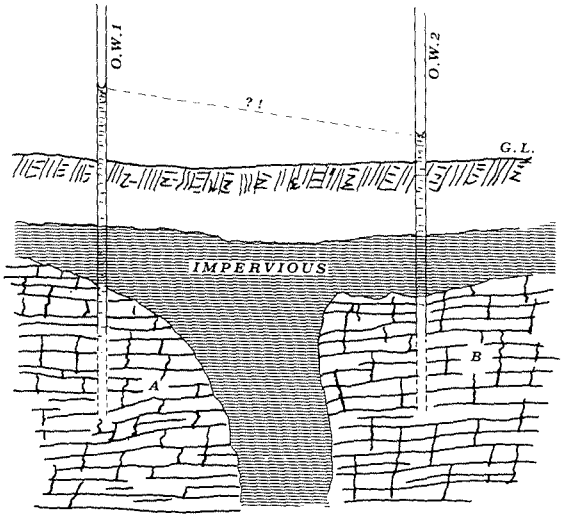

Fig. 6. Interpolation of measured information can be wrong in some frequent patterns of fractured aquifers, where the soil irregularity and the presence of impervious zones can alter the flow continuity.

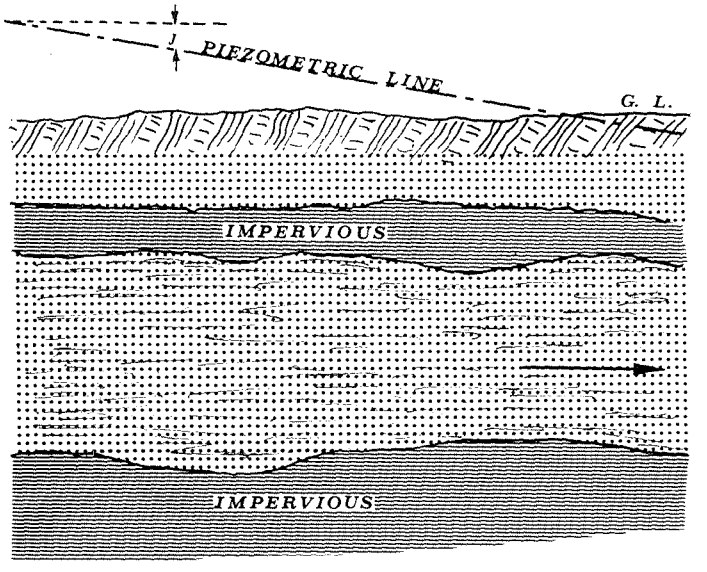

Fig. 7. Typical pattern of confined aquifer where the water-bearing stratum is entrapped between two impervious layers.

COEFFICIENT OF TRANSMISSIVITY

Strictly connected to the permeability is the coefficient of transmissivity, T, defined as:

$$T = bK \tag{6}$$

where b is the aquifer's thickness.

The transmissivity $[L^2T^{-1}]$ is useful mainly to elaborate further the characteristic terms by means of mathematical relationships.

Direct measurement of transmissivity is sometimes performed, especially in *confined aquifers*, i.e., when the water-bearing stratum is interposed between a "bottom" and a "ceiling" of impervious material (Fig. 7). In the *unconfined aquifers* (Fig. 8) the measurement becomes more difficult because the geometric and dynamic aspects of the water table cannot easily be controlled (Wiederhold, 1966).

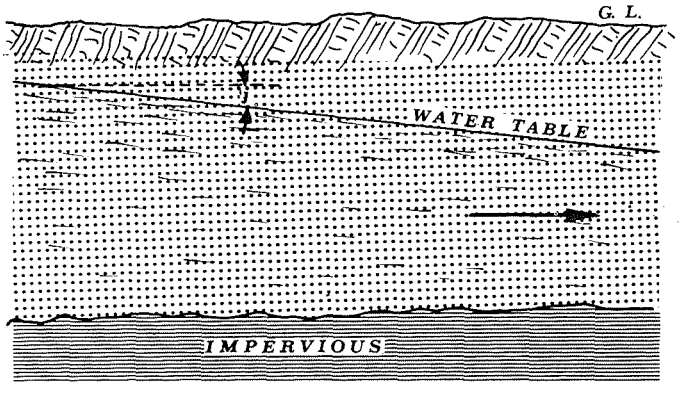

Fig. 8. Typical pattern of unconfined aquifer.

POROSITY

Porosity is another important parameter related to the behaviour of underground water. It is defined as the ratio

$$n = V_v/V_o$$

between the volume V_v of the voids and the total volume V_o considered (it is obviously accepted that $V_o = V_v + V_s$, where V_s is the volume of the solid part).

Porosity depends upon the size of the solid grains, their shape and arrangement. Small grains can fill the empty spaces between larger grains, so an aquifer made up with non-uniform size distribution will have a smaller porosity than one having uniform grains (Fig. 9).

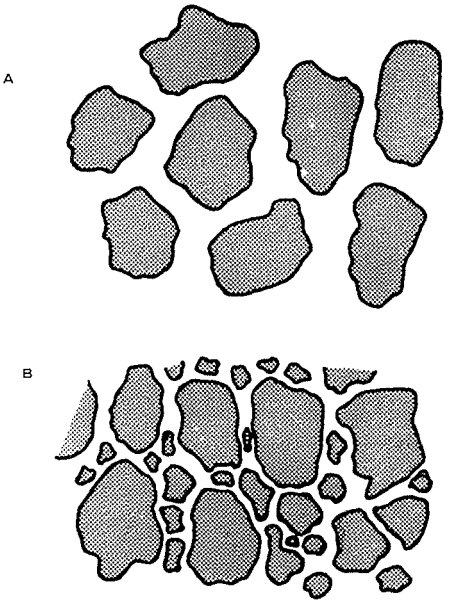

Fig. 9. The effect of grain size on porosity: pattern A, made up with uniform grains, is expected to have a greater porosity than pattern B.

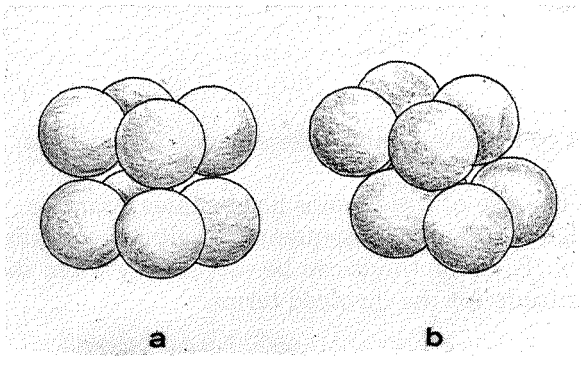

Fig. 10. Graton and Fraser's test: eight spheres set (a) in a cubical array leave a greater porosity (n = 0.476) than (b) in a rhombohedral array (n = 0.260).

Moreover, the way the grains are packed in the solid matrix can affect the porosity. Graton and Fraser's test (Davis and De Wiest, 1967) is well known in which eight spheres, if set in a cubical array, leave a porosity n = 0.476 and n = 0.26 if set in a rhombohedral array (Fig. 10).

The concept of porosity can hardly be transferred to the field of rocky aquifers, where the empty spaces are due to fractures, larger openings and even caves, formed by karstic alterations of joints and faults.

It seems more important to point out the existing relationships between porosity and permeability. Many attempts have been made but the best refer to the so-called "non-indurated sediments", i.e., to aquifers in which the grains still remain uncemented and are therefore free to move relative to one another. In these aquifers the permeability has been found to be proportional to the square of the representative diameter of the grains. Starting from eq. 3 the general expression of permeability is defined by:

$$K = \frac{C}{\nu} d^2 \xi \tag{7}$$

where ξ is a statistical corrective factor which accounts for the size "distribution" of grains.

Recent elaborations consider the density distribution of pore sizes and put eq. 7 in the form:

$$K = \frac{C}{\nu} \int_{d^* = \min} d^{*2} P(d^*) \mathrm{d}d^*$$

where d^* is the mean significant diameter of the pores. The integration is extended above a minimum value of d^*, determined by considering the effect of molecular forces at the liquid—solid boundary. The distribution function $P(d^*)$ is often found to be gaussian", i.e., in accordance with the following law:

$$P(d^*) = \frac{\sigma}{\sqrt{\pi}} \mathrm{e}^{-\sigma^2 d^{*2}}$$

in which σ is a specific constant to be determined after an accurate analysis of the grain pattern.

A statistical investigation on the size of solid grains necessitates a sample to be "abstracted" from the original soil and consequently to alter the natural configuration of the solid matrix. These methods can be useful only when the aim is to assess an order of magnitude for the involved terms.

STORAGE COEFFICIENT

Another fairly important hydraulic parameter of the aquifer is the storage coefficient, S, defined as:

$$S = \rho g(\alpha + n\beta)b$$

where ρ = the density of the water $[FT^2L^{-4}]$
g = the acceleration due to gravity $[LT^{-2}]$
α = the compressibility of the solid skeleton $[L^2F^{-1}]$
β = the compressibility of fluid $[L^2F^{-1}]$
n = the porosity [0]
b = the thickness of the aquifer [L]

The resulting term is non-dimensional.

The occurrence of the storage coefficient is connected to a pressure variation in the aquifer which affects both the volumes occupied by the solid and the liquid components. Although it might seem unrealistic that water compressibility could be involved in problems where usually liquids are deemed incompressible, such a term cannot generally be neglected, since β is of the same order of magnitude as α. Assuming for instance:

$\alpha = 0.2 \cdot 10^{-9}$ m^2 kg^{-1} $\quad$ $\rho = 102$ kg sec^2 m^{-4}

$\beta = 5 \cdot 10^{-9}$ m^2 kg^{-1} $\quad$ $g = 981$ m sec^{-2}

$n = 0.5$ $\quad$ $b = 10$ m

gives: $S = 2.7 \cdot 10^{-5}$

which is a value of the same order as K.

However, the phenomenon of compression of both the solid and the liquid components becomes more remarkable in the case of an aquifer confined between an impervious bed and a ceiling, when the bulky volume variation is impeded by the boundary constraints and therefore the inner masses are more directly stressed. Conversely, in an unconfined aquifer the displacements of the water table can reduce the effect of volume variation in the liquid-grains pattern. Incidentally, the storage coefficient is very small in these aquifers.

The storage coefficient is also a function of the space coordinates x, y, z: $S = S(x,y,z)$. It is therefore expected that this term can vary from site to site and the same concepts can thus be applied to the permeability, including the aspect of homogeneity.

The evaluation of S is generally difficult and in practice it can be achieved only by calculation, starting from accepted values of α, β and n. Very often this determination is obtained by solving the so-called "inverse problem", as will be explained in the next section.

For the sake of simplicity in unconfined aquifers the storage coefficient is very often replaced by the *effective porosity*, defined as the "volume of water which effectively can move into the bulk of the aquifer". Sometimes, because it is small when compared to the other terms for the reasons above specified, it can be neglected.

SOLUTIONS FOR PRACTICAL PROBLEMS

The practical problem of underground water motion is generally solved by means of the following set of equations:

The continuity equation:

$$\frac{\partial(\rho V_x)}{\partial x} + \frac{\partial(\rho V_y)}{\partial y} + \frac{\partial(\rho V_z)}{\partial z} = n\rho \left(\beta + \frac{\alpha}{n}\right) \frac{\partial p}{\partial t}$$

with the above defined symbols and the variation of pressure p over the time t.

The state equation, relating the variability of the aquifer's characteristics with temperature. The problem being isothermal, the equation reduces to:

ρ = const.

The rheological equation:

$$\tau = \mu \frac{dV}{dz} \tag{8}$$

where τ is the shear stress, μ the dynamic viscosity and dV/dz the transverse velocity gradient ("shear rate") between two consecutive layers of fluid in motion.

The equation of forces, i.e., the Darcy equation. The application of this set of equations leads to typical relations able to treat several problems in practice, e.g. the behaviour of pumping wells, drainage tunnels and dispersion pits. After some manipulations, a general equation is obtained using all the terms previously considered and assuming the hydrostatic distribution of pressure ($p = \gamma h$):

$$\frac{\partial}{\partial x}\left(T\frac{\partial h}{\partial x}\right) + \frac{\partial}{\partial y}\left(T\frac{\partial h}{\partial y}\right) + \frac{\partial}{\partial z}\left(T\frac{\partial h}{\partial z}\right) = S\frac{\partial h}{\partial t} \tag{9a}$$

or, if T = const.:

$$\frac{\partial^2 h}{\partial x^2} + \frac{\partial^2 h}{\partial y^2} + \frac{\partial^2 h}{\partial z^2} = \frac{S}{T}\frac{\partial h}{\partial t} \tag{9b}$$

A further term can also be included to account for a "concentrated" activity which with the "plus" means a pumping well located in the area, and with the "minus" means a sink, injecting water into the soil. Eq. 9b becomes:

$$\frac{\partial^2 h}{\partial x^2} + \frac{\partial^2 h}{\partial y^2} + \frac{\partial^2 h}{\partial z^2} \pm q = \frac{S}{T}\frac{\partial h}{\partial t} \tag{10}$$

Eqs. 9a, b, 10 contain h as a characteristic term of water motion as well as T and S as characteristics of the soil. It can be used therefore in two ways if h is to be determined and T and S are known, or vice versa.

The first way gives rise to the so-called *direct problem* which is applied when the behaviour of h has to be ascertained in a given aquifer, especially when the operations of wells or sinks have to be considered.

The second way gives rise to the *inverse problem* which is applied to assess the numerical value of the soil characteristics, starting from in-field measurements of h (Emsellem and De Marsily, 1971; Maione and Troisi, 1972; Troisi, 1975).

The application of the inverse problem is generally a cumbersome task from a mathematical viewpoint since it involves complicated elaborations to assess the stability and the uniqueness of the solution of eq. 10, which becomes very sensitive to the scattering of h due to the errors of measure.

NON-DARCY FLOW

In recent years the problem of *non-darcy flow* has been given increasing importance since it was pointed out that in some typical patterns of soils the water motion is no longer proportional to the hydraulic gradient (Chauveteau and Thirriot, 1967; Benedini et al., 1969, 1971).

Lower and upper limits have been ascertained for the Darcy flow, with theoretical investigations able to support the experimental results (Fig. 11).

A lower limit has been found by observing the flow in a very fine medium, generally clay, at a very small range of hydraulic gradient. For these conditions the linearity between the hydraulic gradient and the seepage velocity disappears and even at zero velocity a non-zero gradient does exist. This means that a positive pressure difference is necessary to start the flow moving.

Many attempts have been made to explain such a phenomenon. Physical and chemical properties of the interaction at the liquid—solid boundary have been used referring to molecular interchange and forces.

From a kinematic viewpoint the best interpretations are those considering the "non-newtonian behaviour" of water, which at the beginning of motion acts preferably as a "Bingham-plastic fluid" owing to the solid—liquid mutual interactions. Instead of having the classic "newtonian" eq. 8 the following law is supposed to hold (Karadi and Nagy, 1959; Benedini, 1969):

$$\tau = \tau_0 + \mu \frac{dV}{dz}$$

in which τ_0 ("yield stress") is a characteristic value to be determined before starting the motion.

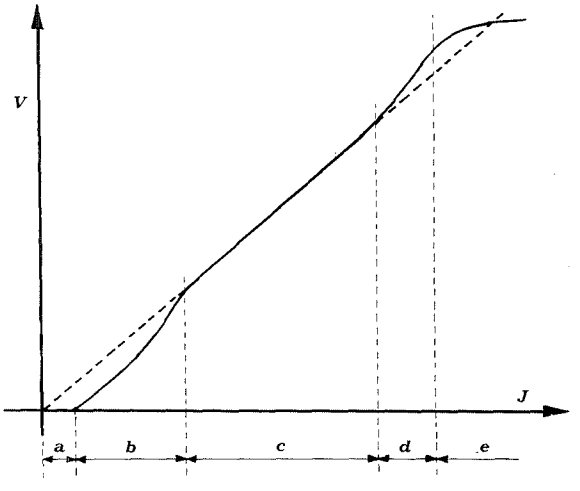

Fig. 11. Qualitative behaviour of water motion in soil: *a* and *b*, non-newtonian; *c*, Darcy flow; *d*, transition zone; *e*, turbulent.

As the velocity increases these interactions become more and more negligible and consequently the behaviour becomes newtonian. The linearity is restored and therefore the validity of Darcy law. Furthermore, the linearity disappears for the highest values of the hydraulic gradient, but this happens quickly in the case of large grains or fractured aquifers (Benedini et al., 1972, 1975). To explain this the fundamentals of fluid dynamics must be used.

As was previously mentioned, the flow within the solid matrix complies with the laws of liquid motion in ducts where for the lowest pressure differences, i.e. the lowest values of the hydraulic gradient, the motion is expressed by Poiseuille's law which gives the proportionality between the velocity and the hydraulic gradient.

As the pressure difference (the energy dissipation) increases the motion of the duct-flow begins to be turbulent and, after a considerable zone of transition, Poiseuille's law must be replaced by one referring to the square root of the hydraulic gradient:

$$V = G\sqrt{J}$$

where G is a factor accounting both for the geometry of the duct and for the roughness on the wall of the duct. The demarcation between the linear and the transition zone in duct-flow is set by the well-known Reynolds number:

$$R_e = Vl/\nu$$

where V is the mean velocity and ν the kinematic viscosity. The geometric term l, which has no universal meaning in fluodynamic problems, is put equal to the diameter in the case of circular pipes or to an "equivalent" diameter (often to the "hydraulic radius") in the case of non-circular ducts. The value of Reynolds number for which the linearity vanishes in pipes and ducts is generally assumed equal to 2,500, while for more than 100,000 the motion is considered fully-developed turbulent.

Similar considerations hold also in the case of underground water motion where the above-mentioned situations of very high pressure gradients or large grains, for which the linearity starts to disappear, can be both quantitatively reduced to a high Reynolds number, either for a large value of the velocity V (to be expected for high-pressure gradients) or for a large geometrical term l, in the broad interstices between the larger grains.

Adaptation of such a theory, albeit cumbersome, has proved fruitful in seepage problems. The main difficulty lies in the choice of an appropriate and meaningful geometrical term l useful for the construction of the Reynolds number. For clay, sand and small gravel it is generally assumed as the mean diameter of the solid grains. Since this term is of the same order of magnitude as the equivalent diameter of the void interstices, such an assumption is strictly in line with the fluodynamical considerations dealing with the fluid motion in ducts.

A substantial difference has been found experimentally, because the transition from laminar to turbulent flow is at a value of 80 for the Reynolds number, which is far less than that ascertained for pipes and ducts.

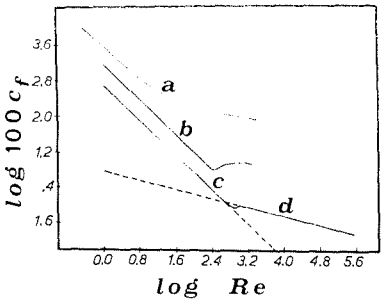

Fig. 12. "Friction factor" (c_f) versus Reynolds number for various types of seepage flow: *a*, porous medium; *b*, fractured medium with rough fissures; *c*, fractured medium with smooth fissures; *d*, smooth-walled tube.

Furthermore, the way in which the transition occurs in the aquifers is different from that in the pipes. As usual, in Fig. 12 the friction factor—Reynolds number diagram can be taken for this purpose. In such a diagram the curve *a* shows the behaviour of a porous aquifer, the curves *b* and *c* are for fractured aquifers (for rough and smooth fissures respectively) and finally the last stretch of the curve *d* shows the behaviour of smooth pipes.

It is easy to see that the transition in the porous aquifers proceeds gently for a large proportion of Reynolds numbers, while in the other cases there is a sudden start. Several attempts have been made to explain similar behaviour: the most reliable one takes into account the fact that, due to the extreme irregularity of the voids' geometry, there are coexisting large and small ducts as well as smooth and rough-walled ones, so that simultaneously some ducts are affected by laminar flow and others are affected by turbulent flow. The represented pattern is therefore the combined result of both laminar and turbulent effects, which progressively shifts towards the fully developed turbulence as the Reynolds number increases.

A similar explanation holds also in the case of fractured aquifers where, in a more detailed investigations both in the field and in the laboratory, some singularities have been found (Le Tirant and Baron, 1972).

In fact, plotting the seepage velocity versus the hydraulic gradient, a very broad transition zone can be observed, with reverse curvature as compared to that of increasing turbulence. This might be due to the progressive pitch of more and more joints in the turbulent flow, but also might be because of their enlargement determined by the pressure of the liquid component. Once the linearity has begun to fail, the basic concept of permeability also vanishes and the main aim is then to find a formal law suitable to replace Darcy's.

Several formulae have been proposed, especially from laboratory investigations, which often have a mere interpolation meaning and therefore are without any direct physical significance. Apart from some details, which concern attempts to specify the proper meaning of the involved terms, the resulting formal interpretations lead to two basic expressions:

(1) The binomial Fochheimer's relationship:

$$\vec{J} = (a + bV)\vec{V}$$

(2) The monomial power law:

$$\vec{J} = wV^{p-1}\vec{V}$$

where a, b and w are constant. The above relationships account both for the transition zone and for the fully developed turbulence, provided appropriate values are given to the coefficients and exponents involved. If complete turbulence is considered it should be expected that: $a = 0$ or, respectively, $p = 2$, but for the transition zone a can assume any positive value, and p can vary between 1 and 2.

In any case the resulting mathematical interpretations give rise to many formal difficulties when further elaborations are requested, especially for the evaluation of both the steady and unsteady conditions of flow.

In practice the problem is more complicated because the three regimes of laminar, transition and turbulent flows can all exist within the same problem. A typical example is the case of a pumping well in a coarse gravel or in a fractured aquifer, where one would expect to find (Fig. 13):

a a fully turbulent zone close to the pumping well;
b a more or less extended transition zone; and
c a linear Darcy zone at the farthest points of the field.

Delineation of one zone from another can be done only after considering the limiting Reynolds number, which can be calculated by means of the assumed holding equations, thereby involving a tedious "trial and error" process.

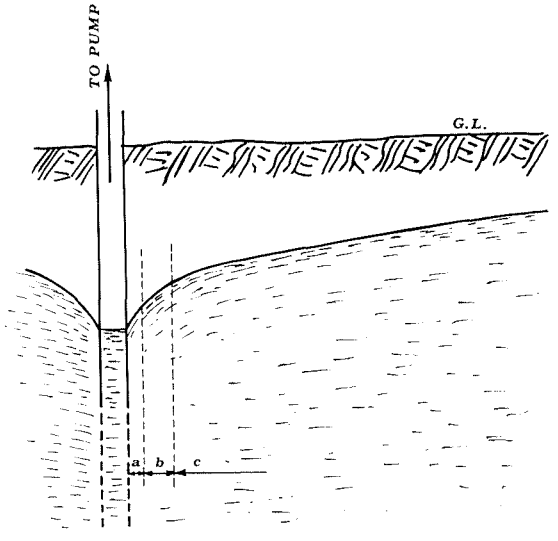

Fig. 13. Typical behaviour in a pumping well: *a*, non linear zone; *b*, transition zone; *c*, turbulent zone.

The logical procedure should be:
(1) evaluate the velocity,
(2) calculate the Reynolds number,
(3) choose the appropriate equation,
(4) compute the velocity,
(5) compare with the value assumed in (1), and start again from (1) with a new cycle.

POLLUTION

Pollution is affecting more and more aquifers, involving further terms and calling for further investigations.

Pollution of groundwater is chiefly due to the transportation of miscible and immiscible pollutants by the surface water penetrating into the ground. Another frequent case of underground water pollution is caused by the mixing of rainfall-originated fresh water with seawater intruded in coastal zones, sometimes enhanced by irrational criteria of exploitation of the existing resources. In fact, to pump water beyond a certain flow ("critical flow"), imposed by the natural balance of the available quantity, can motivate irreversible displacement of the "interface" between fresh and sea water (Cotecchia, 1958; Dracos, 1975). The presence of pollutants in underground water is shown by the concentration:

$$c = c(x,y,z,t)$$

i.e., the mass of pollutants in the unit volume. In metric units c $[FT^2L^{-4}]$ is expressed conventionally in g cm^{-3}.

Concentration is a scalar term that is also affected by the characteristics of the dispersed medium as well as by the liquid one. In its most general way it can also be expressed by a relationship of the following type:

$$c = f(D,\rho,\mu)$$

where D, ρ and μ are the *molecular diffusion*, the *density* and the *dynamic viscosity* of the liquid, respectively. Once the dependence of c upon these terms is ascertained, the concentration can be considered as a *potential* and mapped in the same way as the piezometric head h. The mechanics of pollution are related to the dispersion of polluted particles inside the water, which is indeed a very complex phenomenon (Fig. 14).

Representing the particle by means of a small ball, transported by the flow, the process can be roughly sketched as a continuous splitting of the original ball into smaller and smaller balls shifted in the direction of the flow.

If the dispersion is considered in a more comprehensive way within the aquifer, the presence of the solid matrix must be included because this affects the motion of the smaller balls thereby identifying some preferential paths. Furthermore, the process must be determined by the difference of concentration existing between two contiguous points, since in order to

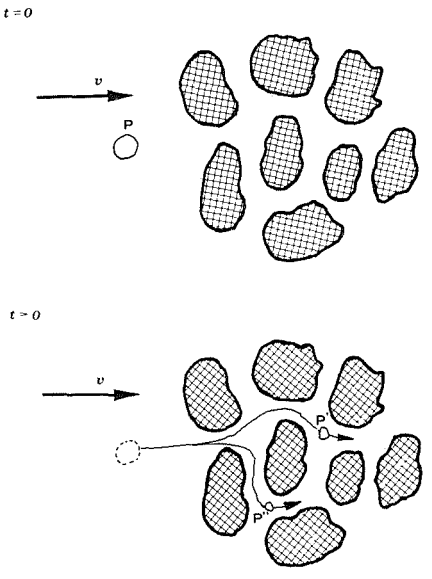

Fig. 14. The mechanism of pollution transfer. The original pollutant particle P at time $t = 0$ is split into two (or more) smaller particles at time $t > 0$.

restore a general equilibrium, the point having the highest concentration is expected to affect that with least number of particles, thus generating a "flow" of particles which initially can be considered proportional to the difference of concentration.

Such a proportionality can be achieved through the definition of a coefficient that plays more or less the same role as the permeability in the Darcy law and is called the *dispersion coefficient.* For the above considerations dispersion appears to be a function of the space coordinates and since it may vary from one direction to the other, being not necessarily parallel to the variation of concentration, in its most general expression it must be a tensor (Fried and Combarnous, 1971; Fried, 1972). Keeping in mind that dispersion is a time-dependent phenomenon, the describing equation may be written in its most comprehensive form:

$$\operatorname{div}\left(k\rho \overrightarrow{\operatorname{grad}}\frac{c}{\rho}\right) - \operatorname{div}\left(\vec{V}c\right) = \frac{\partial c}{\partial t} \tag{11}$$

For the dispersion coefficient k $[L^2T^{-1}]$ considerations hold similar to those for permeability, e.g., those concerning the homogeneity and the isotropy (Krizek et al., 1972). More complexities are involved if the possibility of adsorption and absorption of pollutants by the solid matrix is also included. Some chemical reactions can also occur.

A further complexity is introduced by some pollutants which have a separate "life", e.g., microorganisms of the domestic sewage whose degree of

evolution if connected to the available oxygen. Investigations on these aspects move into the field of hydraulics and invade that of chemistry and microbiology. More information should be collected on this matter and new research begun, both experimentally and theoretically, to enhance this knowledge.

To treat the problem of underground pollution the dispersion eq. 11 must be considered together with the equations of continuity, rheology and Darcy already introduced on pp. 167—168. Moreover the following "state equations" of the mixture should be considered:

$$D = D(c);\ \rho = \rho(c);\ \mu = \mu(c).$$

The solution to this problem can benefit from some experimental law, involving the dispersion coefficient with some other term, e.g.:

$$k = \alpha D \left(\frac{Vd}{D}\right)^m + \beta$$

which refers to the molecular diffusion D, to the mean pore velocity V and to the pore diameter d. The constants α, m and β should be determined experimentally.

The non-dimensional term Vd/D is the well-known Peclet number, very useful in this kind of investigation.

The final solution to this problem can be obtained only after appropriate elaboration of the above mathematical formulations and on the basis of reliable experimental data. It seems worth stressing that more research is still necessary in this field.

The large availability of statistical and advanced mathematical techniques, together with the progress of high speed computers, can probably bring an improvement to the solution by adopting *stochastic and probabilistic procedures*, which have proved very effective in treating dispersion problems in surface water.

UNSATURATED AQUIFERS

A field of basic interest is that of unsaturated aquifers, whose importance is chiefly involved in water balance and irrigation problems (Fig. 15). The phenomenon is related to the presence of a separation surface between air and water which gives rise to the development of molecular forces sometimes having a very high intensity. If referred to the unit surface they form the *surface tension*, the effect of which can influence the motion of water and be superimposed on that of gravity (IAHS, 1900; Kovacs, 1971). If ψ is the surface tension $[FL^{-2}]$, the general law of unsaturated flow, corresponding to the steady-state Darcy's law, is (in the x-direction):

$$V = K_H \frac{\partial(h + \psi/\gamma)}{\partial x}$$

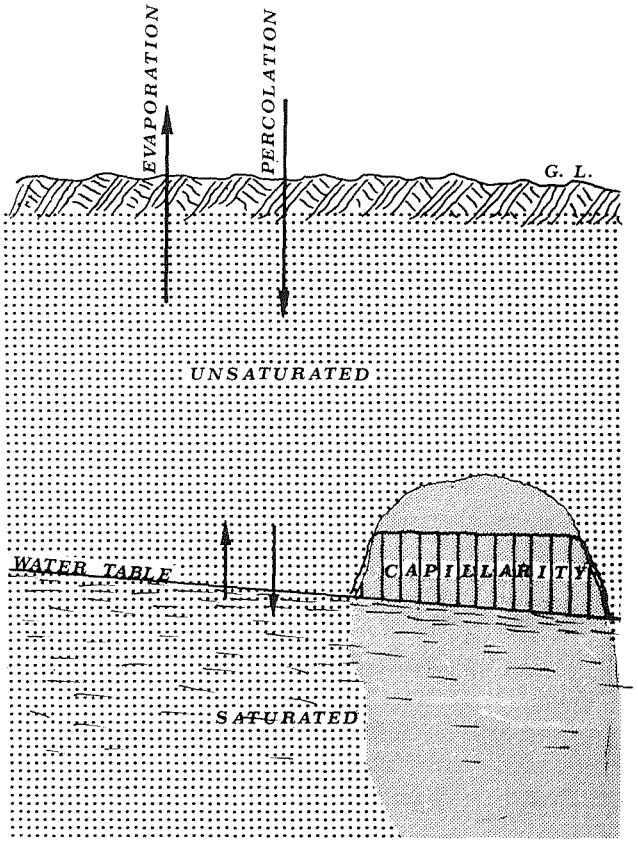

Fig. 15. Above the water table a water—air mixture forms the *unsaturated zone*. The difference in pore size can produce the *capillary rise*.

In vectorial form (γ is the specific gravity of water):

$$\vec{V} = K_H \left(\overrightarrow{\text{grad}}\, h + \overrightarrow{\text{grad}} \frac{\psi}{\gamma} \right)$$

where K_H is the corresponding tensor of *unsaturated conductivity* [LT^{-1}].

The evaluation of the latter term is generally cumbersome, both theoretically and experimentally, since a complete picture of the phenomenon itself is not yet available. As in Darcy flow, it can be helpful to refer to the pipe flow in Poiseuille conditions. Imposing the dynamical balance in an elementary portion of air-water current within the pipe, motivated by the gradient of hydrostatic pressure and surface tension, and hindered by the viscosity forces, after some elaboration the unsaturated conductivity can be expressed in a more or less complicated way as a function of the so-called *coefficient of saturation*, that is the ratio:

$$s = \frac{W}{n}$$

where W is the percentage of water in volume and n is the porosity.

The unsaturated conductivity often is expressed as proportional to the permeability K by means of a relation:

$$K_H = Ks^{\alpha}$$

s being the coefficient of saturation. The exponent can generally vary from 3.0 to 3.5.

Taking account of the molecular forces at the air—water surface does not always allow similar molecular forces acting in the water—solid boundary surface to be neglected. This is achieved by adopting criteria similar to those for the saturated aquifers, when the non-Darcy behaviour can be kinematically described with the non-newtonian flow. For the unsaturated aquifers it is worthwhile to say that further research is still necessary.

CONCLUSIONS

It seems worthwhile to look into the future, pointing out the most important subjects towards which the present research ought to be oriented. To meet the specific requests of the increasing use of underground water for human needs, geophysics can make a useful contribution.

As it can be seen from the previous sections, the field in which further theoretical and experimental research is especially necessary is for a better appreciation of the behaviour and exploitability of fissured aquifers. Geophysics has a very important role to play in this subject, improving at the same time its own knowledge. Indeed, the complexity of this kind of aquifer demands more and more reliable techniques.

The basic concepts of water motion in fissured aquifers should also be confirmed, especially through in-field measurements, in order to ascertain the possibility of applying existing formal relationships or introducing new and perhaps more complete mathematical tools.

Other topics, also of particular interest for the increasing applications of water-intaking techniques, are:

— the behaviour of non-saturated aquifers, and
— natural and man-made pollution, identifying techniques useful for detecting quality aspects in the deepest strata of the aquifers.

Water engineers who are responsible for the use and protection of underground water resources are anxious to hear the progress of geophysics in these fields.

REFERENCES

Benedini, M., 1969. Exploratory Investigation on Some Rheological Background in the Interstitial Motion of Water. XIII Congress of IAHR, Kyoto, 1969.

Benedini, M., Cicioni, G.B. and Giuliano, G., 1969. Sull'applicazione di alcune leggi di moto permanente non lineare a pozzi emungenti. Geol. Appl. Idrogeol., IV.
Benedini, M., Cicioni, G.B. and Giuliano, G., 1971. On the possibility of formulating a mathematical model for the study of unsteady non linear flow in aquifers. Geol. Appl. Idrogeol., VII.
Benedini, M., Giuliano, G. and Troisi, S., 1972. Alcune considerazioni sulla trattazione matematica del problema del moto in acquiferi fessurati. Geol. Appl. Idrogeol., VII.
Benedini, M., Giliano, G. and Troisi, S., 1975. Recherches de Laboratoire sur un Perméamètre fissuré. Réunion Int. AIRH/SIA sur les Nappes Souterraines. Vol. II, Rapperswil.
Chauveteau, G. and Thirriot, C., 1967. Regimes d'écoulement en milieux poreux et limite de la lois de Darcy. La Houille Blanche, 2(1).
Childs, E.C., 1969. An Introduction to the Physical Basis of Soil Water Phenomena. Wiley, New York, N.Y.
Cotecchia, V., 1958. Sviluppi della teoria di Ghyben ed Herzberg nello studio idrogeologico dell'alimentazione e dell'impiego delle falde acquifere, con riferimento a quella profonda delle Murge e del Salento. Geotecnica, 6.
Darcy, H., 1856. Les Fontaines Publiques de la Ville de Dijon. Dalmont, Paris.
Davis, S.N. and De Wiest, R.J.M., 1967. Hydrogeology. Wiley, New York, N.Y.
De Wiest, R.J.M., 1969. Flow through Porous Media. Academic Press, New York, N.Y.
Dracos, T., 1975. Pollution due aux eaux non miscibles. Réunion Int. AIRH/SIA sur les Nappes Souterraines. Vol. I, Rapperswil.
Emsellem, Y. and De Marsily, G., 1971. An automatic solution of the inverse problem. Water Resources Res., VII.
Fried, J.J., 1972. Miscible Pollution of Groundwater: a Study in Methodology. Int. Symp. on Modelling Techniques for Water Resources Systems, Ottawa, 1972.
Fried, J.J. and Combarnous, M.A., 1971. Dispersion in Porous Media. Advances in Hydroscience, Vol. 7. Academic Press, New York, N.Y.
IAHS, 1900. Hydrological investigation of the unsaturated zone. 1st, Vituki, Budapest.
Irmay, S., 1955. Flow of liquid through cracked media. Bull. Res. Counc. Israel, 5(1).
Irmay, S., 1964. Theoretical Models of Flow through Porous Media. Proc. RILEM Symp. on the Transfer of Water in Porous Media, Paris.
Karadi, G. and Nagy, I.V., 1959. Investigations into the Validity of the Linear Seepage Law. IX Congr. IAHR, Dubrovnik, 1959.
Kovacs, G., 1971. Seepage through saturated and unsaturated layers. Bull. IASH, XVI(2).
Krizek, R.J., Karadi, G.M. and Socias, E., 1972. Dispersion of a contaminant in fissured rock. Proc. Symp. on Percolation through Fissured Rock. T3-C, Stuttgart, 1972.
Le Tirant, P. and Baron, G., 1972. Ecoulement dans les Roches Fissurées et Contraintes Effectives: Application à la Fracturation Hydraulique das Reservoirs. Proc. Symp. on Percolation through Fissured Rock. T2-K, Stuttgart, 1972.
Louis, C., 1968. Etude des écoulements d'eau dans les roches fissurées et de leurs influence sur la stabilité des massifs rocheux. EDF, Bull. Div. Etudes Rech., A(3).
Maione, B. and Troisi, S., 1972. Metodi per la risoluzione del problema inverso in una falda sotterranea. Atti XIII Conv. di Idraulica e Costruzioni Idrauliche, Milano, 1972.
Muller-Feuga, R. and Ruby, P., 1960. Mesure de la permeabilité en milieux poreux. L'Hydraulique Souterraine.
Paolillo, A.G.S.: La determinazione della permeabilità in situ. Memorie e note dell'Istituto di Geologia Applicata, Napoli, Vol. XI.
Rouse, H., 1949. Engineering Hydraulics. John Wiley, New York, N.Y.
Todd, D.K., 1959. Ground Water Hydrology. John Wiley, New York, N.Y.
Troisi, S., 1975. Stability of the solution of water flow in heterogeneous aquifers. IFIP Working Conf. on Computer Simulation of Water Resources Systems, Ghent, 1975.
Wiederhold, W., 1966. Interpretation of pumping tests on wells. Proc. of IWS Congr., Barcelona, 1966.

Geoexploration, 14 (1976) 179—193

POSSIBILITIES AND LIMITATIONS OF THE RESISTIVITY METHOD OF GEOELECTRICAL PROSPECTING IN THE SOLUTION OF GEO-HYDROLOGICAL PROBLEMS

J.C. VAN DAM

Delft University of Technology, Delft (The Netherlands)

ABSTRACT

Van Dam, J.C., 1976. Possibilities and limitations of the resistivity method of geoelectrical prospecting in the solution of geohydrological problems. Geoexploration, 14: 179—193.

The resistivity method has proved to be very suitable in determining the distribution of fresh and saline groundwater in sedimentary deposits as occur in the Netherlands. This is illustrated by several examples.

However, the method gives no information about recharge, groundwater flow, geohydrological constants (permeability, transmissibility and hydraulic resistance) and the presence of relatively thin layers of bad hydraulic conductivity which can be of great importance in geohydrological problems.

Difficulties arise also in the interpretation of gradual changes of the groundwater salinity with depth in otherwise homogeneous aquifers.

INTRODUCTION

In present times, with the growing population and rising standards of living, the demand for good quality water is increasing almost everywhere. Depending on the local conditions either surface water, groundwater or occasionally both can be used to meet the demands. However, the demands are not only in terms of quantities of water that meet the quality standards for consumption in domestic and industrial use or for irrigation or sprinkling in agriculture. There are other interests or constraints as well, such as:

(1) Agriculture, in those cases where crop production depends on the depth of the groundwater table, as in large parts of The Netherlands.
(2) Land subsidence and stability of foundations. When lowering the water pressure in the pores, the intergranular stress increases and subsidence can occur. Even foundations on piles can be endangered especially in the cases of wooden piles when the piles fall dry and rot off.
(3) Conservation of nature, which may impose certain conditions on groundwater table levels and on base flow in streams.

Apart from groundwater recovery for the above-mentioned consumptive purposes there are other human activities which can exert their influence on the groundwater regime, such as:

(1) Land reclamation (largely practised in Holland).
(2) Construction of reservoirs for the storage of surface water (in the uplands behind dams, in the lowlands surrounded by circular dikes).
(3) Urbanization.
(4) Artificial recharge of groundwater by
    — infiltration of surface water
    — returning pumped groundwater after use
    — loss of irrigation water by percolation.
(5) Open cast mining.

WATER RESOURCES IN MODELS

With increasing demands and other requirements on the one hand, and harder constraints or at least greater consciousness of the constraints and greater public control on the other, it has become necessary and customary to analyse and to model the system of any water resources project not only in technical terms, but also in socio-economic terms. However, there is a difficulty — and probably it will remain — to account for intangible factors such as nature conservation. Such models enable the optimal solution of a great many of alternative solutions to be found. In terms of this paper such alternatives are, for instance, the use and/or storage of surface water, import of water from elsewhere, or desalting of brackish or saline groundwater.

It is obvious that the results of such a model study are correct only as far as the input data are correct. Part of the input data are formed by the output of a geohydrological model which describes the geohydrological system and its response to its inputs and boundary conditions.

GEOHYDROLOGICAL MODELS

The geohydrological system is characterized by:
(1) The underground, built up of:
    (a) aquifers, characterized by their transmissibilities KH (products of permeability K and aquifer thickness H) and their storage coefficients μ (for phreatic groundwater) or S (for confined or semi-confined groundwater);
    (b) semi-permeable layers or aquitards, characterized by their hydraulic resistance c, expressed in days, which is the thickness d of the semi-permeable layer divided by its vertical permeability K_v;
    (c) impermeable layers or aquicludes.
    Apart from KH, μ, S and c the lateral extent of these layers is essential.
(2) The water present in the underground:
    (a) the groundwater tables, which determine the quantity of water stored;
    (b) the chemical composition of the groundwater, in particular its salinity and hardness.

The flow in this geohydrological system is governed by the inputs and boundary conditions as:

(3) (a) natural recharge with its seasonal variations;
(b) groundwater extraction, characterized by location, depth and quantity of extraction;
(c) artificial recharge, also characterized by its location, the construction and operation of the works;
(d) water tables, whether constant or variable in rivers and canals bounding the aquifers;
(e) artificial control of groundwater tables by controlled surface water tables in areas with great drainage density (polders).

We have now come down to the domain of the geohydrologist who must build the geohydrological model and therefore first collect the required data. In his survey the geohydrologist can derive great support and profit from what geophysicists can do for him, or rather what they can do in mutual cooperation. This paper deals with the possibilities and the limitations of the input by geophysical prospecting and in particular resistivity prospecting. It is based on the author's experience in The Netherlands. Therefore it may be best to give initially some background information on the particular geohydrological conditions prevailing, and on the history of resistivity prospecting in The Netherlands.

GEOHYDROLOGY OF THE NETHERLANDS

The name, The Netherlands (Nederland, les Pays Bas, die Niederlande) indicates that the country has a low elevation. This applies in particular to the numerous so-called 'polders' in the western provinces Noordholland, Zuidholland, Utrecht and Zeeland and to the few large polders in the IJsselmeer (former Zuiderzee). Many polders are reclaimed lakes or parts thereof and have a land-elevation of up to several meters below mean sea-level. See Fig.1. The groundwater tables in these polders are roughly equal to the so-called polder-levels, the water-levels maintained in the dense networks of canals and ditches. The polder-levels are artificially controlled at depths of about 0.3—2 m below land surface by means of embankments, sluices and pumping stations.

The so created depressions in the groundwater table are reflected in the pattern of the piezometric level of the underlying Pleistocene aquifer, as appears clearly from figs. 2 and 3. This Pleistocene aquifer ranges to depths of the order of 200—250 m below mean sea-level and is covered by semi-permeable clay- and peat-layers of Holocene age, ranging from the land-surface to depths of up to 25 m in the western part, decreasing to zero in the eastern part of the areas concerned. The Pleistocene aquifer can be subdivided into more or less permeable layers of sand and gravel with some intercalations of clay-layers of local and regional extent. See Fig.4.

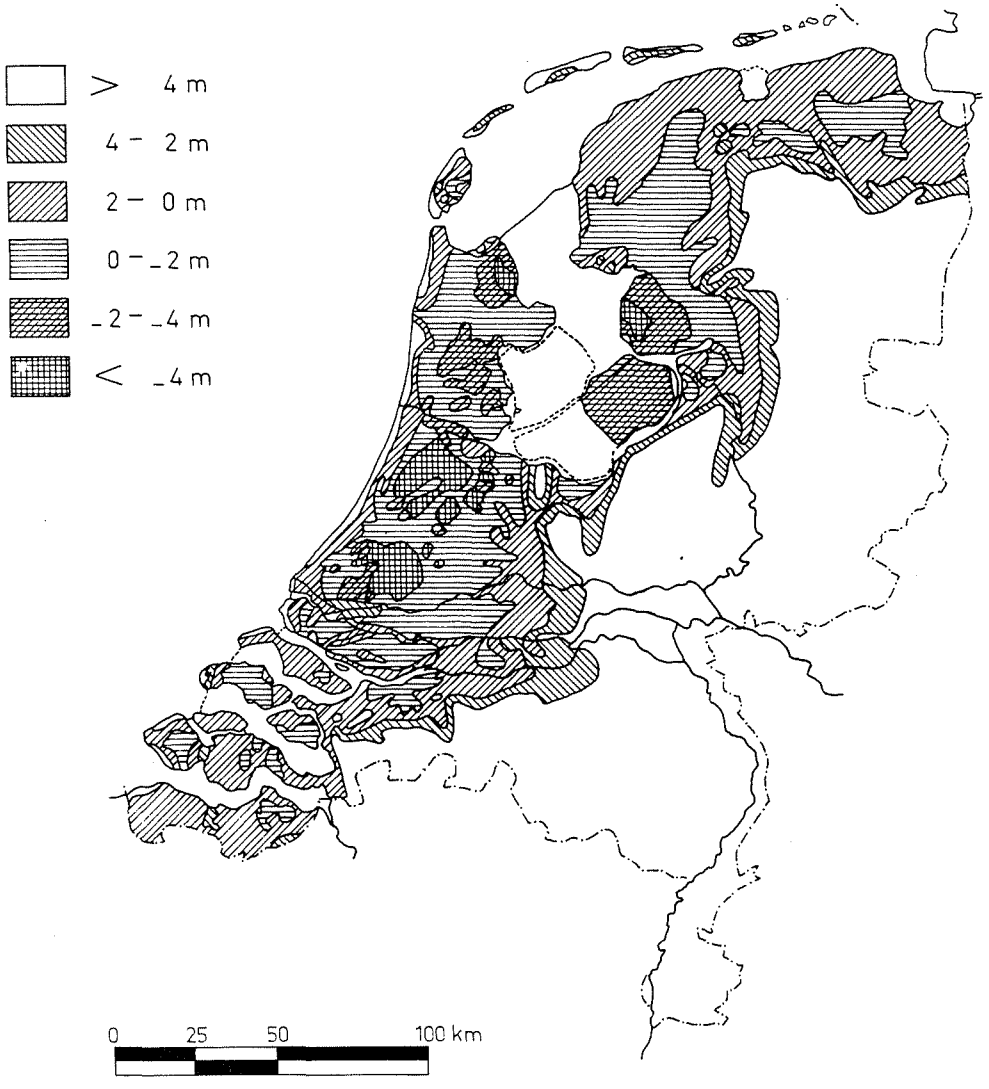

Fig.1. Contour map of The Netherlands. Depths in meters above and below mean sea-level.

The groundwater in the Pleistocene aquifer is partly fresh, partly brackish and saline; generally the salinity increases with depth. In some places there is a rather sharp interface between fresh and saline groundwater, in others the salinity increases gradually with depth.

The present distribution of fresh, brackish and saline groundwater within the polder areas is most complicated both in terms of depth and geographically, see Van Dam and Meulenkamp (1967). This is not surprising since this

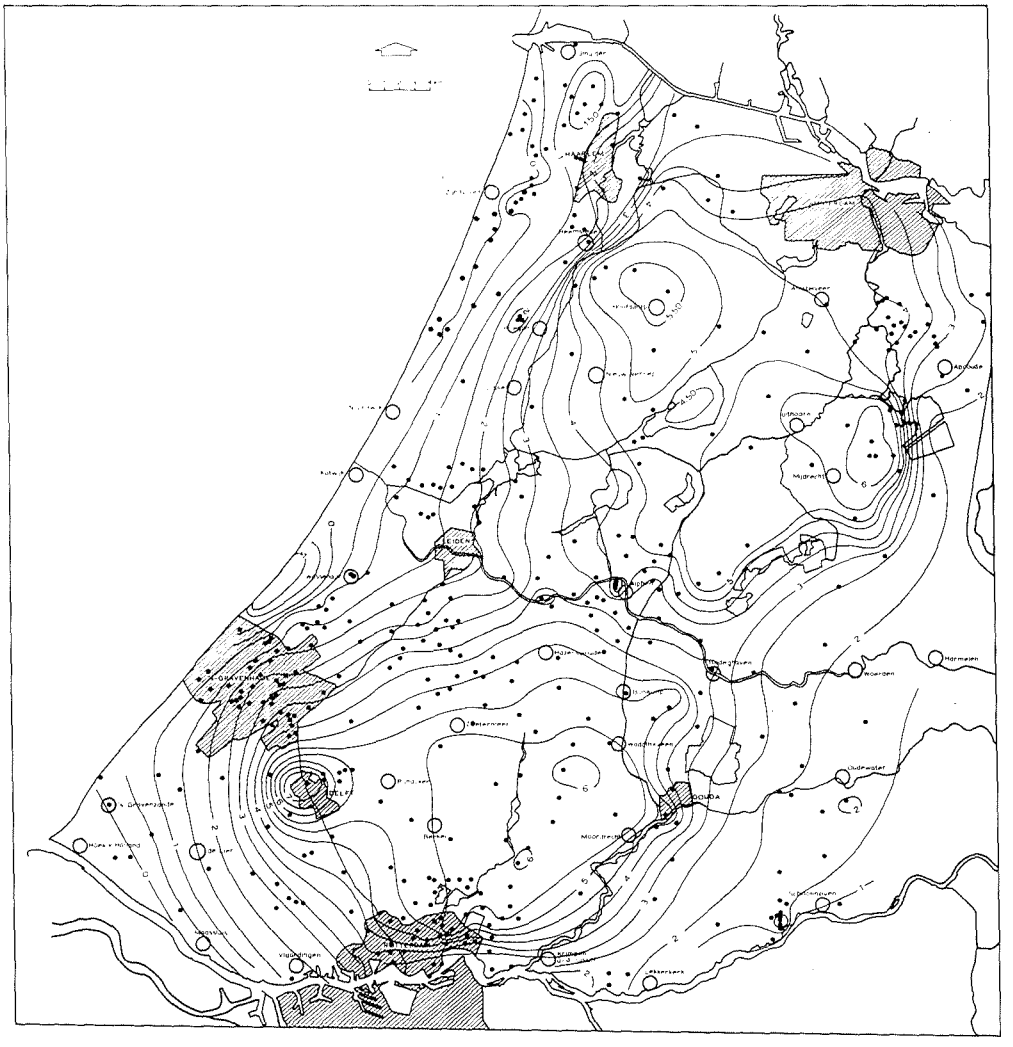

Fig. 2. Isopiestic contourlines of the Pleistocene aquifer, at a depth of 25 m below mean sea-level, in Middle-West-Netherlands. Levels in meters below mean sea-level. Average conditions over 1971. (By courtesy of Mr. K.E. Wit.)

distribution is the result of geologic processes since the end of the Tertiary Age, i.e., during the Pleistocene period (roughly 1,000,000 years) and the Holocene period (roughly 10,000 years) of the Quaternary, as well as the result of intensive human intervention such as diking, land reclamation and groundwater extraction during the very short period of roughly the last 1000 years.

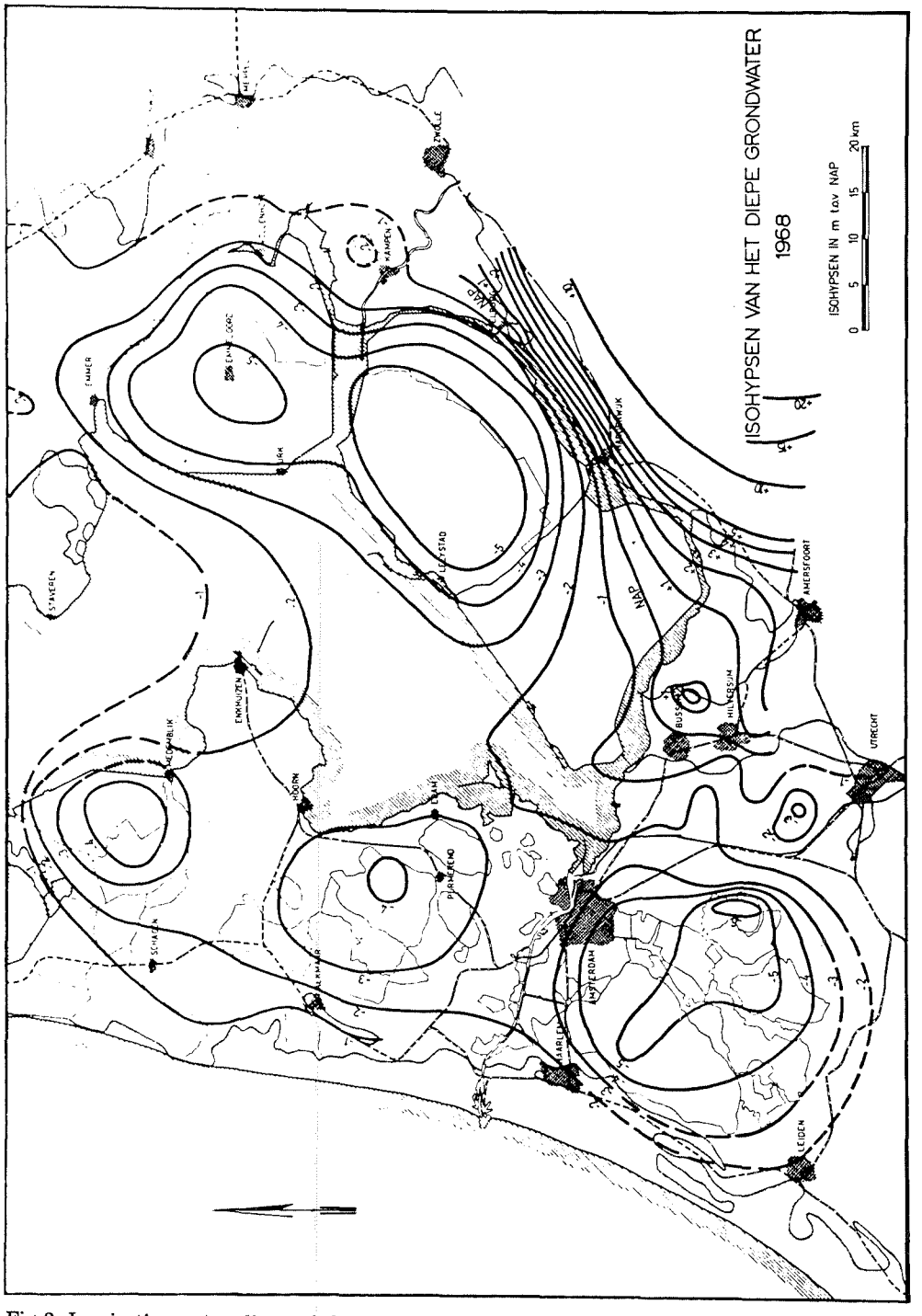

Fig. 3. Isopiestic contourlines of the Pleistocene aquifer in the IJsselmeer-region. Levels in meters above and below mean sea-level. Average conditions over 1968.

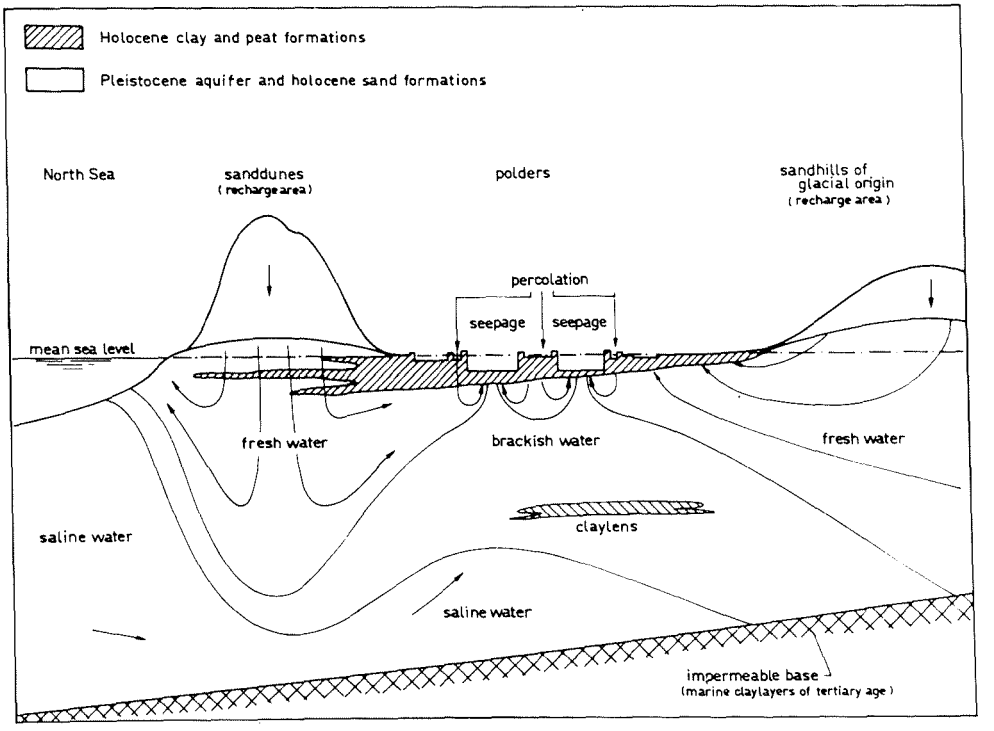

Fig.4. Geohydrological profile of the western part of The Netherlands.

RESISTIVITY PROSPECTING IN THE NETHERLANDS

The history of resistivity prospecting in The Netherlands dates back to the early fifties, when an intensive survey was carried out in the area of the former Zuiderzee, the present IJsselmeer (Dijkstra and Volker, 1955, 1958). This survey was carried out over water with electrodes on a cable laid on the bottom of the shallow lake. The results, about which later, were of great importance for the large-scale reclamation works, i.e., the creation and lay-out of new land on the lake bottom.

The great success of this survey gave rise in 1954 to the formation of a working group with field parties within the Organization for Applied Scientific Research TNO and in 1956 to the formation of a unit within the Service for Water Management of State Public Works (Rijkswaterstaat). The TNO group now forms part of the Groundwater Survey DGV-TNO.

The unit of Rijkswaterstaat started in 1956 a systematic survey of the geo-hydrological conditions, in particular the salinity distribution of the ground-water in the low-lying western and northern parts of the country. The TNO-group took an active part in that survey and also worked for local and regional

water authorities and water supply companies in The Netherlands. From the very beginning till present they took orders from abroad as well. DGV-TNO was not restricted to resistivity prospecting only; it developed and applied several methods of geophysical well-logging, refraction seismics and geothermal prospecting, all sustained by research.

Another activity of DGV-TNO is the installation of so-called salinity-watchers, i.e., permanent electrodes connected to cables left behind in exploration bore-holes.

DGV-TNO is now directed by Rijkswaterstaat to make a geohydrological map 1 : 50,000 of the Netherlands. The results of the resistivity surveys and geophysical well-logging carried out so far and currently undertaken are fitted in.

The author has had an active part in the work done by Rijkswaterstaat and is familiar with the work of DGV-TNO. Being charged with the chair of hydrology at Delft University of Technology, he introduced resistivity prospecting in his courses on geohydrology and in field work done by the students both for the purpose of instruction and as a tool in geohydrological research — about which later.

SOME RESULTS

The above-mentioned survey in the IJsselmeer was done over water in an area where, at that time, no boreholes existed. Only few borehole data on the surrounding mainland were available for gauging. The scanty external information led to the assumption of a rather homogeneous aquifer consisting of 200—300 m sand and gravel, covered by clay-layers of Holocene age of only a few meters thickness. With this assumption any variation in resistivity could be ascribed to variation in salinity of the groundwater. A calibration curve was drawn, relating the chloride content of the groundwater directly to the interpreted resistivities of the formation. In other words both the formation factor $F(\rho/\rho_1)$ and the contents of other than Cl^--ions present in the groundwater were assumed to be invariable with locality (a constant ratio of the contents of other ions to Cl^--ions would also satisfy). By taking this calibration curve for granted it was possible to draw maps for depths of 50, 100, 200 and 300 m, with lines of equal resistivity and to assign fixed values of the chloride content to each of these lines. For further details see Dijkstra and Volker (1955, 1958).

Later, after reclamation, when more borehole data became available and when resistivity surveys were performed in the surrounding areas, the picture became more complete and more detailed and it appeared that the geohydrological conditions were much more complicated than was first assumed. Therefore, the above-described maps are still valuable, but they should be considered only as a rough indication.

The resistivity surveys performed overland in the western and northern parts of The Netherlands aimed at an inventory of the available fresh water.

Information on the distribution of saline and brackish groundwater is also required in calculating the load of salt carried by seepage in the low-lying areas, which in turn is required in the calculation of the amounts of surface water needed for water- and salinity-control. Both the present situation and the prospects for the future are important, as in some polders the seepage is or was once fresh, then turns saline and later on after partial depletion of the saline water becomes fresh for ever. A paper on this subject has been published recently by the present author (Van Dam, 1976).

A most illustrative example of the distribution of fresh and saline groundwater in and around a deep polder is that of the polder Groot-Mijdrecht. A schematic profile is drawn in Fig.5. This roughly circular polder has seepage of saline groundwater in an almost circular area in its centre. In the annular

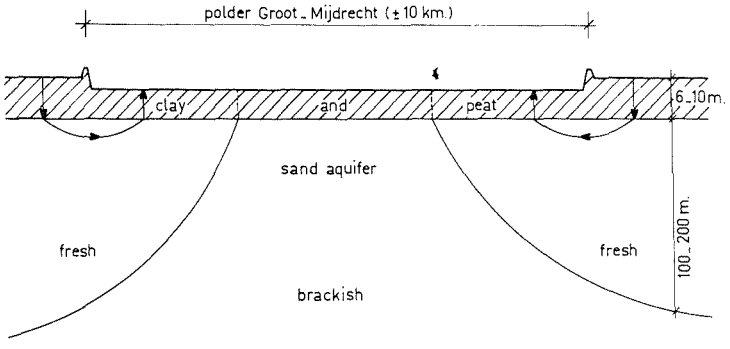

Fig.5. Schematic profile of the polder Groot-Mijdrecht (The Netherlands).

area around that circular area the seepage consists of fresh water. The interface between fresh and saline water in the rather homogeneous sandy aquifer was quite steep, as appears from Fig.5. This result of the resistivity survey was even better understood after studying the Badon Ghijben-Herzberg principle dealing with the different densities of fresh and saline groundwater.

When locating fresh water lenses, currently recharged by effective precipitation, as for example in the sand-dunes along the Dutch coast, the results of resistivity prospecting can be much better understood and interpreted when taking into account the topography and the soil types of the land sur-

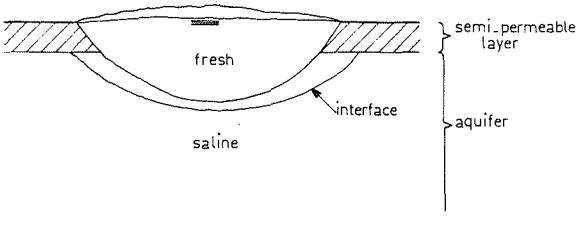

Fig.6. Inverse landscape with fresh-water lens.

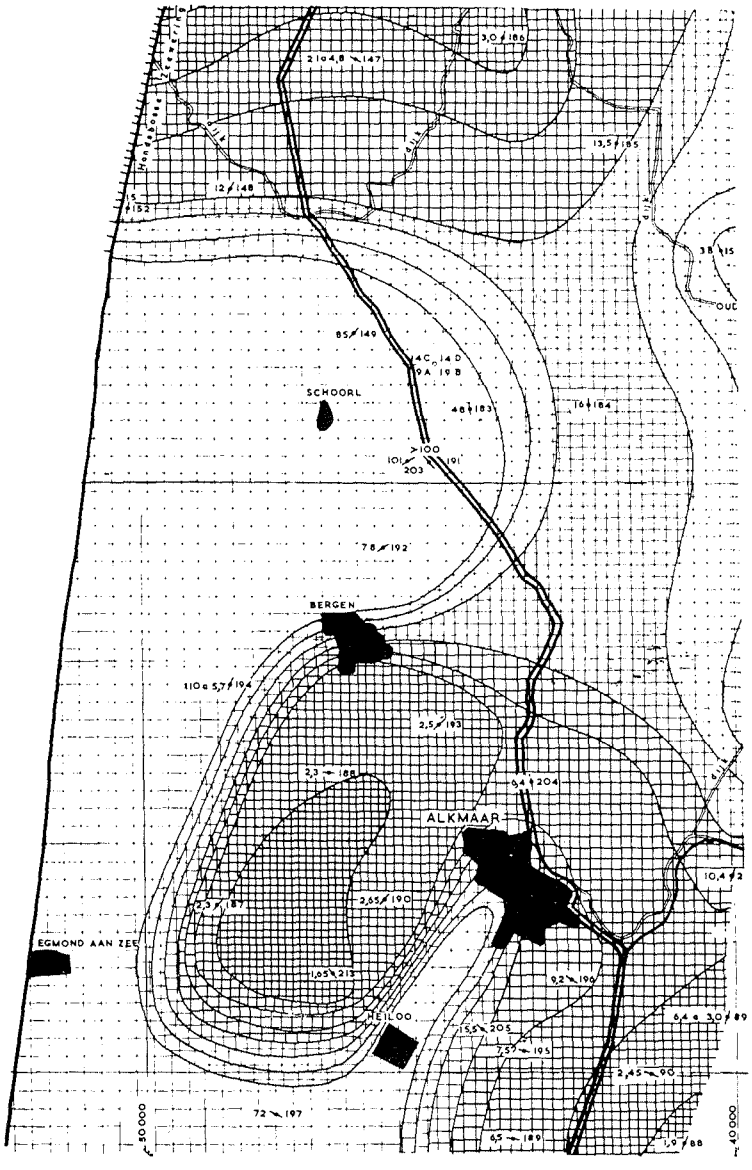
SCHOORL
BERGEN
ALKMAAR
EGMOND AAN ZEE
90 ǀ 25
1st number is spec. electr. resistivity (Ωm), 2nd is No. of measurement
0 1 2 5km
1,5
2,2
4,0
8,6
14,0
25,5
31,5
37
> 37
Spec. electr. resistivity (Ωm)

face as well as information on the elevation of the groundwater table. This latter in combination with understanding of the Badon Ghijben-Herzberg principle is very helpful. Apart from the fresh-water lenses in the sand-dunes with thicknesses of up to some 200 m, fresh-water lenses were also found in so-called creek-ridges, which are elongated sand bodies embedded in the Holocene clay- and peat-layers. These sand bodies were formed by deposition of sand particles in former tidal creeks. Later on, the adjacent clay- and peat-layers have undergone greater compaction than the sand in the creeks and so an "inverse landscape" was formed. See Fig.6. The small differences in elevation and the different soil types were perfect indicators of the presence of fresh-water lenses, which could then be mapped in detail by means of resistivity prospecting.

Another useful experience was the possibility of detecting the presence and extent of clay-layers, the thicknesses of which are small in relation to their depths. The detection of such thin clay-layers intercalated in sand- and gravel-aquifers is normally difficult or even impossible due to the principle of suppression, the resistivity of the clay often being only one-third or one-half the resistivity of the sand or the gravel. An exception is the case where the salinity of the groundwater in the aquifer above the clay-layer is higher than the salinity of the groundwater in the aquifer below the clay-layer. In the absence of a clay-layer the situation would be unstable. The heavier saline groundwater would percolate downward thus forcing the fresh water to flow upward. The presence of a clay-layer prevents this exchange. So the presence and the depth of the clay-layer is found indirectly ; its thickness still remains unknown. A clay-layer separating fresh water above from saline water below cannot be detected in this way because such a situation can equally well exist in the absence of such a clay-layer.

The above described principle enabled the author to detect an Eemien clay-layer of some 5 m thickness at depths between 25 and 35 m and extending over a large area in the province of Noordholland. The groundwater below the clay-layer was unexpectedly fresh to a considerable depth. It was protected against the exchange with sea-water by transgressions of the sea during which this clay-layer was first deposited and leaving saline water in the sandy formations subsequently deposited on the clay. The body of fresh groundwater thus conserved is not recharged in present times; it is a one-time reserve.

Another example is the case shown in Fig.7. The map indicates the electrical resistivity at a depth of 15 m below mean sea-level. The saline groundwater occurring in the area indicated by dense hatching is enclosed between the fresh-water lens in the sand-dunes west of that area, another fresh-water lens in the sandy ridge east of that area, and a clay-layer of a few meters thickness at a depth of some 25 m. The groundwater below the depth of the clay-layer was fresh. This pointed to the presence of the clay-layer acting as

Fig.7. Electrical resistivity at a depth of 15 m below mean sea-level in the area west of Alkmaar (The Netherlands).

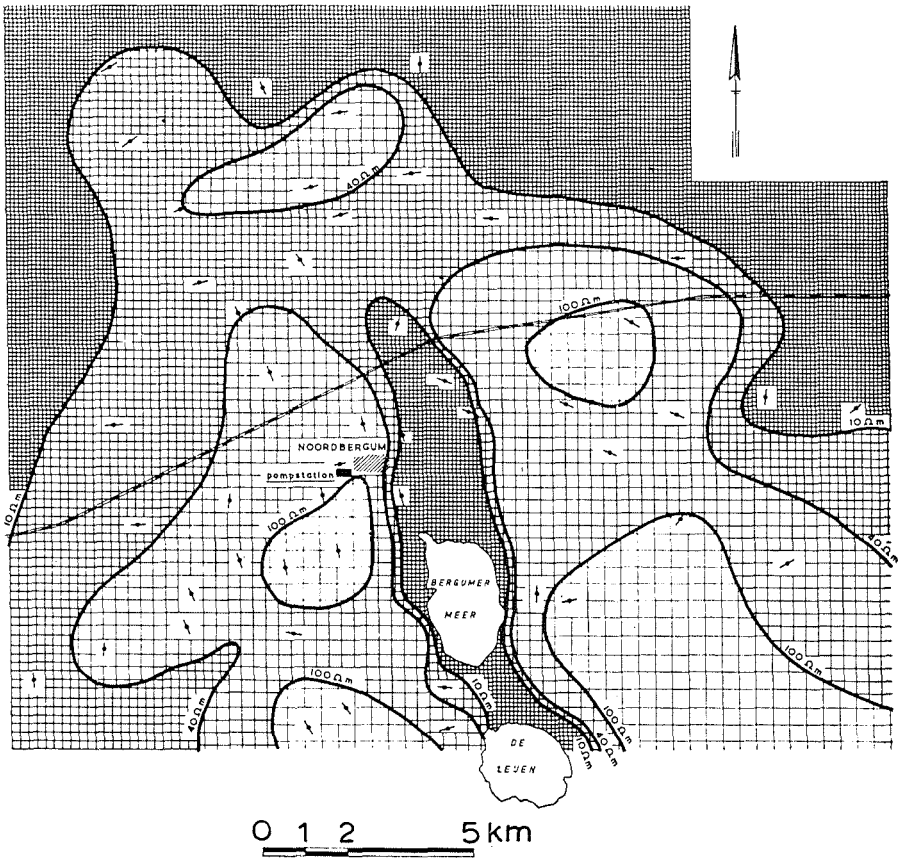

Fig.8. Electrical resistivity at a depth of 60 m below land surface in the vicinity of Noordbergum (The Netherlands).

the bottom of the box. The information obtained by resistivity prospecting and the geological knowledge of that area proved to be complementary.

In the north of The Netherlands the Pleistocene aquifer contains local bodies of highly impermeable clay in the form of filled up gullies of several tens of meters depth. The resistivity of this clay was clearly distinct from the resistivity of the sandy aquifer. It was easy therefore to map the clay bodies as shown in the example of Fig.8, which is a map of the resistivity distribution at a depth of 60 m below landsurface.

CHANGES WITH TIME

The result of any resistivity survey is an instant picture. When repeating the survey some time later the distribution of resistivities may be different due to a changed composition of the groundwater in the invariable formations. The

composition of the groundwater can change due to flow. There are only few places where the changes due to flow are great enough to be determined accurately enough by repetition of the resistivity survey with intervals of one or a few years. A good example of where this was possible is the growth of the fresh water lens on the Haringvreter. The Haringvreter is an island of roughly 1.8 km × 0.7 km in the lake Veerse Meer. The Veerse Meer was formed in 1961 by the closure of a dam in the Veerse Gat, until then a tidal inlet. Before closure the Haringvreter was a sand-shoal, flooded twice a day at high tide. Since its closure the water level in the newly-formed lake is artificially controlled and the sand-shoal has fallen permanently dry. From that moment on a fresh-water lens is being built up by effective precipitation. The growth of this lens is followed annually by civil-engineering students doing their field work in this research project. The results of the 1965 survey (by Rijkswaterstaat) and the 1972 survey (by students) are presented in Fig.9. In the mean time two graduate students calculated the final shape of the lens and some transitional stages. Their calculations based on the Badon-Ghijben-Herzberg principle, yielded a maximum final depth of 14.5 m.

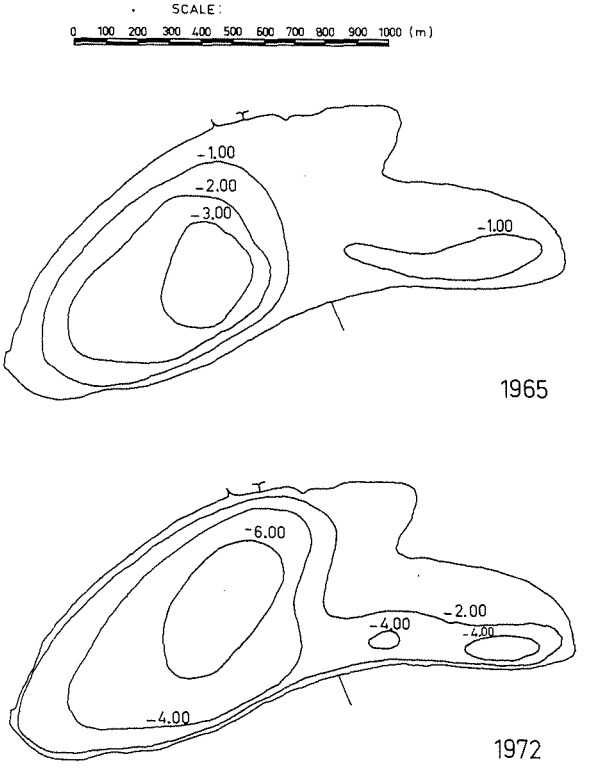

Fig.9. Depth of the fresh-water salt-water interface on the Haringvreter island. Figures in meters below lake-level.

Another possibility to detect vertical changes in the position of a fresh water—salt water interface is the installation of the salinity-watchers, mentioned earlier in this paper. These permanently installed cables have numerous electrodes in one vertical line. Any combination of four successive electrodes can be connected to portable measuring instruments at the surface. Such measurements are repeated at time intervals of say 6 months. A great number of such salinity-watchers has already been installed in the intake areas for public water supply to check the uprising of saline water. It is, so to speak, the finger on the pulse.

POSSIBILITIES AND LIMITATIONS

The examples described so far indicate clearly the possibilities of resistivity prospecting, particularly in mapping the salinity distribution and under certain conditions, indirectly, the presence of clay-layers. However, the method has its limitations.

When checking the list given in the section on Geohydrological Models one must conclude:

(1) a: Resistivity prospecting does not provide any information on the transmissibility KH. Therefore pumping-tests remain indispensable. Under favourable conditions the thickness H of an aquifer can be determined. Research is now being carried out by DGV-TNO on the relationship between the permeability and the porosity p and the formation factor F. The storage coefficients μ and S cannot be determined by resistivity prospecting.

b: The hydraulic resistance c cannot be determined by resistivity prospecting. Even if it were possible to determine d and K_v separately the practising (geo)-hydrologists would handle the c-value calculated as d/K_v with great care as the actual c-value depends greatly on the presence of leaks caused by inhomogeneities.

c: The top of impermeable layers can, under favourable conditions, be found by resistivity prospecting. Whether a layer is really impermeable can only be checked by boreholes.

(2) a: Groundwater tables can only roughly be determined by resistivity prospecting. In fact one finds the top of the capillary fringe. For calculation purposes a more accurate figure is required than resistivity prospecting can provide.

b: For the determination of salinity and hardness of the groundwater, resistivity prospecting can render good service as was illustrated by several examples in this paper.

(3) Resistivity prospecting does not provide any direct information about flow or recharge of groundwater. Data on groundwater extraction and surface water tables can only be obtained directly.

In addition to this summing up it may be worthwhile to report the following findings, both as a warning to (geo)-hydrologists and as a challenge to geophysicists:

(1) Without additional information it is impossible to distinguish between sand- or gravel-layers saturated with brackish water, and clay-layers with fresh water.

(2) In practice the vertical distribution of salinity often shows a gradual increase with depth, as appears by water sampling in boreholes and by resistivity logging. So far the interpretation of resistivity surveys is only possible in terms of a limited number of clearly distinct layers. When increasing the number of resistivity steps the accuracy could be increased so long as the principle of equivalence does not impose its restrictions to the resolving power.

REFERENCES

Dijkstra, J. and Volker, A., 1955. Détermination des salinités des eaux dans le sous-sol du Zuijderzeé, par prospecting géophysique. Geophys. Prospect., III (2).

Dijkstra, J. and Volker, A., 1958. Geo-elektrisch onderzoek op het IJsselmeer. Rapporten en Mededelingen betreffende de Zuiderzeewerken, no. 6. Staatsdrukkerij- en Uitgeverijbedrijf, The Hague.

Van Dam, J.C., 1976. Partial depletion of saline groundwater by seepage. J. Hydrol., 29: 315—339.

Van Dam, J.C. and Meulenkamp, J.J., 1967. Some results of the geo-electrical resistivity method in groundwater investigations in The Netherlands. Geophys. Prospect., XV (1).

Geoexploration, 14 (1976) 195—206

THE ROLE OF A GEOLOGIC CONCEPT IN GEOPHYSICAL RESEARCH WORK FOR SOLVING HYDROGEOLOGICAL PROBLEMS

H. FLATHE

Federal Institute for Geosciences and Natural Resources, Hannover (F.R.G.)

ABSTRACT

Flathe, H., 1976. The role of a geologic concept in geophysical research work for solving hydrogeological problems. Geoexploration, 14: 195—206.

Modern computer techniques today allow a comprehensive physical interpretation of direct current resistivity measurements. The principle of equivalence and anisotropy, however, are still a real handicap in translating the physical results into hydrogeological facts. This situation, often causing a misunderstanding between geophysicist and geologist in practice, is outlined in this paper. Some striking examples will demonstrate the importance of a geological concept in collaborations between the geologist and the geophysicist to overcome the difficulties arising from the fundamental limits of the resistivity method.

INTRODUCTION

Direct current resistivity measurements have been used for about 50 years to obtain quantitatively the resistivity distribution below the surface in a vertical direction from data registered at the earth's surface.

The four-point method proposed by Wenner (1916) and C. and M. Schlumberger (1920) was developed for routine work in the following decades for prospecting mainly a horizontally stratified underground — regarding measuring techniques and interpretation as well — and has been brought to a very high standard today. Since Slichter (1933) has shown the unique—unique relation between the surface data ρ_a (apparent resistivity) and the true resistivities ρ in the case of a horizontally-stratified earth, direct methods of interpretation (starting with Pekeris, 1940) have been proposed running parallel with a rapid development of the indirect interpretation, i.e., the theoretical computation of master curves used in combination with the so-called auxiliary point diagrams and Maillet's (1947) "Dar Zarrouk" curves (see, for example, Zohdy, 1965 and 1974). In recent years there has been a "boom" in writing computer programs so that it is rather difficult to mention the authors without missing one of them. All deal with the problem:
surface data $\rho_a \leftrightarrow \rho(z)$ vertical resistivity profile
This is the mathematical-physical aspect of the interpretation. It seems, however, that there is an important "missing link" in the step:
$\rho(z) \rightarrow$ geologic structure (lithological log)

To point out this fact, i.e., the role of a geological concept in the interpretation of resistivity measurements, is the aim of this paper.

PRINCIPLES

To understand what we are doing the fundamental principle of electrical sounding — following the classical description of Krajew (1952, German edit. 1957) — will be described in a few words illustrated by Fig.1. Let us assume two layers with the resistivities ρ_1 and ρ_2 ($\rho_2 \gg \rho_1$) divided by a plain horizontal interface at depth h. The flow of the current fed into the earth by two

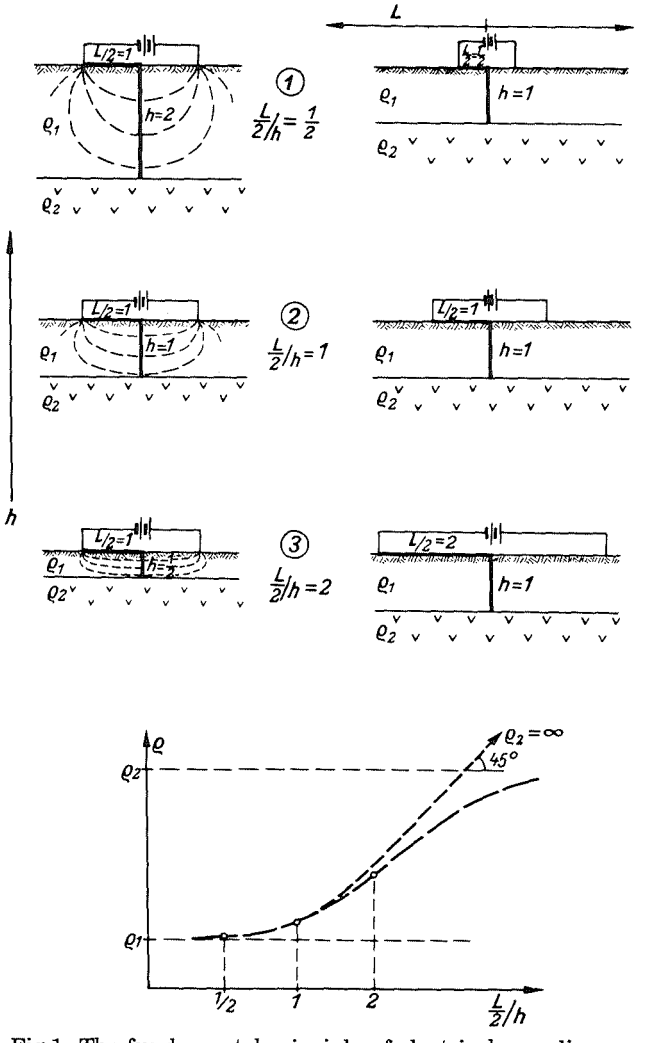

Fig.1. The fundamental principle of electrical sounding.

electrodes with a spacing L is marked by dotted lines in the underground for different values of the depth h (left side of the figure) assuming $\rho_2 = \infty$ (insulator). Decreasing h and constant L mean an increasing current density at the surface: the current density j at the surface is proportional to L/h. On the other hand j is proportional to the potential difference ΔV measured between two potential electrodes (not plotted in the figure) in the centre of the four-point arrangement. This potential difference ΔV is itself proportional to the so-called "apparent resistivity" ρ_a, i.e., ρ_a expresses the current density at the surface as a function of L/h. Because on the left-hand side of the figure L is constant and h is decreasing, on the right-hand side of the figure h is, according to the given geological situation, of course fixed. The process of "pulling up the underground" is here simulated by enlarging L. We obtain the same quotient L/h on both sides of the figure which means that from the change of the current density j at the surface, expressed in the value of the "apparent resistivity" ρ_a, the depth h of the interface between the two layers can be determined by enlarging the electrode spacing L from a sounding graph $\rho_a(L/h)$. L/h is a quotient. Thus the logarithmic scale is adequate for plotting this graph as shown in the lower part of the figure (taking $L/2$ instead of L is a convention after Schlumberger). Thinking over this process again we get the following result. The data measured at the earth's surface and plotted in log—log-scale as a sounding graph $\rho_a(L/2)$ reflect the variations in the current density at the surface* caused by enlarging the electrode spacing L, thus simulating a "pulling up" of the underground layers.

RANGE OF THE METHOD

The question which arises now is: How far can an underground layer be recognized from a sounding graph with regard to its depth, thickness and resistivity, if the accuracy of measured data is ± 5%? The author, having been confronted by this problem for the last 25 years, has tried in a series of publications (1955, 1958, 1963, 1964, 1969, 1970, 1974) to approach this problem. In collaboration with geologists and hydrogeologists he came to the conclusion that without a geological concept an interpretation of geoelectrical measurements is almost impossible if the number of layers concerned exceeds three. The resolution of sounding graphs not only depends on the classical principle of equivalence discussed with respect to the three-layer-case, but also on the relative thickness, the "effective" relative thickness and the from case-to-case changing resistivity distribution. Maillet's Dar Zarrouk curves are integrated in these considerations especially with respect to anisotropy.

To obtain a relevance to practical work concerning prospection on groundwater the large range of resistivity variations occurring in this field is demon-

* Just "below our feet" in the centre of the four-point arrangement.

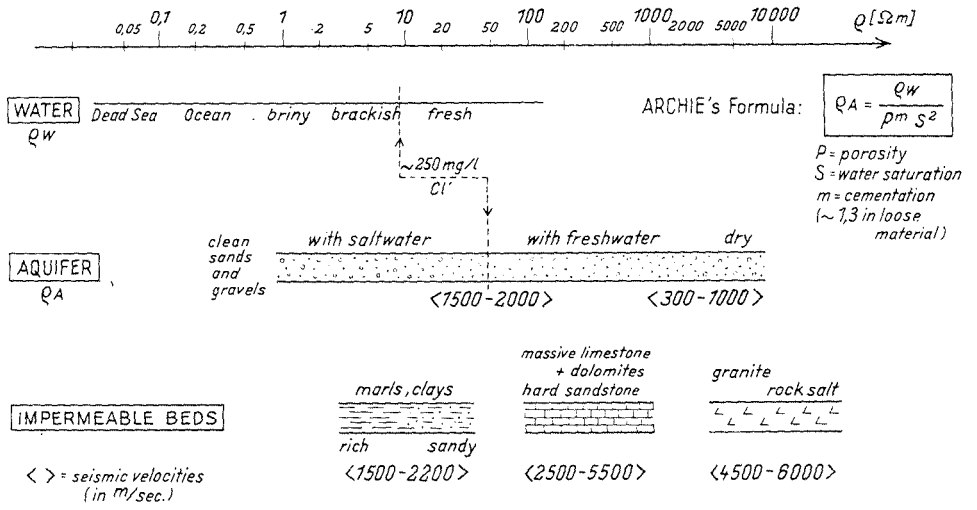

Fig.2. Electric resistivities and seismic velocities.

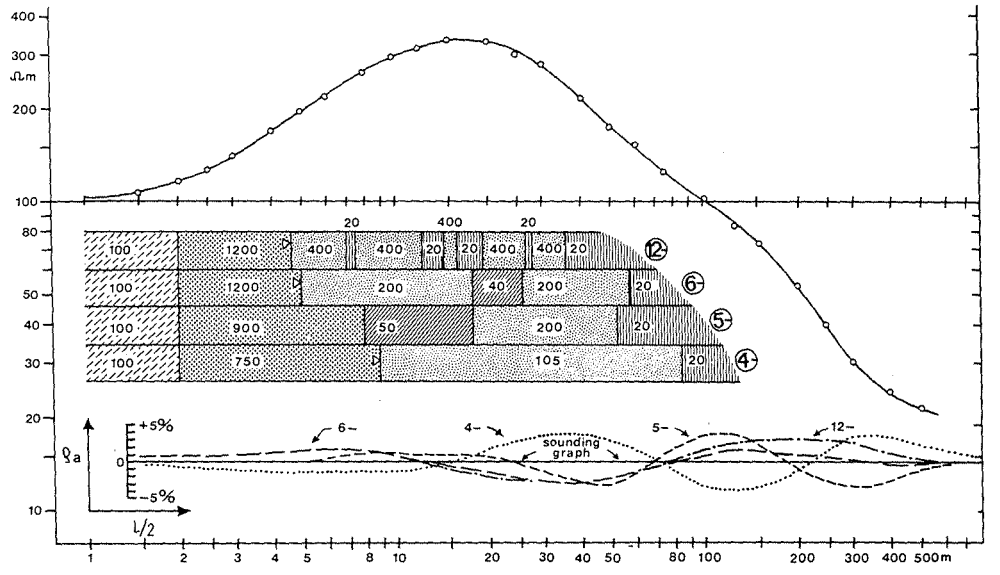

Fig.3. Geoelectrical sounding graph $\rho_a(L/2)$.
The vertical profiles plotted in logarithmic scale (using the $L/2$-scale as depth scale simultaneously) and provided with the layer resistivities in Ωm represent equivalent interpretations as 4-, 5-, 6- and 12-layer cases. The deviation of the theoretically calculated values of ρ_a from the measured data (in %) is given at the bottom of the diagram.

strated in Fig.2. The reason for only using direct current resistivity measurements in solving hydrogeological problems becomes obvious from this figure which also shows, however, where supplementary information by seismic measurements are necessary.

DISCUSSION ON THE INTERPRETATION OF RESULTS

The field data of a geoelectrical sounding usually consist of about 25 measured apparent resistivities $\rho_a(L/2)$ combined (by hand) to a sounding graph. Fig.3 shows a field result as it occurs very often in practice if below a surface layer of a few meters of dry sand with a relatively high resistivity cover, a series of aquifers, and impermeable clayey layers of unknown thickness underlain by an impermeable substratum (20 Ωm). If the hydrogeologist has no idea about the underground the geophysicist can offer him a few physically-exact solutions within the accuracy of measured data. Four of them are plotted in profiles in log scale within the figure.

(a) At first glance the sounding graph seems to represent a 4-layer case, consisting at the beginning of a dominating maximum, followed by a double descending branch. The physical interpretation — using the most simple hydrogeological model — results in dry sands (750 Ωm) below a 100 Ωm-top layer above an aquifer (105 Ωm) down to 80—85 m below surface.

(b) Assuming a near surface boulder clay (50 Ωm) and below this an aquifer (200 Ωm), we will get the 20 Ωm-substratum already at 52 m depth (5-layer case).

(c) A two-aquifer-system leads to a 6-layer case, where the separating boulder clay (40 Ωm) has its upper boundary just at the depth of its lower boundary found for the five-layer case. But not enough:

(d) Without any concept the geophysicist may offer a 12-layer case to the hydrogeologist bringing up the impermeable clayey substratum to 38 m. The chance to find water thus varies between the 38 m and 82 m depth, i.e. a difference > 100%.

After this statement by the geophysicist, in an attempt to check the content of the information in his sounding graph the geologist will draw vertical profiles in linear scale, as is done in Fig.4, and present this picture to his colleague, the geophysicist, asking him: "Why did I use the relatively expensive geophysical method to answer my questions? Can't you by means of your computer techniques distinguish between those 4 layers and these 12 layers. There *must be* a difference." The geophysicist's answer would be: "Theoretically there *is* a clear difference, but not in practice. Look at Fig.5. Here the extreme cases of the 4- and 12-layer cases are represented in their sounding graphs calculated theoretically. The field data lay in between. There is no chance to decide if I would rather have a geological concept. If you, for instance, could tell me that a two-aquifer-system is needed, then I would follow up the 6-layer case by making more measurements with this concept."

Supplementary measurements taking into account the concept of a 2-aqui-

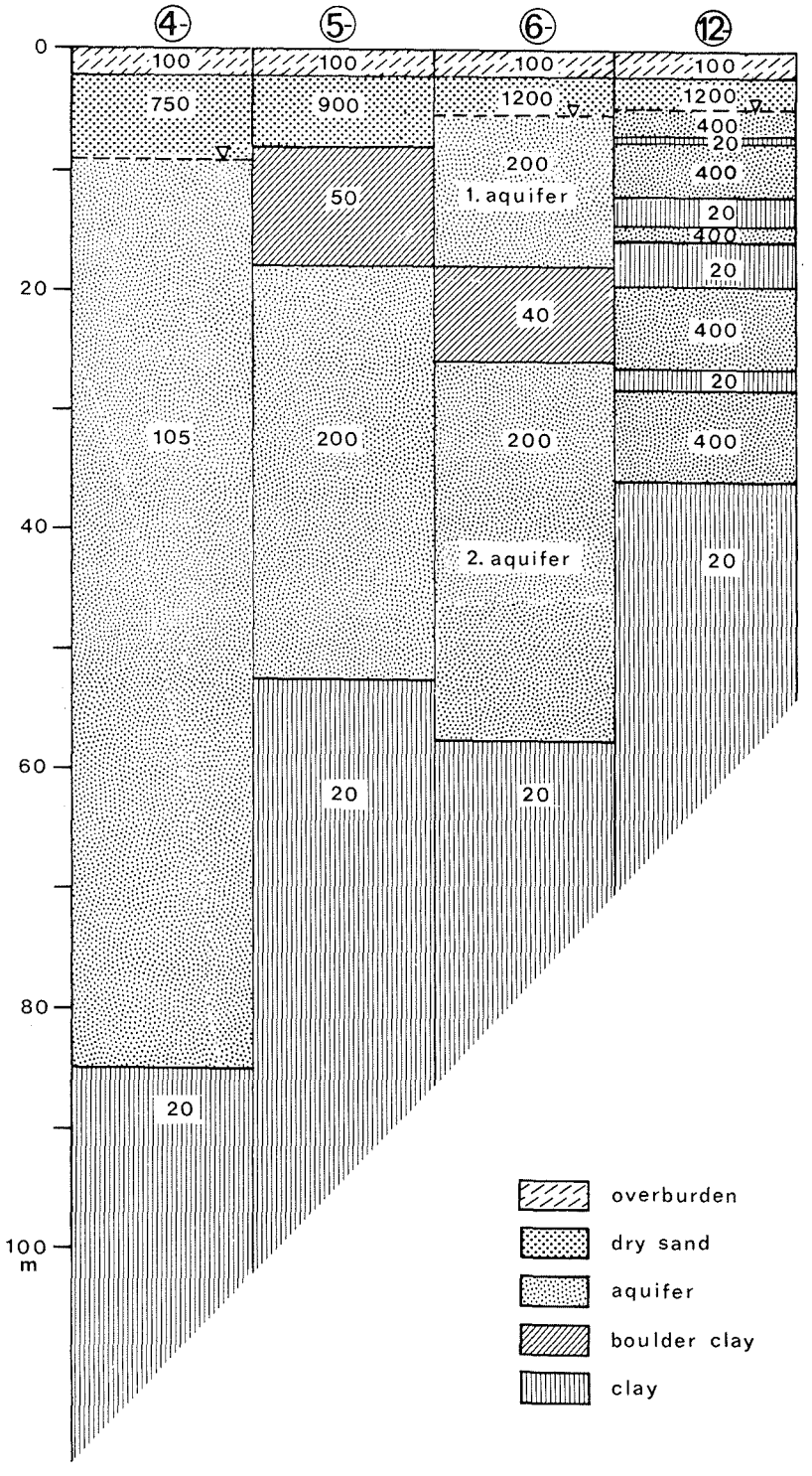
④
⑤
⑥
⑫
0
20
40
60
80
100
m
100
750
105
20
100
900
50
200
20
100
1200
200
1. aquifer
40
200
2. aquifer
20
100
1200
400
20
400
20
400
20
400
20
400
20
overburden
dry sand
aquifer
boulder clay
clay

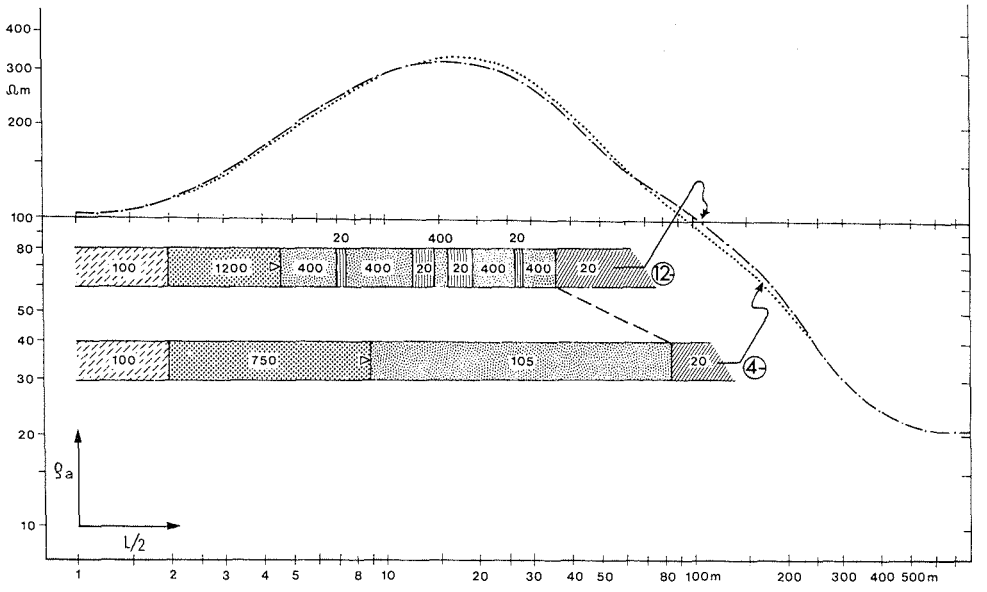

Fig.5. Theoretically calculated master curves for the 4- and 12-layer case in Figs. 3 and 4.

fer-system resulted in the sounding graphs plotted in Fig.6. From these graphs the true resistivities of the layers could be calculated. The whole result is given in Fig.7. From this it can be concluded that a discussion on a single sounding graph between the geophysicist and the geologist may lead to a quantitative result only if:

(a) the geologist gives a clear concept to the geophysicist,
(b) the geophysicist gets the chance to carry through supplementary measurements, and
(c) the concept may be confirmed by test drillings at typical soundings proposed by the geophysicist.

ANALYSIS OF RESULTS

Analysing the results it can easily be seen from Fig.5 that at least four layers are concerned.

Due to the principle of equivalence the resistivities and thicknesses of the layers within the 12-layer case cannot be calculated from the sounding graph. The resolution of the method is too weak. In the sounding graph the sequence of layers appears as a series which can in its electrical influence at the surface (i.e., variations of the current density) be replaced by two homogeneous iso-

Fig.4. Equivalent layer sequences (in linear scale) resulting from the interpretation of the sounding graph in Fig.3 (resistivities of the layers in Ωm).

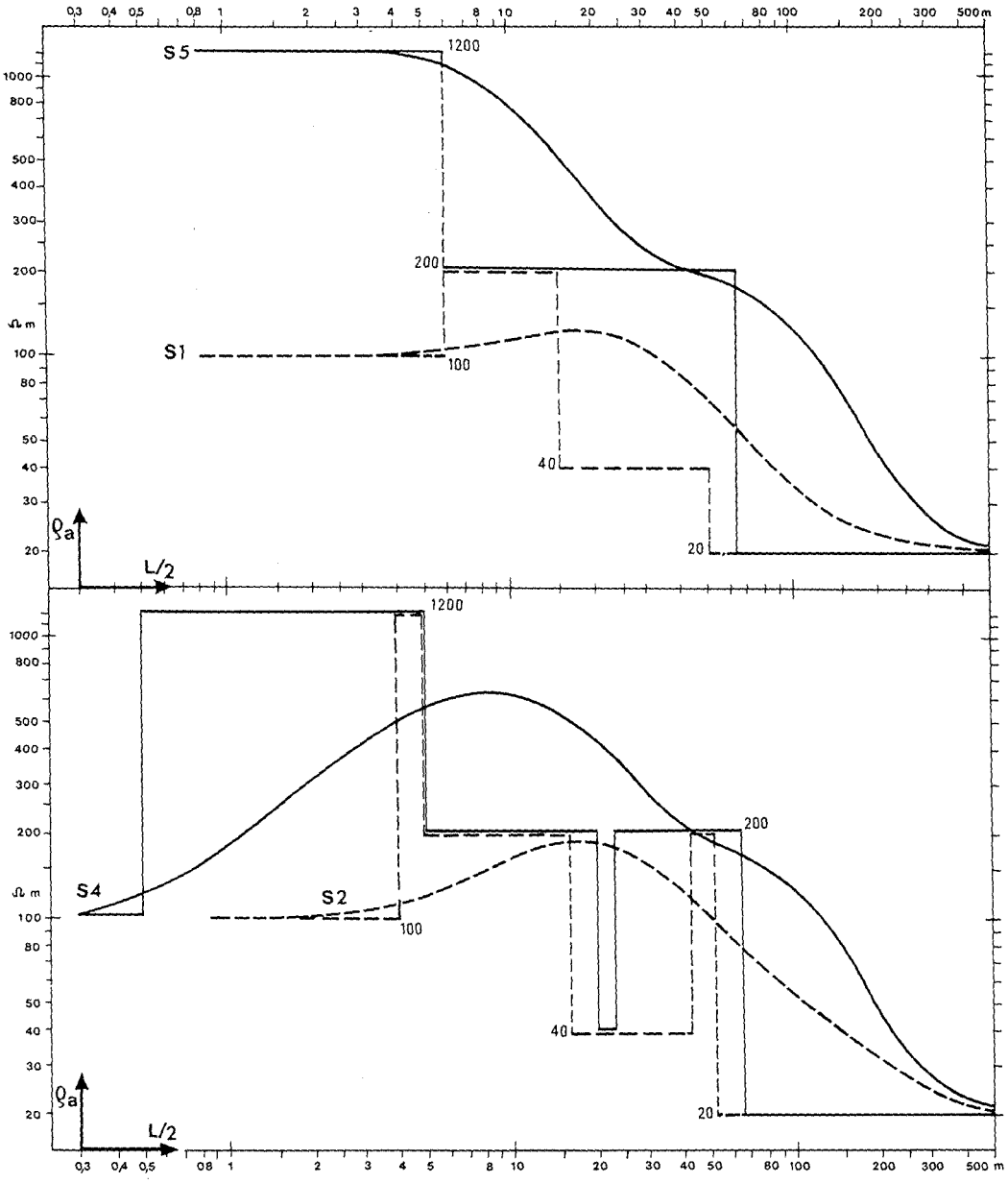

Fig. 6. Master curves calculated for the vertical profiles S 1, 2, 4 and 5 in Fig. 7. The corresponding resistivity logs are plotted using the $L/2$-scale as depth scale and the ρ_a-scale as resistivity scale, simultaneously.

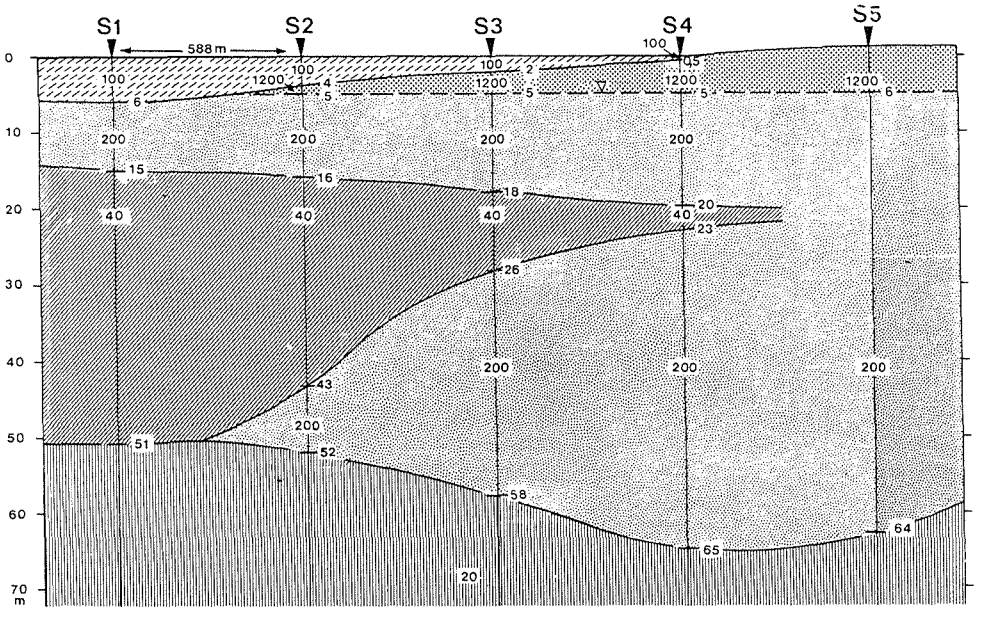

Fig.7. Vertical cross section with geoelectrical soundings S1—5 (signatures from Fig.4). The depths of the interfaces are plotted in the diagram in meters below surface.

tropic layers with resistivities of 750 and 105 Ωm (4-layer case). This, however, results in an enlargement of the thickness pushing the 20 Ωm-substratum from 36 m down to > 80 m below surface. To get the real depth of 36 m an *anisotropy* within the layer series has to be taken into account. But there is no information on the factor of anisotropy contained in the field curve. The value of this factor, which reduces the thickness of the series, has to be taken from "outside"-information, e.g. test drillings. It is obvious that just at that point where the resolution of the resistivity method begins to fail the anisotropy becomes the real problem for the geophysicist.

In borehole-geophysics we distinguish between a macro- and a micro-anisotropy of a sequence of layers. The phenomenon of anisotropy is caused by a difference in longitudinal and transversal resistivity (Maillet, 1947). Penetrating a sequence of layers the electric log within a borehole detects the macro-anisotropy, but not, however, the micro-anisotropy of a layer. The latter fact has already been observed by Maillet and Doll (1932) who have shown that only the longitudinal resistivity of a layer is contained in the formation of a resistivity log (so-called "anisotropy paradoxon"). This is the reason why resistivity data from borehole measurements cannot be used for the interpretation of surface measurements, because the latter are influenced both by the longitudinal and the transversal resistivity.

The macro-anisotropy as observed in borehole measurement has another meaning in surface measurements especially if deep soundings are concerned.

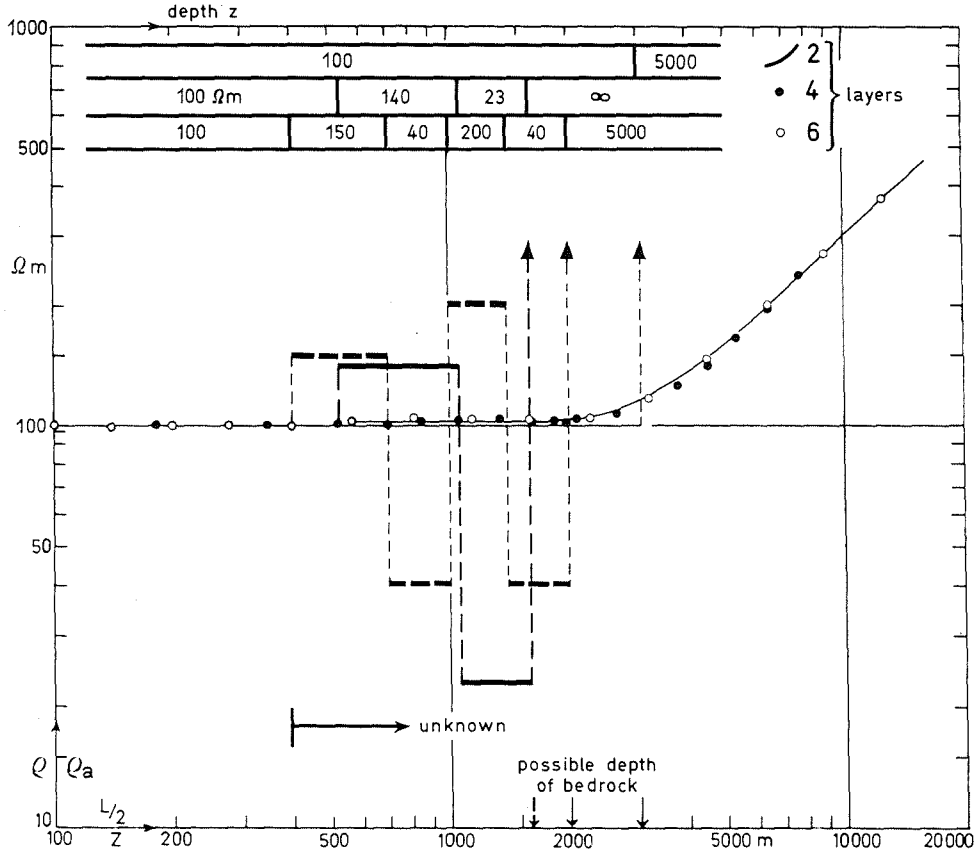

Fig. 8. Equivalent interpretation of a two-layer curve as a 4- and 6-layer curve.

In Fig.8 a sounding graph with the character of a 2-layer curve is drawn and compared with theoretical data for a 4- and 6-layer case. Within the possible measuring accuracy all three cases are equivalent. If a 3000-m deep borehole existed the electrical log would supply the macro-anisotropy and from the layer thicknesses an interpretation of the sounding graph would be possible. Having a borehole only 400 m deep, it would depend on the knowledge of the geologist whether the depth of bedrock would be expected at 1600 m, 2000 m or 3000 m in the cases plotted in the figure or at any other depth < 3000 m for other possible concepts. The sounding graph gives no information because the resolution fails; it is a two-layer curve and nothing else! The geologist thinking in linear scale (see Fig.9, left-hand side) would be surprised that such a good conducting clay (23 Ωm), 500 m thick in a depth of about 1000 m, was not visible in the sounding graph.

In Fig.9 the author compares the linear scale with a logarithmic one. Although this is mathematically not correct, a normalization with respect to

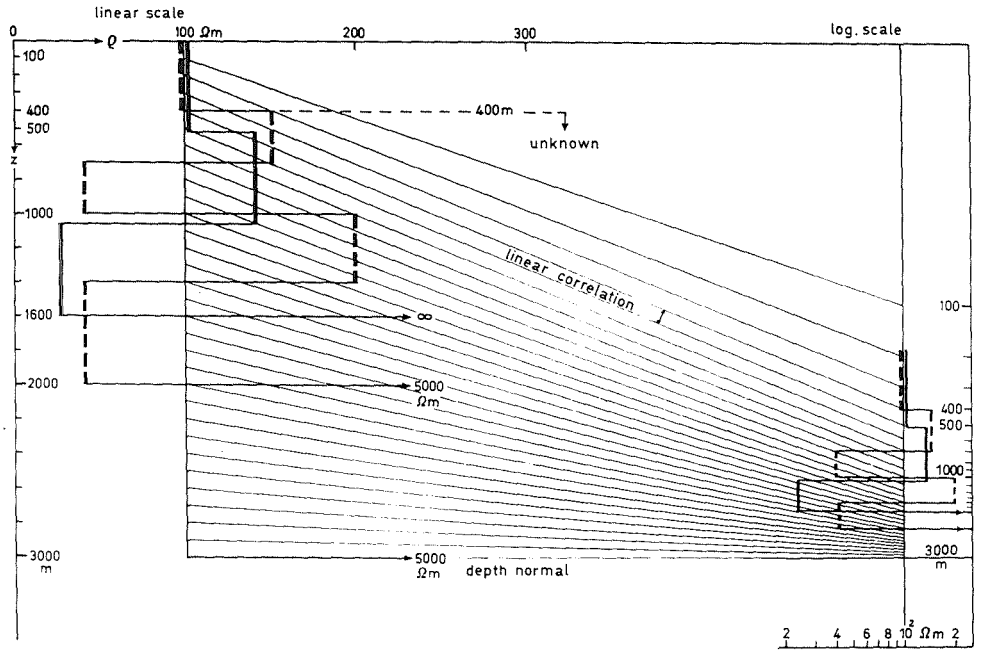

Fig. 9. Resistivity logs of layer sequences according to Fig. 8 in linear scale (left) and logarithmic scale (right).

the given situation seems to project a useful picture. This normalization was done in the following way. The interpretation of the sounding graph as a two-layer case results in a depth of 3000 m for the bedrock. This boundary has been fixed in both scales. Assuming that deeper than 400 m the underground is unknown, this depth of 400 m has been taken as a linear relation between both scales, i.e., in this depth the straight lines connecting the linear with the logarithmic scale are running parallel in this 400 m-depth range. Now from this comparison it is obvious that the macro-anisotropy of the linear scale is changed into a micro-anisotropy within the logarithmic scale thus making it impossible to recognize the individual layers in the surrounding graph of Fig. 8. One remark should be added: the anisotropy does not always increase with the number of layers in a series. The 4-layer case in our example shows a larger anisotropy than the 6-layer case.

CONCLUSIONS

This paper, in which the limits of the resistivity method have been outlined in a somewhat rigorous way, may perhaps lead to some depression with respect to the value of the method at all. Modern computer techniques, however, only provided the theoretical base for this paper; the computer is not

the means to surpass the fundamental limits of the method. The dialogue of the geophysicist and his computer should in future increasingly be replaced by the dialogue between the geophysicist and the geologist to overcome the difficulties arising by closer teamwork.

REFERENCES

Flathe, H., 1955 a. Possibilities and limitations in applying geoelectrical methods to hydrogeological problems in the coastal areas of North-west Germany. Geophys. Prospect., 3: 95—110.

Flathe, H., 1955b. A practical method of calculating geoelectrical model graphs for horizontally stratified media. Geophys. Prospect., 3: 268—295.

Flathe, H., 1958. Geoelectrical investigations on clay deposits in Western Germany. Geophys. Surv. Min., Hydrogeol. Eng. Proj., pp. 170—185.

Flathe, H., 1963. Five-layer master curves for the hydrogeological interpretation of geoelectrical resistivity measurements above a two-storey aquifer. Geophys. Prospect., 11: 471—508.

Flathe, H., 1964. New ways for interpretation of geoelectrical resistivity measurements in the search for and delimentation of aquifers. Bull. IASH, 9 (1): 52—61.

Flathe, H., 1969. The geophysicist's role in teamwork for groundwater prospecting. IHD-Expert Meeting, Budapest.

Flathe, H., 1970. Interpretation of geoelectrical resistivity measurements for solving hydrogeological problems. Min. Groundwater Geophys./1967, Ottawa, Econ. Geol. Rep., 26: 580—597.

Flathe, H., 1974. Comment on the "automatic fitting of a resistivity sounding by geometrical progression of depths. Geophys. Prospect., 22: 176—180.

Krajew, A.P., 1952. ОСНОВЫ ГЕОЭЛЕКТРИКИ. German Edit. VEB-Tech., Berlin, 1957.

Maillet, R., 1947. The fundamental equations of electrical prospecting. Geophysics, 12: 529—556.

Maillet, R. and Doll, H.G., 1932. Sur un théorème relatif aux milieux électriquement anisotropes et ses applications à la prospection électrique en courent continu. Erg. H. Angew. Geophys., III, 1.

Pekeris, C.L., 1940. Direct method of interpretation in resistivity prospecting. Geophysics, 5: 31—42.

Schlumberger, C., 1920. Étude sur la Prospection Électrique du Sous-Sol. Gauthier-Villars, Paris.

Slichter, L.B., 1933. The interpretation of resistivity prospecting method for horizontal structures. Physics, 4: 307—322, 407.

Wenner, F., 1916. A method of measuring earth-resistivity. Bull. U.S. Bureau Stand., 12: 469—478.

Zohdy, A., 1965. The auxiliary point method of electrical sounding interpretation, and its relationship to the Dar Zarrouk parameters. Geophysics, 30: 644—660.

Zohdy, A., 1974. Use of Dar Zarrouk curves in the interpretation of vertical electrical sounding data. Geol. Surv. Bull. Wash., 1313-D.

Geoexploration, 14 (1976) 207—213

APPLICATION OF ELECTRICAL RESISTIVITY MEASUREMENTS FOR THE DETERMINATION OF POROSITY AND PERMEABILITY IN SANDSTONES

D.H. GRIFFITHS

Department of Geological Sciences, The University of Birmingham, Birmingham (Great Britain)

ABSTRACT

Griffiths, D.H., 1976. Application of electrical resistivity measurements for the determination of porosity and permeability in sandstones. Geoexploration, 14: 207—213.

The paper discusses the background to and development of a method for determining porosity (and hence indirectly, permeability) in British Triassic sandstones which is based on surface resistivity measurements supplemented by data from borehole cores. The practical aim of the method is to assist in the siting of abstraction wells in the development of aquifers. The starting point is the formation factor F, defined as:

$$F = \rho_o/\rho_w$$

where ρ_o = sandstone resistivity and ρ_w = resistivity of saturating electrolyte. If clay is a minor constituent of the sandstones, current flows not only through the electrolyte but via the clay. ρ_o/ρ_w then gives F_a an apparent formation factor.

Various formulae have been devised connecting F_a and ρ_w, e.g.:

$$\frac{1}{F_a} = \sum_{i=0}^{n-1} A_i \rho_w{}^i$$

$$\log_{10} F_a = \sum_{i=0}^{n-1} A_i (\log_{10} \rho_w)^i$$

where $n = 2$ or 3 in practice, and A_i are constants.

These relationships are discussed, and examples shown of the variation of rock resistivity with pore water conductivity determined in laboratory experiments.

INTRODUCTION

As a result of the increasing need for water in Great Britain and the difficulty of developing surface sources there has been of late a greater interest in the use of groundwater. Apart from chalk the most extensively developed and useful aquifers in the United Kingdom are the Permo-Triassic sandstones.

More intensive development brings with it the need for more careful preliminary study of the aquifer. It is necessary to have as much information as

possible relating to its lateral and vertical extent, its continuity and structure, possible sources of recharge, degree of saturation and chemical quality of the groundwater and, equally important, the formation characteristics. The latter have classically been determined by geological mapping, drilling of boreholes and examination of cores, and by pumping tests. This contribution summarises recent work carried out in the Department of Geological Sciences of the University of Birmingham, the aim of which has been to see how far surface electrical techniques could be developed as an alternative or parallel approach to conventional methods, particularly for the study of intergranular porosity and permeability. The methods have developed mainly as a result of work carried out in the Fylde area of Lancashire since 1968. In a number of ways the area is ideal for a study of this nature. The aquifer of interest, the Triassic Bunter Sandstone, is virtually everywhere overlain by thick drift but even at the outset of the study a considerable number of boreholes had already been drilled, and cores were available for measurement. There are no major intra-formational marl bands and the aquifer appears to be generally hydrologically continuous. Although the evidence was uncertain fissuring did not seem to be of major importance. Pumping tests made by the Fylde Water Board suggested a wide range of permeability even over quite limited areas.

DETERMINATIONS

In the initial stages an electrical resistivity survey of the area was carried out (Worthington, 1972). In the laboratory extensive measurements were made on borehole cores of fractional porosity, intergranular permeability and electrical resistivity (Barker and Worthington, 1973).

The electrical resistivity soundings were made with a Wenner electrode system and the data reduced using the tripotential method of smoothing developed by Habberjam (1967). In general it was possible to map the base of the drift (up to about 30 m thick) and to obtain satisfactory resistivities for the Bunter Sandstone. Where practicable the expansions were extended to determine the thickness of the sandstone, at least 120 m, and in some places greater than 200 m. Marked lateral changes in resistivity were noted in the sandstone, sometimes over a distance of less than 1 km.

Electrical logging of boreholes revealed large variations of resistivity with depth, although these appeared to be mainly confined to relatively thin layers. The surface soundings in general revealed no well-defined resistivity interfaces within the Bunter, so in any one area it seems probable that marked resistivity variations are on a small scale, perhaps mainly the result of random variations due to local layering. The resistivity obtained from the surface measurements is therefore reasonably representative of the formation. In fact the average longitudinal resistivity of 79 Ωm, calculated from a borehole log, showed excellent agreement with a value of 80 Ωm interpolated from the results of five nearby surface soundings (74, 104, 94, 65 and 82 Ωm).

Measurements on samples showed that the Bunter Sandstone is electrically

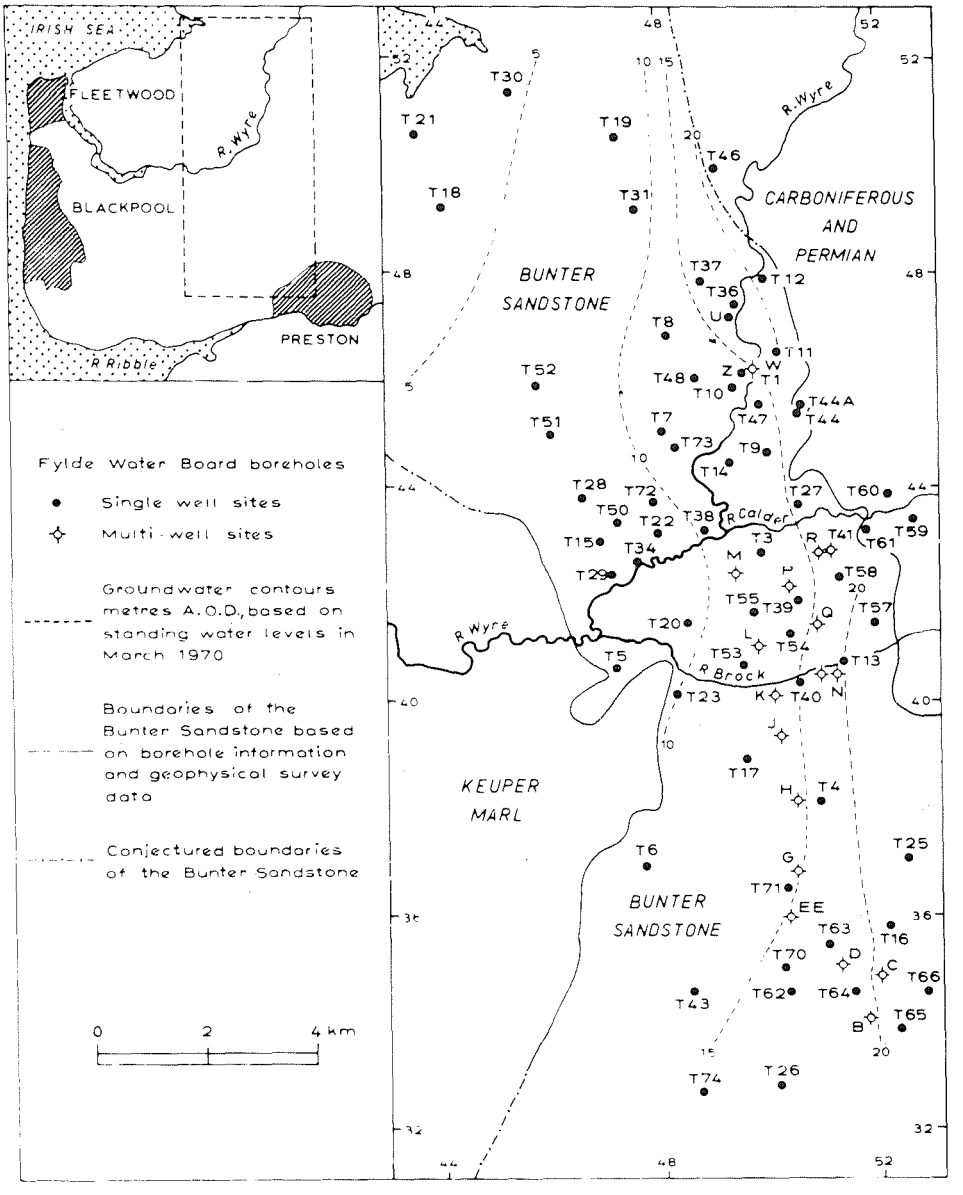

Fig. 1. The Fylde, Lancashire, showing the sub-drift geology and borehole locations. (From Worthington and Griffiths, 1975, with permission.)

almost isotropic, but there is significant hydraulic anisotropy.

Information on water quality was available from borehole data. Fig. 1 shows the geology, borehole positions and water-table contours. For the most part electrolyte content varies smoothly over the area and can be interpolated at any point with a fair degree of confidence.

BACKGROUND

For saturated unfissured sandstones which are "clean" (i.e., in which there is no solid conducting cement or matrix and electrical conduction takes place only through the electrolyte in the pores) Archie (1942) defined a quantity known as the "formation factor" as:

$$F = \rho_o/\rho_w$$

where ρ_o is the resistivity of the saturated sandstone and ρ_w the resistivity of the saturating solution. Furthermore, the formation factor has been found to be related to fractional porosity ϕ by an equation of the form:

$$F = a/\phi^m$$

where a and m are constants for a given formation that can be determined by laboratory measurements on samples. For example, Barker and Worthington (1973) have determined $a = 1.05$ and $m = 1.47$ for the Bunter Sandstone in the Fylde. In certain sandstone formations a somewhat less well-defined relationship exists between formation factor and permeability K. This has the form:

$$F = E/k^l$$

where E and l are constants for the formation (for the Bunter Sandstone, $E = 3.3$, $l = 0.17$, see Barker and Worthington, 1973).

In principle, therefore, a method is available for deriving permeability from surface resistivity measurements and values of groundwater conductivity. There are, however, certain practical difficulties. The first is in the determination of the formation factor. The Bunter Sandstones are clay-bearing; thus conduction takes place by two paths, through the clay, and through the electrolyte, so the formation factor (defined above) is not a true but an apparent value. Before F can be used to derive porosity or permeability some method of correcting this "apparent" formation factor F_a to a "true" value must be found. Various methods have been tried. Worthington and Barker (1972) give three possible expressions relating F_a and ρ_w:

$$F_a = \sum_{i=0}^{n-1} A_i \rho_w^i \tag{1}$$

$$\log_{10} F_a = \sum_{i=0}^{n-1} A_i (\log_{10} \rho_w)^i \tag{2}$$

$$\frac{1}{F_a} = \sum_{i=0}^{n-1} A_i \rho_w^i \tag{3}$$

where n = 2 or 3, A_i are constants, and ρ_w = electrolyte resistivity. Experiments were carried out on a range of sandstone samples saturated with various concentrations of saline solution. It was shown that eq.1 did not fit the data well. Eq.2 is basically the expression used by Hill and Millburn (1956). They made the reasonable assumption that as the conductivity of the electrolyte in the pores increased the relative contribution of conduction through the clay matrix would decrease. Consequently the true formation factor, they considered, could be defined as $F_a = F$ when $\rho_w = 0.01\ \Omega m$. If one substitutes $A_0 = \log_{10}F + 4b$ and $\rho_w = 0.01$ then:

$$\log_{10}F_a = \log_{10}F + b\,(\log_{10}100\rho_w)^2$$

where b is a constant for the sample, and a measure of the matrix conduction. For reasons given by Worthington and Barker this formula was found to have certain limitations when applied in the Fylde area. The best results were obtained with the third expression. For n = 3 the second order coefficients were found to be small, and the linear fit (n = 2) was felt to be acceptable. This is essentially Patnode and Wyllie's (1950) formula:

$$\frac{1}{F_a} = \frac{1}{F} + A\rho_w$$

DISCUSSION

According to Patnode and Wyllie conduction through the matrix is unaf-

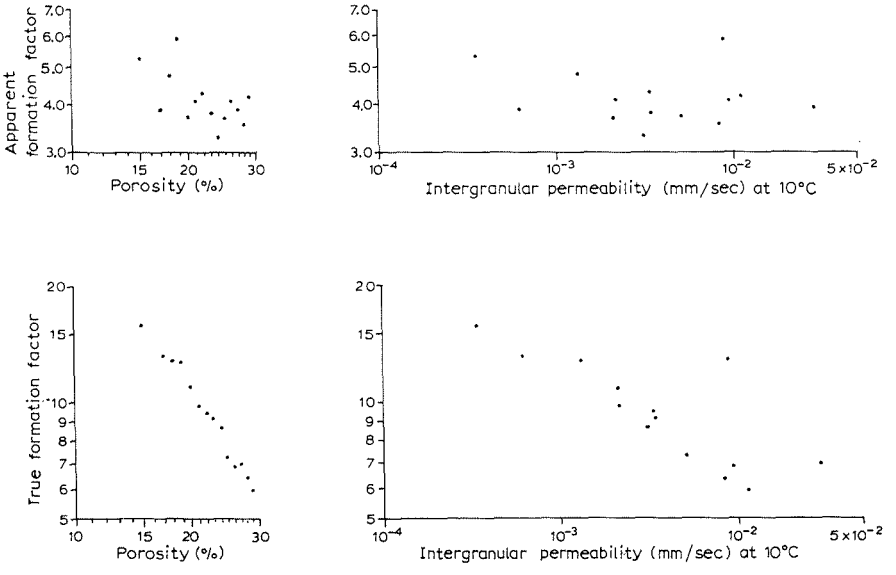

Fig. 2. Variation of true and apparent formation factor with porosity and permeability for samples from the Bunter Sandstone of the Fylde. (From Worthington and Griffiths, 1975, with permission.)

fected by electrolyte concentration (i.e., A is a constant). The total resistance is thus the sum of two resistances in parallel, one due to the matrix, the other to conduction through the pore fluids. The formula implies a straight line relationship between $1/F_a$ and resistivity, the intercept at $\rho_w = 0$ giving the "true" value of F. In fact the relationship is not strictly linear and the assumptions may well not be entirely correct. However, in practice extrapolation back to the axis does give adequately accurate values of F.

Fig. 2 shows the relationship of both the apparent and the true formation factor to porosity and permeability for 14 samples from 3 boreholes. The correlation is excellent between the correction formation factor and both porosity and permeability, but not significant before correction.

In theory we can now determine intergranular porosity and permeability if we know the formation resistivity, groundwater conductivity, and have sufficient information from borehole samples to interpolate everywhere a satisfactory value for the matrix conductivity, since we can then calculate the "true" formation factor.

The following example from Worthington and Griffiths (1975) illustrates the method. Fig. 3 shows an area in the Fylde where the physical properties of the sandstone are known to vary considerably over short distances. A number of wells had already been drilled and pump tested. Hydraulic conductivity at T9 had a value of $4.6 \cdot 10^{-3}$ mm sec^{-1}.

Interpolating values from surrounding wells gives $2.5 \cdot 10^{-2}$ mm sec^{-1} which we know to be an overestimate.

Let us suppose that T9 had not been drilled, and we wish to estimate the hydraulic conductivity by geophysical methods. Depth averaged values of the matrix conductivity obtained by measurements on samples from the sur-

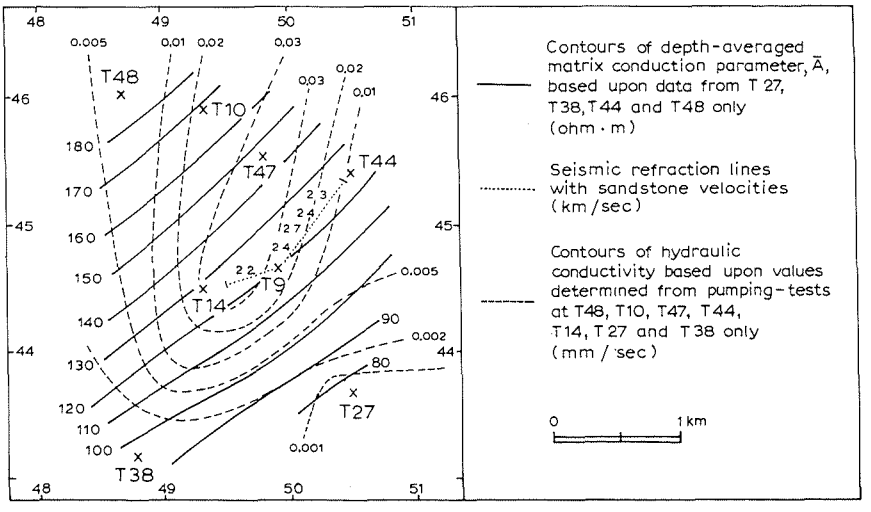

Fig. 3. Location of wells in the vicinity of T9 and data used in the calculation of hydraulic conductivity. (From Worthington and Griffiths, 1975, with permission.)

rounding wells were used to contour and interpolate a value for this parameter at T9, of 120 Ωm. Groundwater resistivity at the site is 20 Ωm, and the surface measured resistivity at T9 is 67 Ωm. Using the formula of Patnode and Wyllie leads to an apparent formation factor of 3.35. The true formation factor is calculated as 7.6, from which a value of $7.4 \cdot 10^{-3}$ mm sec^{-1} is obtained for the hydraulic conductivity. This is considerably better than the directly interpolated value. Although it has been possible to make only a few tests of this kind they do suggest that in suitable conditions the method could prove to be useful. The range of permeabilities, as measured on samples in the Fylde, is from 10^{-5} to $5 \cdot 10^{-2}$ mm sec^{-1}. Pumping tests indicate values from $3 \cdot 10^{-4}$ to $1.0 \cdot 10^{-1}$ mm sec^{-1}.

If sandstone resistivity, matrix conduction factor and water conductivity can be determined to within 10%, then the error in the permeability determination is not likely to be greater than perhaps half an order of magnitude, considerably less than the full range observed. However, it must be stressed again that the approximations involved in the calculation are considerable. An "average" value of resistivity for the whole formation is being used, and the true formation factor calculated using averaged and interpolated values of the matrix conduction factor. Equally important the formation factor/permeability relationship is only approximate.

REFERENCES

Archie, G.E., 1942. The electrical resistivity log as an aid in determining some reservoir characteristics. Trans. Am. Inst. Min. Metall., Eng., 146: 54—62.

Barker, R.D. and Worthington, P.F., 1973. Some Hydrogeophysical Properties of the Bunter Sandstone of north-west England. Geoexploration, 11: 151—170.

Habberjam, G.M. and Watkins, G.E., 1967. The Reduction of Lateral Effects in Resistivity Probing. Geophys. Prospect, 15: 221—235.

Hill, H.J. and Milburn, J.D., 1956. Effect of clay and water salinity on electrochemical behaviour or reservoir rocks. Trans. Am. Inst. Min. Metall. Eng., 207: 65—72.

Patnode, H.W. and Wyllie, M.R.J., 1950. The presence of conductive solids in reservoir rocks as a factor in electric log interpretation. Trans. Am. Inst. Min. Metall. Eng., 189: 47—52.

Worthington, P.F., 1972. A geoelectrical investigation of the drift deposits in north-west Lancashire. Geol. J., 8(1): 1—16.

Worthington, P.F. and Barker, R.D., 1972. Methods for the calculation of true formation factors in the Bunter Sandstone of north-west England. Eng. Geol., 6: 213—228.

Worthington, P.F. and Griffiths, D.H., 1975. A strategy for the application of geophysical methods in the exploration and development of sandstone aquifers. Q.J. Eng. Geol., 8(2).

Geoexploration, 14 (1976) 215—228

THE COMPARISON OF SOUNDING RESULTS AND THEIR INTERPRETATION IN THE ABSENCE OF BOREHOLE CONTROL

G.M. HABBERJAM

Department of Earth Sciences, University of Leeds, Leeds (Great Britain)

ABSTRACT

Habberjam, G.M., 1976. The comparison of sounding results and their interpretation in the absence of borehole control. Geoexploration, 14: 215—228.

Resistivity sounding curves are first examined as a site characteristic and the 'association parameter' defined as an objective assessment of site differences. Magnitudes of this parameter are examined and its use to investigate structure indicated. The use of an appropriate 'window of comparison' to limit surface variations, and the use of the L.I.I. to screen uncharacteristic sounding results, are discussed.

Resistivity curves as profiles of four electrode resistivity space are then considered, with the problems of sounding interval and orientation dependence, in constructing resistivity space sections. The use of such sections for indicating favourable sites for depth interpretation is stressed.

The form of some theoretical square array resistivity spaces is then considered. Layered medium resistivity spaces can readily be generated for the square array using the normal curve calculation procedures, or, to a close approximation, Schlumberger curves can be plotted at the equivalent square array spacing. The dipping interface problem has also been calculated for the extremes of square array orientation and these results are summarised by the β—J locus presentation. From the β—J locus, the corresponding resistivity space is quickly recovered. Full spatial solutions for the square array have also been derived for the outcropping vertical dyke problem. Observed spaces seldom correspond to such simple models, but regions of the observed space may frequently correspond to them.

INTRODUCTION

If orientation effects are ignored, a sounding curve of apparent resistivity against electrode spacing can be considered to provide a description of the site occupied by the sounding.

Direct comparisons between sites can thus be made on the basis of the observed sounding curves. Since with the commonly used configurations (Wenner α; Schlumberger or square), resistivities are only negative on extremely rare occasions, the $\log_{10}$ measure of resistivity is generally useful, and has the merit that percentage changes in resistivity are not influenced by the resistivity magnitude.

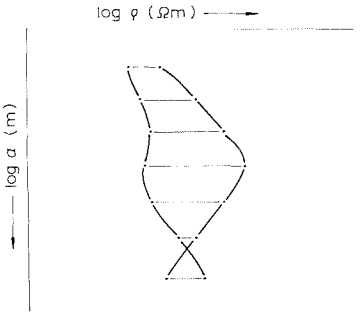

Fig. 1. Log/log representation for comparison of two soundings.

The spacing, likewise, is also positive and can range (theoretically) from the infinitesimal to the infinite, so that again a $\log_{10}$ scale is appropriate. The normal log/log presentation used for interpretation is therefore also suitable for normal sounding display and spacing is normally increased by a constant factor. See Fig. 1.

Soundings at two sites, i and j, conducted using the same pattern of spacing expansion (constant factor, or nearly so), can be effectively compared by correlating on the basis of these logarithmic variables. This may be summarised in the 'association parameter', A_{ij} defined as:

$$A_{ij} = \frac{1}{n+1} \sum_{r=0}^{r=n} [\log_{10} \rho(a_{r,i}) - \log_{10} \rho(a_{r,j})]^2$$

where, $\rho(a_{r,i})$ is the resistivity on the r-th spacing (a_r) at site i, etc. A_{ij} has the particular significance that (1) it is zero only if the sounding curves at i and j are alike, both in form and magnitude, and (2) that a percentage variation at low resistivity levels is as great as at high resistivity levels.

Consistent observational discrepancies of 2% in reoccupying a single site, would yield:

$$A_{ii} = \frac{1}{n+1} \sum_{r=0}^{r=n} [\log_{10} 1.02]^2 = 0.00007$$

Although earth resistances are commonly measured to a higher precision than this, discrepancies in reoccupation also arise from repositioning of electrodes, and unless special location precautions are taken, reoccupation can commonly yield an A_{ii} value of 0.0001.

(Although developed here as a site comparison index, the association parameter is also of importance in assessing the 'goodness of fit' between an observed field curve (o) and a master or calculated curve (c). Clearly if A_{oc} is less than A_{ii}, curve fitting is being carried beyond its useful limit.)

As against this minimum level, if contrasts within an area can be as great at 100, maximum A_{ij} values of 4 could occur. A wide scale of comparison is thus possible.

WINDOW OF COMPARISON

Clearly, a practical sounding only samples apparent resistivity over a limited range of spacing ($a_0 \rightarrow a_n$, say) and, for computation of A_{ij} values, sampling within this range should be at constant logarithmic intervals (i.e., a constant expansion factor should be used and the square array factor of $\sqrt{2}$ is adequate). In comparing soundings the full observed range $A_{ij}[a_0,a_n]$ or a partial range $A_{ij}[a_p,a_q]$ can be used. The spacing range can be regarded as the window of comparison and, if desired, the range of larger spacings $a_q \rightarrow a_n$ could be used to examine likeness at depth only.

THE USE OF LIKENESS DIAGRAMS

The association parameter can be used on raw sounding data in a preliminary search for geological symmetry.

Thus, considering a line of soundings disposed as in Fig. 2 over a 'two-dimensional' structure (it is assumed that the soundings are conducted as collinear soundings parallel to the strike), it will be apparent, that certain 'like' sites exist, e.g. sites 1, 5 and 7.

Adopting a criterion of 'likeness', two sites will be considered 'like' if $A_{ij} < C$ (a small constant); the complete results of sounding comparison can be represented on a likeness diagram, Fig.3, where basic symmetry elements can be seen.

Thus, in squares 1—5 the simple cross-pattern is compatible with a simple fold, the block of square 8—11 with uniform ground, and squares 6 and 7 with fault repetition (note also the small pseudo-cross of squares 5—7, where the fault has produced a small cross which could be misinterpreted as a fold).

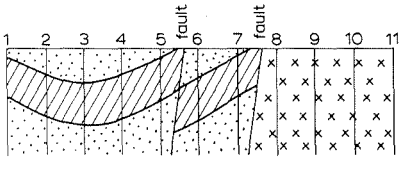

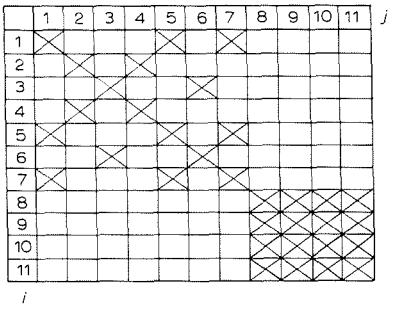

Fig. 2. Geological section (vertical scale exaggerated).

Fig. 3. Likeness diagram showing the results of sounding comparison.

The main function of such diagrams is to assist in dividing the sounding results into groups before subsequent interpretation (say by normal curve matching), where ambiguity can lead to improbable solutions.

The diagram can also be of more direct help, as indicated by the correspondence of rows 1—3 of the diagram, with the actual section.

LIKENESS PROFILES

An alternative to the above procedure is to construct profiles of A_{ij} for each row of the likeness diagram (i fixed). See f.i. Fig. 4.

On the previous example, it would be expected that A_{13} would be approximately the same as A_{16}, whereas here it can be seen that A_{16} is much larger. This could arise if the line of sounding 6 was affected by the fault 5/6. This could show on the L.I.I. value from sounding 6 if it were carried out using the tripotential system (Habberjam and Watkins, 1967).

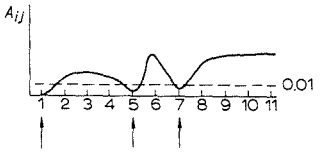

Fig. 4. Profile of A_{ij} for each row of Fig. 3 with i fixed.

Essentially here, orientational variation is destroying likeness and the L.I.I. can be used to diagnose the offending site. In examining a traverse of soundings, it may thus be profitable to exclude sites having large L.I.I. values in the main search, although soundings at such sites would remain of local interest.

Such likeness profiles can also be helpful in relating isolated sounding sites to a master sounding traverse in order to test which site on the master traverse most closely resembles the isolated sounding.

GENERAL SEARCH METHOD

In examining a group of soundings by such methods, three stages should be considered.

(1) Likeness diagrams can be produced for the 'full' range of spacings. In our criterion of likeness ($A_{ij} < C$), C is set at various levels and the corresponding patterns examined. Obviously, low C values would be desirable, but extreme likeness will only exist in very intensive work. On the other hand, high C values will mean that unlike sites may be grouped together.

(2) If it is apparent that surface cover is unconformable with the main structure of interest, comparison based only on the larger spacings may be used.

(3) If high L.I.I. values are encountered, these sites can be omitted in examining likeness (the A.I.I. could similarly be used with square soundings).

RESISTIVITY SPACE SECTIONS

The likeness technique is strictly applicable to any group of soundings, but the search for symmetry is obviously aided when a traverse of soundings is initially used. When such traverses are sufficiently intense for usable likeness patterns to emerge, it will generally be profitable to construct a resistivity space section. On such a section each sounding result is entered at a vertical depth equal to its spacing directly below its location and iso-resistivity contours constructed. Such a space section should, of course, be constructed using a single configuration but, even so, it will not be unique unless a constant array orientation has been used (in which case the space relates to that orientation), *or* unless an orientationally invariant sounding technique has been used.

Tactically, it is frequently inconvenient to carry out constant orientation soundings and, furthermore, even when these are carried out strike directions can vary in relation to a given traverse and these changes can make subsequent interpretation difficult.

Using the square array (preferably in its modified version; Habberjam, 1975), estimates can be made of the extent of orientational variation and, if this exceeds the required limits, crossed square soundings can be used.

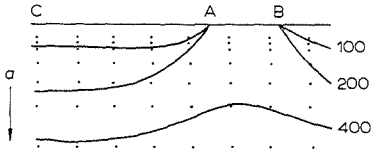

Fig. 5. Example of a resistivity space section diagram.

On an observed space section, Fig. 5, regions such as A and B, where the contours are steep, can be expected to develop large A.I.I. values, whilst site C with flat contours would appear suitable for depth interpretation, provided that A.I.I. values are low (implying that cross dips are low).
are low).

SOME THEORETICAL SQUARE ARRAY SPACES

Although Schlumberger sounding data can be used for the interpretation of square array soundings, it would be helpful if some basic square array space distributions were known for elementary models.

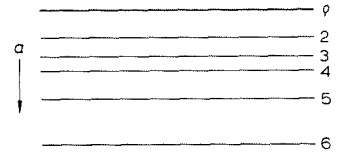

Fig. 6. Horizontal layer space.

The form of the horizontal layer space consists of contours parallel to the surface and can be readily calculated. Alternatively, and within normal drafting accuracy, a Schlumberger master curve can be used to provide a square array space if its resistivity value ρ_s corresponding to the Schlumberger spacing s is plotted at the square array spacing $a = s/1.17$.

DIPPING INTERFACE

Solutions for the dipping interface problem have been published (Broadbent and Habberjam, 1971).

Basically, a single interface in real space produces a pattern of plane contours converging on the line of outcrop in resistivity space (just as with the two-electrode configuration). See Fig. 7. The form of these spaces has been summarised in Fig. 8 by a polar plot of J against β, for different values of α and k, for the two extremes of orientation (θ) of the square array.

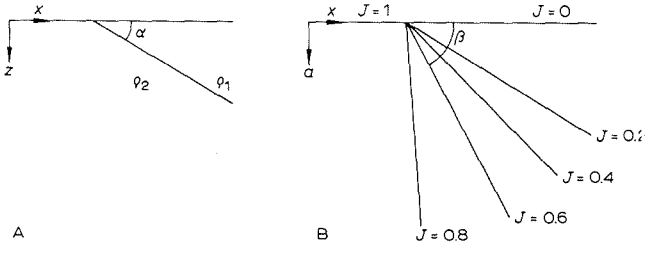

Fig. 7. A. Real space resistivity distribution, $k = (\rho_2 - \rho_1)/(\rho_2 + \rho_1)$. B. Apparent resistivity space. For the contour of the angle β the apparent resistivity $\rho = \rho_1 + J(\rho_2 - \rho_1)$.

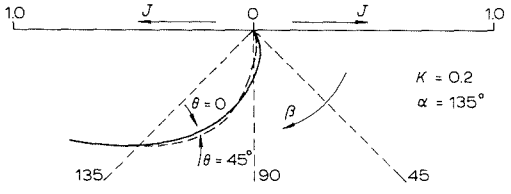

Fig. 8. The β-J locus.

From these curves, the corresponding square array spaces can quickly be constructed.

Resistivity spaces for the outcropping vertical dyke problem have also been worked out (Broadbent, 1970).

Although these space distributions give an insight into the form of apparent resistivity space, practical problems are usually more complex. However, convergences due to outcropping beds are often observed.

INTERPRETATION SYSTEMS FOR SPACE SECTIONS

1. Qualitative interpretation

Before applying quantitative assessments, the observed resistivity section may be of very direct assistance in geological interpolation. This is evidenced in Fig. 9, where the linking of two exposures in a synclinal structure is apparent.

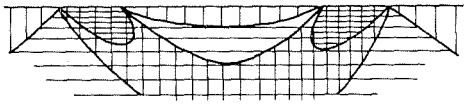

Fig. 9. Diagram showing the apparent linking of two exposures in a synclinal structure.

2. Horizontal layer solutions

These may legitimately be used when the space contours are reasonably flat within a region corresponding to about twice the maximum spacing used (this should also be confirmed by low A.I.I. values, as before). The problems of interpretation are then the normal problems of equivalence and suppression which cannot be resolved without borehole control.

In seeking a solution, in the absence of borehole control, we can only seek *a* solution which will account for the observed space, rather than *the* solution (the actual space), as the latter may be beyond the resolution of the method. Unjustified complexity of solution should thus be avoided by seeking a minimum parameter solution for each sounding. This involves, in curve matching and auxiliary point techniques, not using a four-layer interpretation where a three-layer one will do. Here some criterion of adequacy of fit is required and this can be done by first calculating the layered curve for the solution derived and comparing it with the observed curve, using the association parameter. Clearly, if this lies within the limits which can arise from orientational variation, a more complex solution is unjustified on the basis of a single sounding.

A problem still arises, however, where the results from several soundings are assembled, in that the interpolation between successive soundings — unless very close together — may be obscure. For general use the following

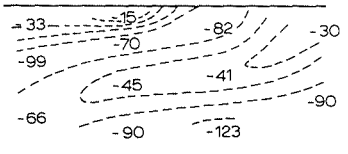

Fig. 10. Contours of "true" resistivity values.

procedure is suggested. The derived resistivity for each layer is plotted vertically below each sounding location at a depth corresponding to the mid-point of the bed and the lowest 'layer' (extending to infinity), is plotted at a depth below its upper surface equal to half its cover. This distribution of 'true' resistivity values is then contoured.

This represents an attempt to explain the observed resistivity space in terms of a distribution of true resistivity in the subsurface. Apart from the assumption of stratification to obtain depth solutions, no geological postulates are involved in this process and the solution is thus unbiased by geological information. Interpretation can be extended, if such information is available, but in a drift covered area none may exist.

Such a solution will commonly only be *a* solution because even within the minimum parameter context ambiguity exists. Some simplification of the contour pattern can sometimes be effected by re-examining isolated sounding results.

Automatic procedures

As an alternative to seeking sounding solutions in terms of depths and resistivities of layers, several automatic procedures have been suggested where, for a fixed succession of layer thicknesses, resistivity successions are derived which correspond to the observed curve. In particular, even bed thicknesses can be proposed which, if sufficiently thin, can approximate any resistivity succession. This is shown in Fig. 11A, where t is the layer thickness. With this type of solution, ambiguity again asserts itself and many solutions are possible. It would appear that we are trying to extract too much information from the resistivity curve. Fig. 11B shows a distribution used by Marsden (1973) which effectively proposes a logarithmic increase of thickness. In Marsden's model, the initial bed thickness t may be either fixed or allowed to acquire its best value. Clearly, there is little point in seeking depth solutions beyond the maximum spacing used and Marsden's sequence is thus limited to layers whose mid-point is less than the maximum field spacing.

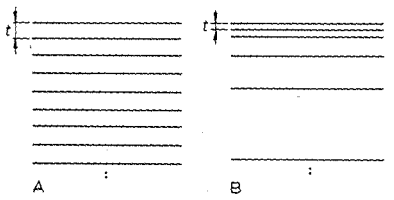

Fig. 11. Examples of layer systems used to achieve sounding solutions.

Although the Marsden technique fits a more limited number of variables, it is still subject to some ambiguity when layers of resistivity substantially greater (or less) than their surrounding beds are encountered. In this respect it is a compromise solution in that in certain cases higher resolution is possible.

Having obtained solutions from a traverse of soundings these can again be contoured in the manner previously described.

In recent trials, using both auxiliary point and Marsden fittings, it was found that qualitatively similar results were obtained for an extensive resistivity section using both techniques, but that the Marsden technique gave shallower and more contrasting solutions. This finding is perhaps not surprising when one considers the natural desire to keep contrasts in auxiliary point solutions to a minimum.

Both solutions were considered satisfactory, as the association parameters were in all cases brought to low levels (A r.m.s. for the Auxiliary point technique was 0.0006 and the corresponding A r.m.s. for the Marsden technique was 0.0007).

Orientational effects were small in this area, the maximum observed A.I.I. being less than 0.4 from which the maximum A value *arising from orientational variations should be less than 0.0003.*

3. Complex resistivity spaces

When the observed resistivity space is no longer flat, appeal must be made to other model solutions of which the dipping interface or outcropping vertical dyke are of limited use only. Although, as yet, these are the only models available for square array resistivity space, their usefulness can be extended considerably to complex two-dimensional models by the use of Composition Rules.

These rules and the approximations involved are discussed in detail by Habberjam and Jackson (1974).

Rule 1. Concerns combining two resistivity spaces when the contrast surfaces do not intersect one another on being combined.

Consider two separate subsurface models of the true resistivity distribution representing vertical interfaces (Fig. 12).

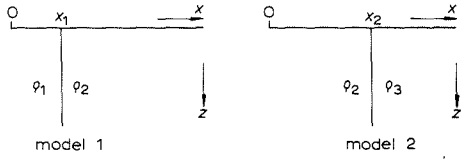

Fig. 12. Two subsurface models of the true resistivity distribution (vertical).

For model 1 the resistivity at any point is $\rho(x,z)_1$, and clearly:
$\rho(x,z)_1 = \rho_1$, for $x < x_1$, and $\rho(x,z)_1 = \rho_2$, for $x > x_1$.
This space can be represented in normalised form as:
$\rho(x,z)_1/\rho_1$ (= 1, for $x < x_1$), (= ρ_2/ρ_1, for $x > x_1$).
Similarly model 2 yields:
$\rho(x,z)_2/\rho_2$ (= 1, for $x < x_2$), (= ρ_3/ρ_2, for $x > x_2$).

If these normalised spaces are multiplied together they will yield a new space, $rho(x,z)$, such that:

$$rho(x,z) = \frac{\rho(x,z)_1}{\rho_1} \times \frac{\rho(x,z)_2}{\rho_2}$$

$$= 1, \text{ for } x < x_1$$

$$= \rho_2/\rho_1, \text{ for } x_1 < x < x_2$$

$$= \rho_3/\rho_1, \text{ for } x > x_2$$

which can be converted to the progression $\rho_1{:}\rho_2{:}\rho_3$, simply by multiplying by ρ_1. A combined space $\rho(x,z)_c$ can thus be formed as $\rho_1 \times rho(x,z)$, and will have the form shown in Fig. 13.

It is the proposition of *rule 1* that, to a reasonable approximation, the square-array apparent resistivity space, for the combined model shown, can be formed from the known apparent resistivity spaces of models 1 and 2 using the same operations. This is shown in Fig. 14. This rule is accurate provided that x_2-x_1 is substantially greater than the maximum spacing. As this condition is departed from, errors arise, but provided the contrast is not too great ($|K| < 0.6$) the maximum error is less than 30% and general error levels are substantially less than this. For the latter reason, it has been found profitable to use the rules at higher contrasts.

This simple rule, here demonstrated with vertical interfaces, can equally well be used with dipping interfaces and with more than two interfaces as demonstrated in Fig. 15. Example A is obviously a common one and the approximation will be relatively poor if the bed thickness becomes small. Example B will be a good approximation when the interface separation is substantial and this will also be true for example C.

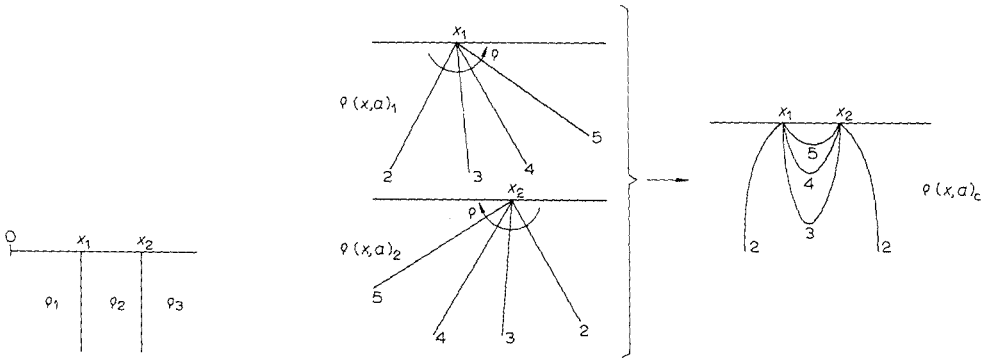

Fig. 13. Schematic representation of a combined resistivity space.

Fig. 14. Scheme of the formation of the combined space by multiplication of the apparent resistivity spaces.

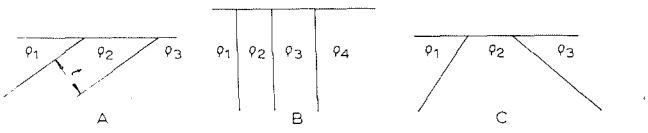

Fig. 15. Rule 1 applied to different interfaces.

Rule 2. Concerns the combination of resistivity spaces when contrast surfaces intersect.

The composition process follows the sequence shown in Fig. 16.

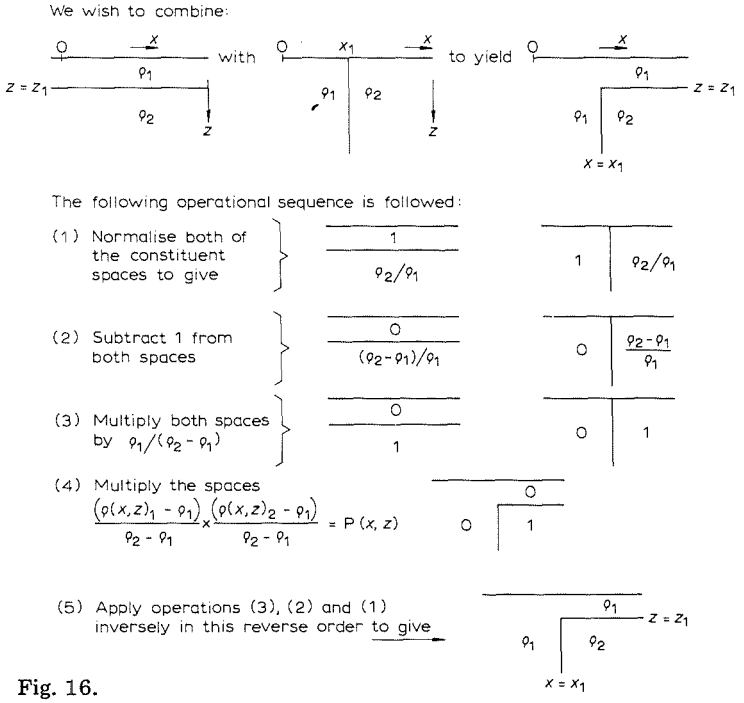

Fig. 16.

As with *rule 1*, *rule 2* proposes that this sequence of operations can be applied to the constituent apparent resistivity spaces.

Thus, calling the apparent resistivity spaces $\rho(x,a)_1$ and $\rho(x,a)_2$ the combined resistivity space $\rho(x,a)_c$ can be written as:

$$\rho(x,a)_c = \left\{ \left[P(x,a) \times \frac{\rho_2 - \rho_1}{\rho_1} \right] + 1 \right\} \rho_1$$

$$= P(x,a) \cdot (\rho_2 - \rho_1) + \rho_1$$

where:

$$P(x,a) = \frac{(\rho(x,a)_1 - \rho_1)}{\rho_2 - \rho_1} \times \frac{(\rho(x,a)_2 - \rho_1)}{\rho_2 - \rho_1}$$

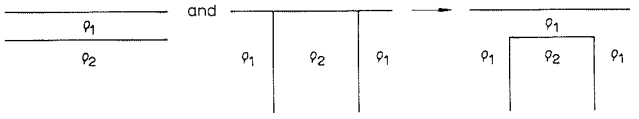

Fig. 17. Application of rule 2 to the concealed dyke model.

This rule can readily be used for the concealed dyke model by combining an outcropping dyke space with a two-layer solution, as shown in Fig. 17. The accuracy of this composition declines as the depth of burial increases, but useful solutions at a depth of burial equal to one-half the dyke width have been obtained, even for a high contrast model.

RANGE OF APPLICATION OF THE RULES

Provided that interfaces are reasonably separated there is a wide range of two-dimensional problems that can be tackled by these rules, using layered models with the dipping layer solution and, where appropriate, the outcropping dyke solution.

It is axiomatic in a successful composition that when a complex theoretical constituent space can be readily calculated, this will be used, rather than composing it using the rules.

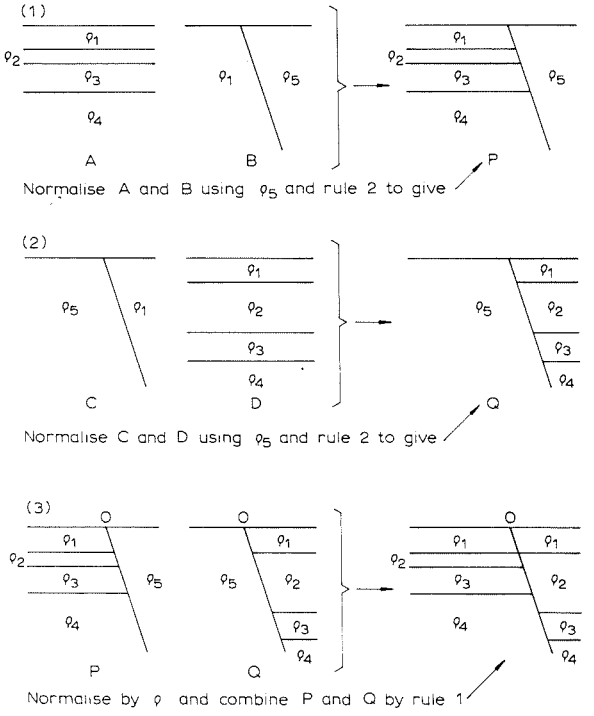

Fig. 18.

A slightly more complex example of a concealed fault is given in Fig. 18 and it will be clear that a succession of faults would entail little difficulty.

Although approximations to complex models can readily be generated in this way it remains important that when borehole control is lacking minimum parameter solutions only should be sought.

With this qualification, the composition rules can be used to extend the interpretation of resistivity space into regions where normal depth interpretation techniques would be unreliable.

SUMMARY

The most complete objective of surface resistivity investigations is to provide an insight into the three-dimensional distribution of resistivity within the subsurface. Such an insight can only be as precise as the inherent ambiguity of the method will allow.

Short of such a full enquiry, scattered sounding curves can be used to investigate geological likeness and symmetry, provided that due attention is paid to orientational resistivity variations.

In more intensive work resistivity sections can be built up which are capable of a considerable degree of quantitative interpretation in terms of two-dimensional structures and the methods indicated may even be crudely useful in three dimensions. Apart from problems of ambiguity, the degree of precision sought in such interpretations must also have regard to the complexity of the observed resistivity field and the precision with which it has been determined (that is, on the intervals between the locations and orientations sampled).

With regard to inherent ambiguity, precision can be added by the use of borehole soundings, when effectively the boreholes will enable a 'most' probable geological interpretation to be made.

Much of the 'noise' encountered in surface resistivity investigations is in fact geologic in origin, and its meaning can only be assessed by intensive investigation. In that the latter is time consuming, there would appear to be scope, at least for improving methods of data acquisition. The requirement of extensive wire laying would appear to be unavoidable.

REFERENCES

Broadbent, M., 1970. Ph.D. Thesis, Leeds University.

Broadbent, M. and Habberjam, G.M., 1971. A solution of the dipping interface problem using the square array resistivity technique. Geophys. Prospect., 19: 321—338.

Habberjam, GM., 1975. Apparent resistivity, anisotropy and strike measurements. Geophys. Prospect., 23: 211—247.

Habberjam, G.M. and Jackson, A.A., 1974. Approximate rules for the composition of apparent resistivity sections. Geophys. Prospect. 22: 393—420.

Habberjam, GM. and Watkins, G.E., 1967. The reduction of lateral effects in resistivity probing. Geophys. Prospect., 15: 221—235.

Marsden, D., 1973. The automatic fitting of a resistivity sounding by a geometrical progression of depths. Geophys. Prospect., 21: 266—280.

Geoexploration, 14 (1976) 229—241

THE APPLICATION OF ELECTROMAGNETIC FREQUENCY SOUNDING TO GROUNDWATER PROBLEMS

O. KOEFOED and D.T. BIEWINGA

Geophysical Laboratory, Delft University of Technology, Delft (The Netherlands)

ABSTRACT

Koefoed, O. and Biewinga, D.T., 1976. The application of electromagnetic frequency sounding to groundwater problems. Geoexploration, 14: 229—241.

The use of an electromagnetic frequency sounding method in groundwater investigations seems to be attractive for two reasons.

First, a change in depth penetration of the current by changing the frequency is far more convenient than displacing the current electrode as is done in resistivity sounding.

Secondly, in arid areas with a highly resistive surface layer the difficulties of introducing the current into the ground that are encountered in resistivity sounding are avoided. Our institute has carried out experimental electromagnetic frequency sounding surveys in two arid areas in South Tunisia. Our choice between the different varieties of this method was controlled mainly by practical considerations. Thus, we avoided the use of a mixed method in which either at the transmitting or at the receiving side conductive contact with the ground is used. We also avoided, because of the instrumental complications involved, methods in which the phase difference between the transmitted and the received signal is determined, and we restricted the measurements to the absolute value of the magnetic field. Finally, we used only horizontal transmitting coils because these allow a far greater strength of the transmitted field than vertical coils.

The methods remaining after this elimination are the horizontal coils method and the perpendicular coils method. Both methods were used during the first months of the survey. It was found during this period, however, that the vertical coils system is far more sensitive to lateral changes in resistivity than the horizontal coils method. For this reason, the perpendicular coils method was abandoned. Using the horizontal coils system, in 85% of the cases response curves were obtained that permitted a good interpretation in terms of 2, 3 or 4 resistivity layers.

INTRODUCTION

The electromagnetic frequency sounding method has been used for the last ten years, particularly in eastern Europe, mainly for the purpose of very deep investigations. As might be expected, however, the method also offers certain advantages when applied to groundwater investigations. The first advantage of the electromagnetic sounding method is that depth penetration of the current can be changed by changing the frequency, which is far more convenient than displacing the current electrodes as is done in resistivity

sounding. The second advantage of the electromagnetic sounding method applies in particular in arid areas where the highly resistive surface layer causes difficulties in introducing the current into the ground by means of conductive contact; this difficulty is entirely avoided when the electromagnetic method is used.

To try out the utility of the electromagnetic frequency sounding method in the conditions described above, a suitable instrument was built, interpretation theory developed, and experimental surveys carried out in two arid areas in South Tunisia.

FIELD PROCEDURE

Our choice between the different varieties of electromagnetic sounding methods was controlled mostly by practical considerations. Thus, because of the difficulty of making conductive contact with the ground, we avoided the use of a mixed method in which either at the transmitting or at the receiving side conductive contact with the ground is used. We also avoided, because of the instrumental complications involved, methods in which the phase difference between the transmitted and the received signal is determined, and we restricted the measurements to the absolute value of the magnetic field. Finally, we decided to use only horizontal transmitting coils, because these allow a far greater strength of the transmitted field than vertical coils. The methods remaining after this elimination are the horizontal coils method and the perpendicular coils method. Both methods were used during the first months of the survey. Later the perpendicular coils method was abandoned, because field experience showed that it had certain undesirable features. The instrument that was used could be set at 13 different frequencies, covering the range from 100 to 10,000 Hz. Thus six observations per decade were obtained. Computations of response curves for theoretical models, which had been made in advance, had shown that this spacing of the observation points would give sufficient detail. The field survey was carried out using two landrovers, one for the transmitter and one for the receiver. Two different types of transmitting coil were used. The first consisted of ten windings of wire laid out on the ground in a circle with a radius of 10 m. The second transmitting coil, which has been used during the greater part of the survey, consisted of 32 windings which were rigidly mounted on a square frame of two by two m, which could be transported on the roof of the landrover. The receiving coil consisted of 430 windings on a circular frame of a diameter of 1.20 m.

In an electromagnetic survey the time required for topographic surveying may well become larger than the time required for the electromagnetic survey. It is therefore essential to use very fast surveying methods. The locations of the measuring stations were determined from aerial photographs; sometimes distances to stations were also determined using special kilometre counters that were mounted on the cars. Only the distance between the transmitting and receiving coil was measured by tape.

RELATION BETWEEN THE RESISTIVITY LAYERING AND THE SHAPE OF THE RESPONSE CURVES

The mutual impedance ratio in the horizontal coils system, Z/Z_0, is equal to the ratio between the actual value of the vertical component of the magnetic field strength and its free space value. For brevity, in what follows this mutual impedance ratio will be referred to as the response. The relation between this response and the parameters of the subsurface layers is:

$$(Z/Z_0) = 1 - \int_0^{\infty} r^3\lambda^2 \cdot R(\lambda) \cdot J_0(\lambda r) \cdot d\lambda \qquad (1)$$

where r is the coil spacing, J_0 is the Bessel function of zero order, and $R(\lambda)$ is a kernel function that depends on the layer parameters ρ_i and d_i and on the period T. This kernel function is defined by the recurrence relation:

$$R(\lambda) = R_{0,n}(\lambda)$$

$$R_{(i-1),n} = (\lambda) = \frac{v_{(i-1),i} + R_{i,n}(\lambda) \cdot e^{-2d_i v_i}}{1 + v_{(i-1),i} \cdot R_{i,n}(\lambda) \cdot e^{-2d_i v_i}} \qquad (2)$$

$$R_{n,n}(\lambda) = 0$$

where n is the number of subsurface layers, and:

$$v_i = \lambda \sqrt{1 + \gamma_i^2/\lambda^2}$$

$$\gamma_i^2 = j \cdot 2\pi \mu_0/\rho_i T \qquad (3)$$

$$v_{i,k} = (v_i - v_k)/(v_i + v_k)$$

If we introduce the logarithmic variables $x = \ln(r)$ and $y = \ln(1/\lambda)$ then eq. 1 can be written:

$$Z/Z_0 = 1 - \int_{-\infty}^{+\infty} R(y) \cdot e^{3(x-y)} \cdot J_0(e^{x-y}) \cdot dy \qquad (4)$$

The right-hand side of eq. 4 is a convolution integral, and consequently the response can be computed from the kernel function by the application of a linear filter. This is a much faster procedure for computing the response than numerical evaluation of the integral.

It may be seen from eqs. 2 and 3 that the kernel function depends only on the products and ratios $(\rho_1 T \lambda^2)$, (ρ_i/ρ_1) and $(d_i\lambda)$. Since the independent variable of the filter function is $(x-y) = \ln(\lambda r)$ this entails that the response depends only on the ratios $(\rho_1 T/r^2)$, (ρ_i/ρ_1) and (d_i/r). Thus if the response curves are plotted on a logarithmic horizontal scale a change in ρ_1, T or r,

provided that (ρ_i/ρ_1) and (d_i/r) remain the same, results in a horizontal shift of the response curve.

Fig. 1 shows the response curve for a homogeneous earth with a resistivity of 100 Ω and a coil spacing of 300 m in the horizontal coils system. It follows from what has been said above that, if the resistivity were higher, then the response curve would be shifted to the left, the shape remaining unchanged on a logarithmic horizontal scale, because the response is uniquely controlled by the quantity $\rho\ T/r^2$. Likewise the response curve shifts to the left when the coil spacing is decreased; this fact can, to some extent, be utilised for displacing the interesting parts of the response curve towards the range of periods in which the measurements are made.

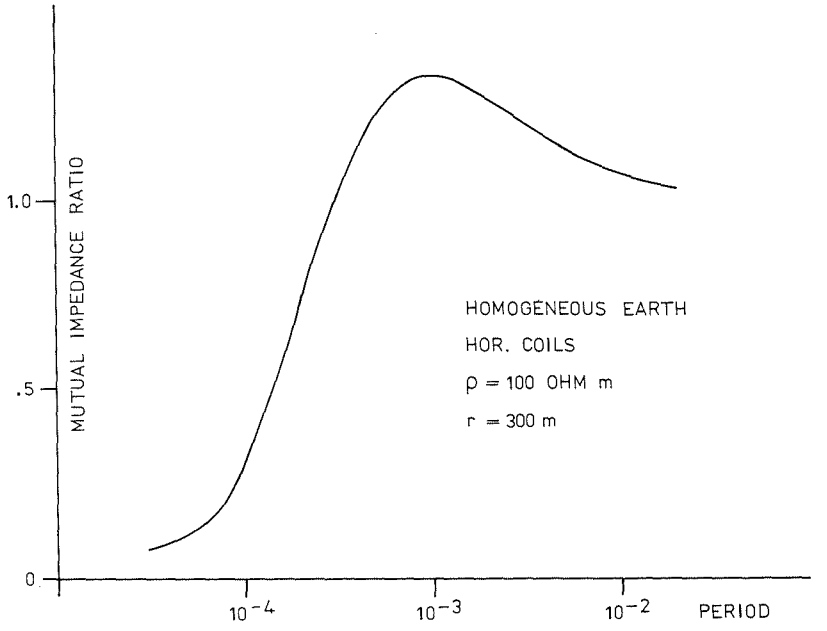

Fig. 1. Response curve for a homogeneous earth.

Fig. 2 shows a set of response curves for two-layer cases with $d/r = 0.2$ and varying values of ρ_2/ρ_1, ρ_2 being smaller than ρ_1. At small values of the period the response curve is mainly controlled by ρ_1. At larger periods, that is greater penetration depth of the current, the effect of ρ_2 becomes increasingly strong which shifts the response curve to the right. The period at which the response curve departs from the homogeneous earth curve depends on the ratio d_1/r. This is shown in Fig. 3, which shows a set of response curves for two-layer cases with $\rho_1 = 1000$ Ω and varying values of d_1/r.

It can be seen from this figure that as d_1/r increases the penetration depths and consequently the period at which the influence of the second layer becomes effective, also increases.

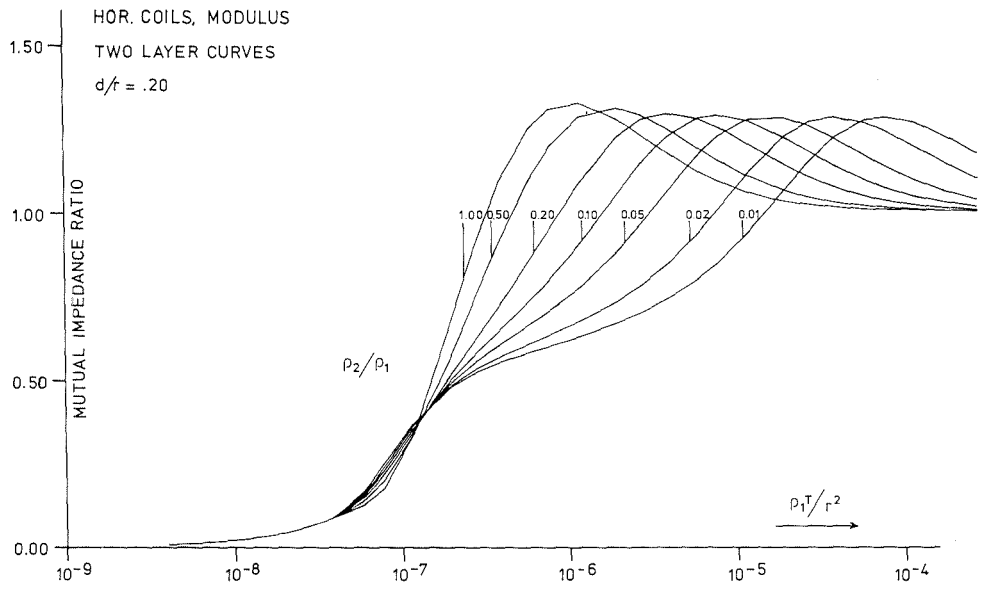

Fig. 2. Response curves for two-layer cases with $d_1/r = 0.2$ and various values of $\rho_2/\rho_1 < 1$.

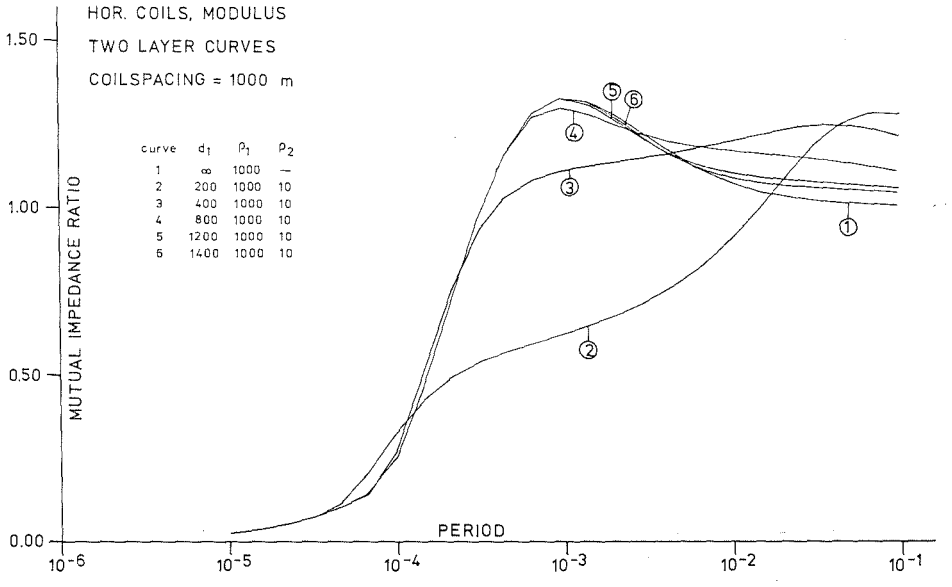

Fig. 3. Response curves for two-layer cases with $\rho_2/\rho_1 = 0.01$ and various values of d_1/r.

Fig. 4 shows a set of response curves for two-layer cases with $d_1/r = 0.2$ and varying values of ρ_2/ρ_1 which are greater than one. Comparing this fig. with Fig. 2 it is seen that the effect on the shape of the response curve of a deeper

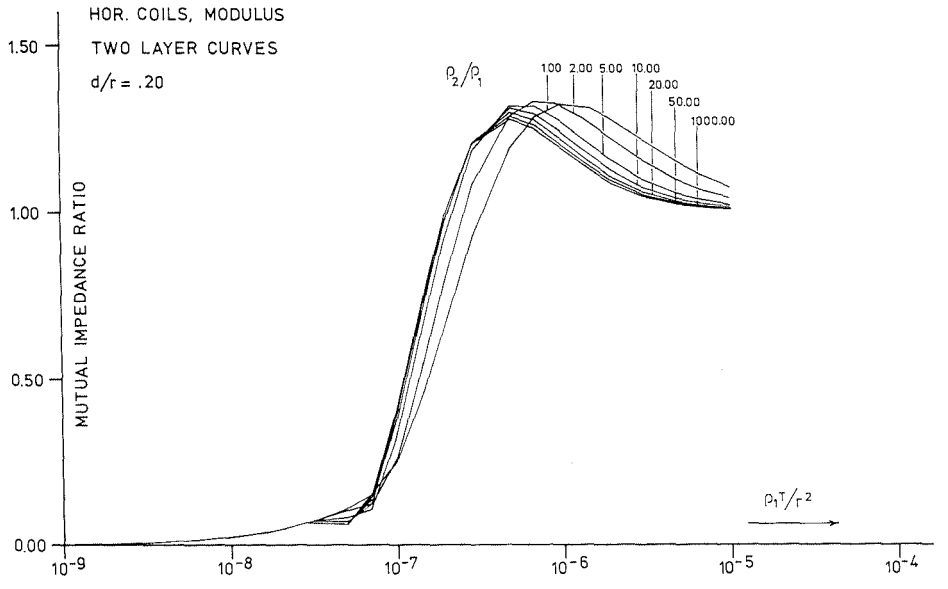

Fig. 4. Response curves for two-layer cases with $d_1/r = 0.2$ and various values of $\rho_2/\rho_1 > 1$.

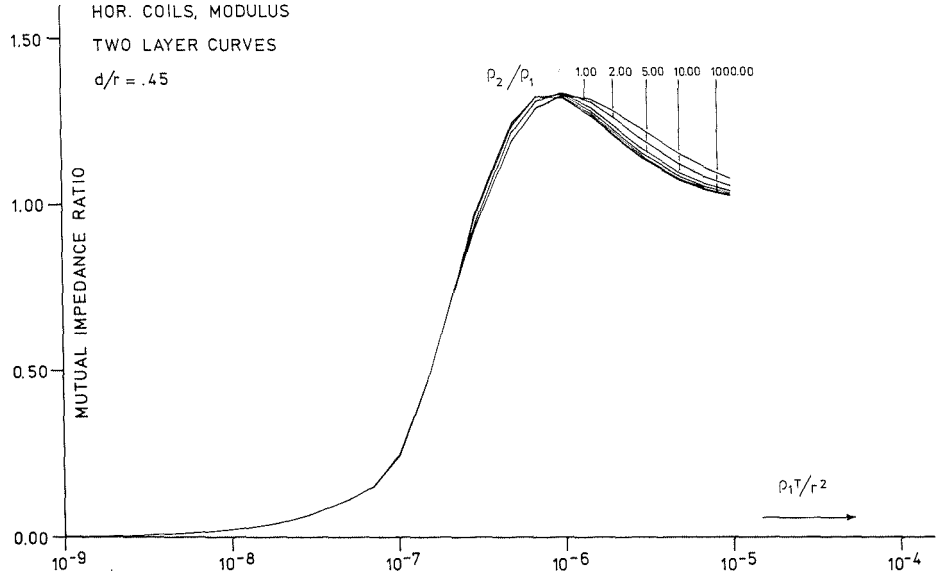

Fig. 5. Response curves for two-layer cases with $d_1/r = 0.45$ and various values of $p_2/\rho_1 > 1$.

layer with higher resistivity is considerably smaller than that of a deeper layer with lower resistivity. The reason for this is that the possibility for a deeper layer with higher resistivity to change the shape of the curve is restricted by the fact that the response curve must be single valued and therefore a vertical

line through the point of departure represents the maximum possible deviation. It is also seen that there is some sort of saturation effect with regard to the value ρ_2/ρ_1; once this ratio has reached a value of ten, a further increase gives hardly any further change in the shape of the response curve. In Fig. 5 a similar set of response curves is shown for a value d_1/r of 0.45. Comparing this figure with Fig. 4 it is seen that the increase in depth shifts the point of departure to the right; also the effect of the second layer on the shape of the response curve is considerably smaller in the case of Fig. 5 than in Fig. 4.

The limitations of the effect of the deeper layer with higher resistivity are considerably smaller in the case of three-layer curves of the bowl type. This is shown in Fig. 6 on a three-layer curve with $d_1/r = d_2/r = 0.1$, $\rho_1 = 1000\ \Omega$, $\rho_2 = 200\ \Omega$ and varying values for ρ_3. The right-hand curve in this figure is the two-layer curve for $\rho_1 = 1000\ \Omega$ and $\rho_2 = 200\ \Omega$. It is seen that, due to the effect of the second layer, the slope of the response curve is considerably less steep than that of a homogeneous earth curve, so that there is more scope for the third layer to make the curve depart to the left. Nevertheless, in this case the saturation effect, which was described above, is clearly noticeable.

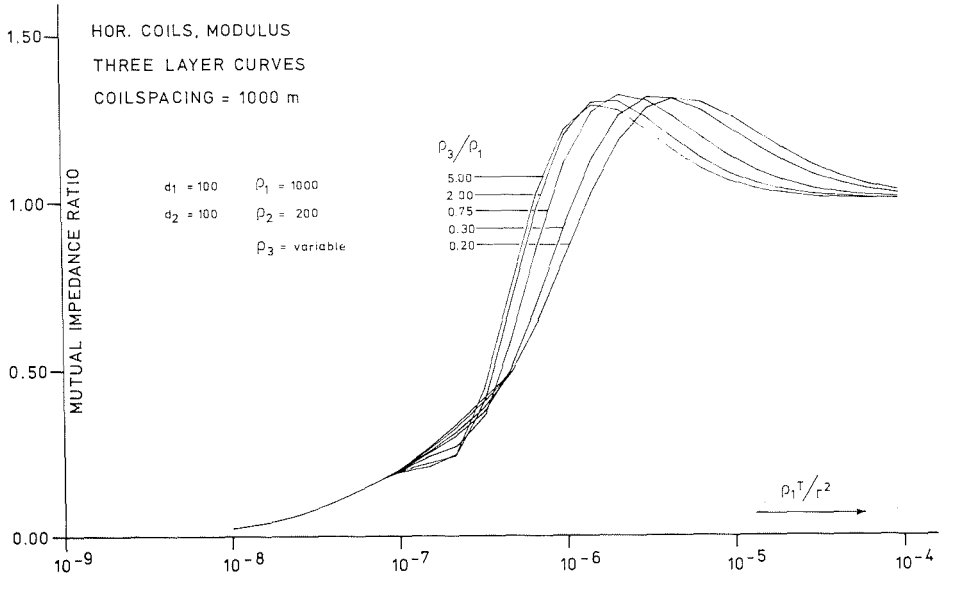

Fig. 6. Response curves for three-layer bowl-type cases with various values of ρ_3/ρ_1.

FIELD EXPERIENCE

Fig. 7a and b show the field observations at one of the stations with two different values of coil spacing. Both curves fit the same three-layer model, the theoretical curve for which is also shown on the figures. The homogeneous earth curve and the two-layer curve are shown as dashed lines to emphasise

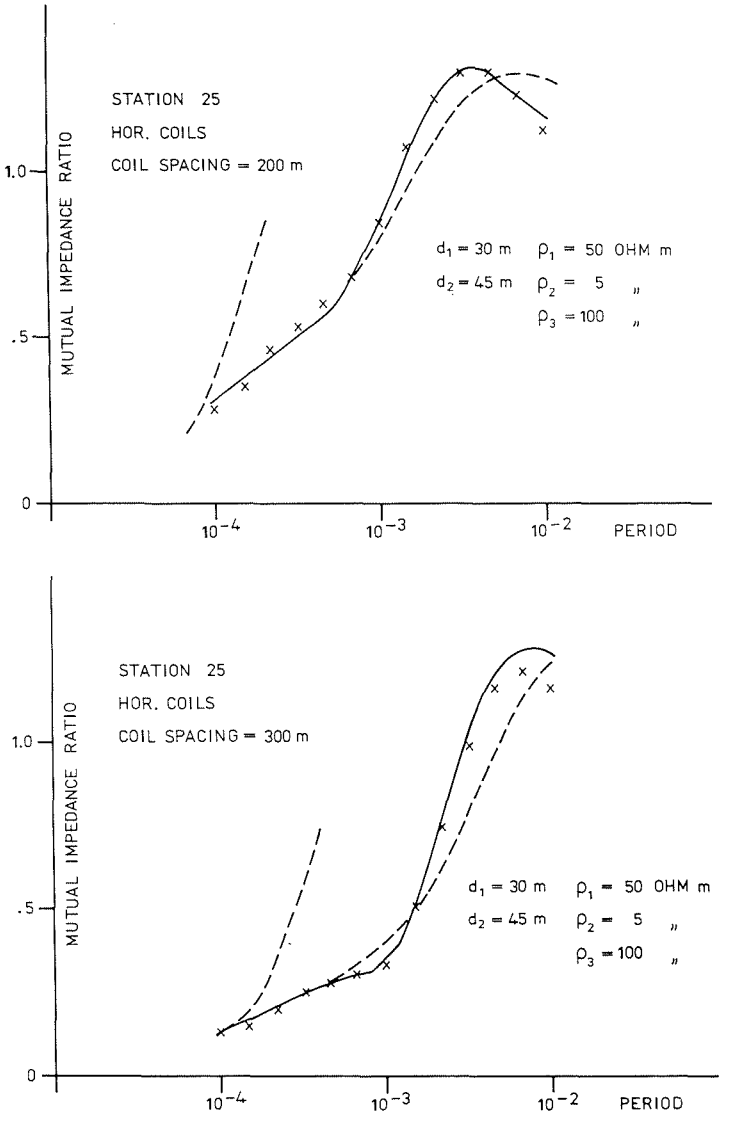

Fig. 7. Field observations with the horizontal coils system at coil spacings 200 m (a) and 300 m (b) and interpretation.

the points of departure of the three-layer curve. The points of departure lay lower down the curve for the measurements taken with larger coil spacing since the ratio of thickness over coil spacing is less. The third layer in this example corresponds to a water-bearing limestone layer; the second layer corresponds to a clay layer which seals off the limestone. A similar layering is encountered rather frequently in groundwater problems. Electrically it

corresponds to a bowl-type case which, as was seen above, is fairly favourable for obtaining a good interpretation. At the station illustrated in Fig. 7 the measurements taken with the perpendicular coils system also gave a good agreement with the theoretical curve for the same layering model. In other cases, however, results obtained with the perpendicular coils systems were often very unsatisfactory.

This is illustrated by Fig. 8, in which measurements with the perpendicular coils system are shown with the best fitting theoretical curve. In the perpendicular coils system the theoretical curve shows a maximum, the value of which can vary between certain limits. The maximum value can become small only for curves which are considerably broader than that shown in Fig. 4. For no layer model can a low value of the maximum be combined with a small width of it, such as the measurements yield.

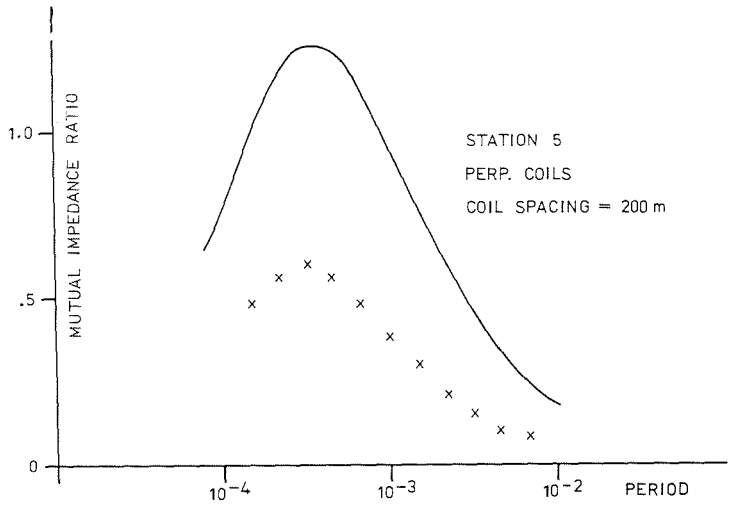

Fig. 8. Field observations with the perpendicular coils system and model curve.

The reason for the abnormal results of the measurements must be sought in lateral variations of the resistivity, to which the perpendicular coils method is far more sensitive than the horizontal coils method. This was established by measuring the horizontal component of the magnetic field in a direction perpendicular to the line connecting the transmitter and the receiver. In a model where the resistivity varies only in a vertical direction, this component must be zero. At stations where results were obtained such as illustrated in Fig. 8, it was found that the component of the magnetic field in this direction was of the same order of magnitude as those in the other directions.

Figs. 9a and b show the measurements at two different values of the coil spacing at an other station. In this case a four-layer interpretation of the bowl-type fitted the observations on both coil spacings. It must be noted, however, that in this instance the saturation effect makes it impossible to determine

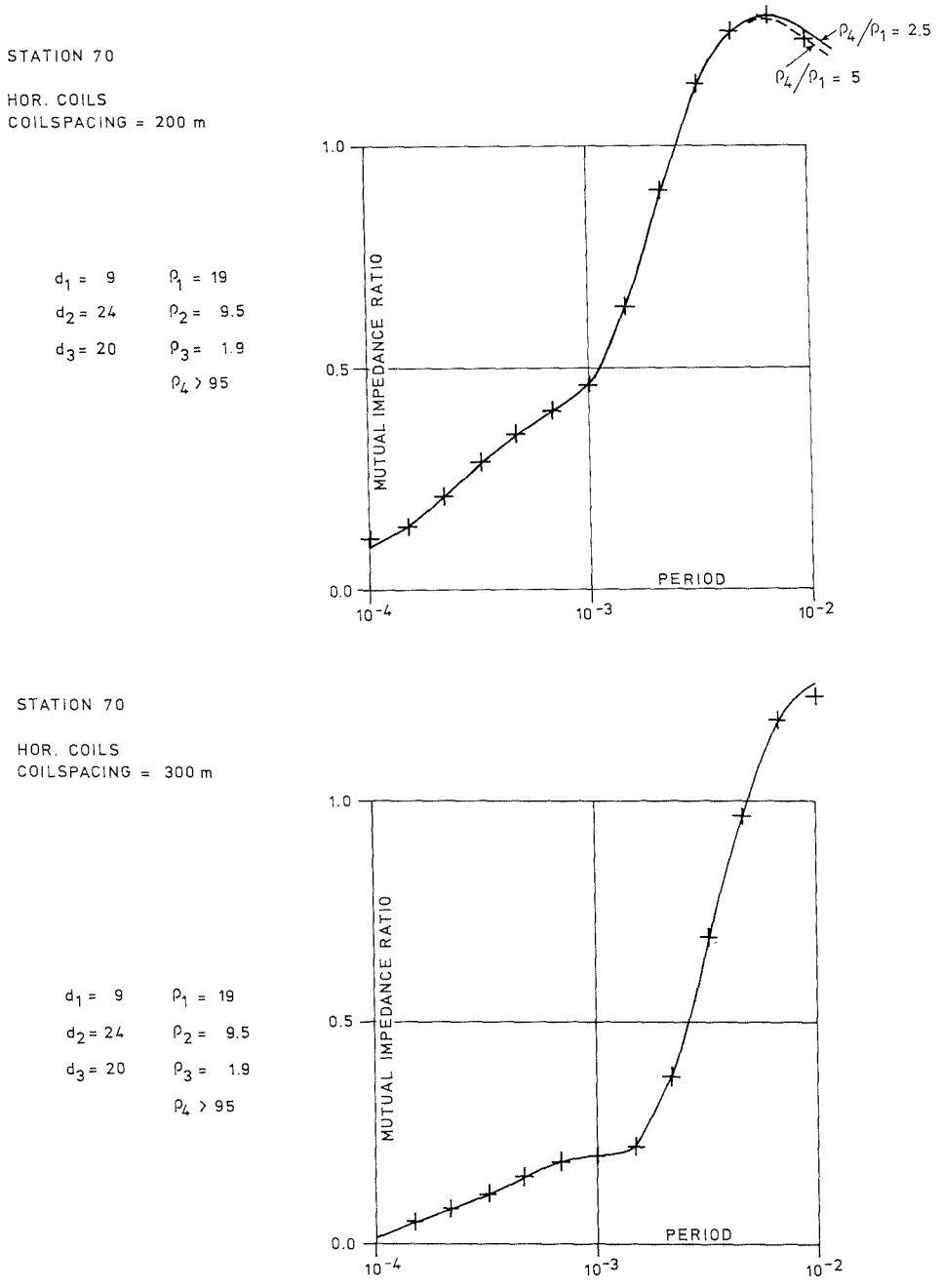

Fig. 9. Field observations with the horizontal coils system at coil spacings 200 m (a) and 300 m (b) and interpretation.

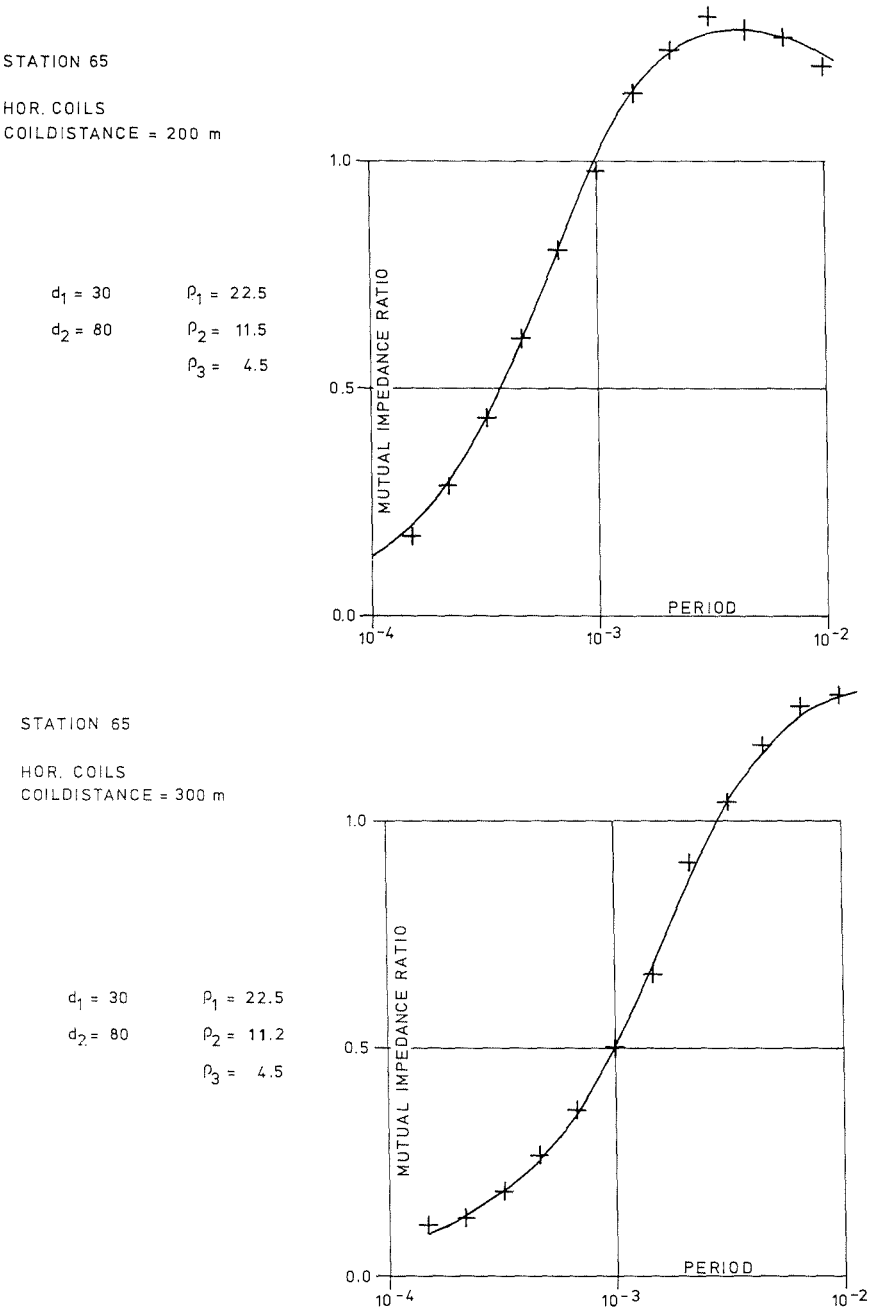

Fig. 10. Field observations with the horizontal coils system at coil spacings 200 m (a) and 300 m (b) and interpretation.

the resistivity of the deepest layer; only a minimum value for this resistivity can be derived. This effect is a rather serious drawback of the method, because it makes it impossible to distinguish, on the basis of the value of the resistivity, between a water-bearing and a dry part of the limestone layer.

Figs. 10a and b show the observations at two different values of the coil spacing at another station. The observations fit a three-layer model of the descending type. The limestone layer at the location of this station was too deep to be reached by the measurements.

In Table I a comparison is shown between the results of the electromagnetic soundings and the drilling at stations where drilling data were available. The agreement is seen to be very satisfactory.

TABLE I

Comparison between electromagnetic sounding results and drilling results

Station No.		Drilling	E.M. sounding
14	overburden	10 m	9 m (18 Ω m)
	limestone	present	present (90 Ω m)
31	overburden	7.20 m	6 m (10 Ω m)
	limestone	present	present (200 Ω m)
32	overburden	> 82 m	20 m (8 Ω m) 7 m (4 Ω m) ? (2 Ω m)
	limestone	not present	not present

CONCLUSIONS

In some instances unreasonable results were obtained with the horizontal coils method; usually this could be attributed to the presence of a fault. In 85% of the cases, however, good interpretations proved to be possible in terms of 2-, 3-, or 4-layer models. Thus, the detail obtained with the frequency sounding method is less than that which is usually obtained with the resistivity method. Nevertheless the method has proved to be capable of giving very valuable information. The most serious drawback of the method is the impossibility, at least in a number of cases, to determine the resistivity of the water-bearing layer. On the other hand, the field measurements in electromagnetic sounding can be carried out considerably faster than in resistivity sounding. The time required for the measurements at one station using two different values of the coil distance was 20 minutes including the time required for measuring out the distances between the coils.

To improve the information obtained by this method it will be necessary to improve the sensitivity of the instrument and to increase its frequency

range. Increasing the sensitivity implies both an increase in the strength of the transmitted field, and an increase in the selectivity of the receiver, by which the signal-to-noise ratio would be improved. An increase in the frequency range is necessary because sometimes, depending on the values of the resistivities, interesting parts of the response curve lay outside the range of the measurements.

Geoexploration, 14 (1976) 243—250

RECENT DEVELOPMENTS IN THE DIRECT INTERPRETATION OF RESISTIVITY SOUNDINGS

O. KOEFOED

Geophysical Laboratory, Delft University of Technology, Delft (The Netherlands)

ABSTRACT

Koefoed, O., 1976. Recent developments in the direct interpretation of resistivity soundings. Geoexploration, 14: 243—250.

The application of the direct interpretation of resistivity soundings using the resistivity transform, has in practice encountered the difficulty that absurd results may be obtained, such as negative resistivity values.

An analysis of this phenomenon has led to the conclusion that it is causally related to the error magnification that occurs in the process of reducing to a lower boundary plane. The errors involved are of two kinds. In the first place there is the error of observation leading to errors in the transform values. In the second place the asymptotic approximation to the transform curve by a two layer curve leads to an error in the determination of the thickness of the first layer. Both of these errors may have the result of driving the denominator in the reduction equation through zero, thus causing negative values of the reduced transform. At the same time, the above mentioned error magnification is the cause of the phenomenon known as equivalence. The magnitude of the error magnification depends on the ratio of the coordinates of a point of the transform curve to the parameters of the layer that is being removed. Insight into this relation makes it possible to avoid the difficulties in the direct interpretation method by a combination of two measures: (a) not to apply the reduction to parts of the transform curve where the error magnification is too large; (b) to compute the limits of reliability of the reduced transform in the marginal section of the transform curve. With these measures the direct interpretation method provides a solution within the margins defined by equivalence; in addition information may be obtained regarding the range of parameter values within which equivalence is possible.

Another development which has been worked out in our institute, is the derivation of an approximate interpretation method, which is based upon the fundamental equations of the direct interpretation method, but which is applied directly to the apparent resistivity curve. With this approximate method, solutions can be obtained in favourable conditions for multi layer cases with an error of about 20% in the layer thicknesses and in a computation time of a few minutes.

DESCRIPTION OF THE DIRECT INTERPRETATION METHOD

In the direct interpretation method of resistivity observations, as developed at the Geophysical Laboratory at Delft, the first step is to derive from the apparent resistivity values the values of the resistivity transform, T. The formal relation between these two quantities is:

$$\rho_{\text{app. Schl.}} = r^2 \int_0^\infty T(\lambda, d_j, \rho_j) \cdot J_1(\lambda r) \cdot \lambda \, d\lambda \qquad (1)$$

where r is half the distance between the current electrodes, d_j and ρ_j are the thicknesses and the resistivities of the layers, and J_1 is the Bessel function of the first order.

The practical computation of the resistivity transform from the apparent resistivity is carried out by the application of a linear filter. To this end sample values of the apparent resistivity are taken at abscissa values that are equidistant on a logarithmic scale, the sample distance corresponding to one third of $^{10}\log 10$. The resistivity transform is then obtained by the equation:

$$T_n = \sum_{i=-2}^{i=6} f_i \, \rho_{\text{app.}}(n-i) \qquad (2)$$

where f_i are the coefficients of the linear filter. The numerical values of these filter coefficients are given in Table I.

TABLE I

The filter coefficients

f_{-2}	f_{-1}	f_0	f_1	f_2	f_3	f_4	f_5	f_6
−0.0723	0.3999	0.3492	0.1675	0.0858	0.0358	0.0198	0.0067	0.0076

The second step in the direct interpretation method is the successive reduction of the transform values to lower boundary planes. The fundamental equation of this process is:

$$T_{j+1} = T_j(1-w_j\rho_j/T_j)/(1-w_jT_j/\rho_j) \qquad (3)$$

where: $w_j = \tanh(d_j/u)$; u is the abscissa value which is equal to $1/\lambda$ (compare eq. 1); T_j is the transform that would have been obtained if the first $(j-1)$ layers were missing and the measurements were carried out directly on the top of the j-th layer.

The procedure is as follows. First, the early part of the transform curve is approximated by an asymptotic two-layer transform curve, which gives the values of d_1 and ρ_1. Then the transform curve is reduced to the T_2-curve by the application of eq.3. The early part of the T_2-curve is then approximated by an asymptotic two-layer curve, which gives the values of d_2 and ρ_2. Then the T_2-curve is reduced to the T_3- curve by means of eq.3, etc. The procedure is repeated until a reduced transform curve is obtained that can be matched completely with a two-layer transform curve.

LIMITATIONS OF THE DIRECT INTERPRETATION METHOD

The direct interpretation method, as described above, has found little application in practice. One of the reasons for this is that the method, in particular when it is carried out on a computer, may lead to absurd results, such as negative values of layer resistivities.

These difficulties in the practical application of the direct interpretation method are connected with an inherent ambiguity of resistivity observations that is usually referred to as the phenomenon of equivalence. This phenomenon involves that widely differing layer distributions may yield apparent resistivity curves that differ so little, that they cannot be distinguished from each other within the accuracy of the observation. In other words: when one tries to derive the resistivity—depth function from the ($\rho_{app.}$—r)-function, then a very small error in the latter may lead to a very large error in the former.

If one wants to circumvade the above mentioned difficulties in the application of the direct interpretation method, then it is necessary to understand in which stage of the calculation and in what manner the error magnification occurs. This problem will be discussed in the following paragraphs.

It can be shown that no error magnification occurs in the transition from the apparent resistivity curve to the resistivity transform curve. In the asymptotic approximation of the early part of the transform curve by a two-layer transform curve a small error in the determination of d_1 may be made of the order of a few percent.

A serious error magnification may occur, however, in the application of the reduction equation (eq.3) both as a result of initial errors in T_j and those in d_j. Initial errors in T_j are caused by observational errors in the apparent resistivity, errors in d_j may be incurred in the asymptotic approximation by a two-layer curve. We shall consider the effect of errors in T_j, which is the more serious of the two. The error magnification, M, can then be expressed as the ratio of the relative change in T_{j+1} over the corresponding relative change in T_j, or:

$$M = \frac{T_j}{T_{j+1}} \cdot \frac{\delta T_{j+1}}{\delta T_j} = \frac{\delta \ln (T_{j+1})}{\delta \ln (T_j)} \tag{4}$$

The expression for M can be derived by differentiation of eq.3 with respect to T_j. It turns out that M can be written as a function of the two variables (T_j/ρ_j) and (u/d_j). This function is shown in graphical form on Fig.1. Superposition of this figure upon a transform curve, with the origin of the figure at the point of the transform curve graph with coordinates d_j and ρ_j, shows immediately the value of the error magnification in each point of the transform curve. The error magnification is particularly large in the neighbourhood of the 45° diagonal through the point with coordinates d_j, ρ_j.

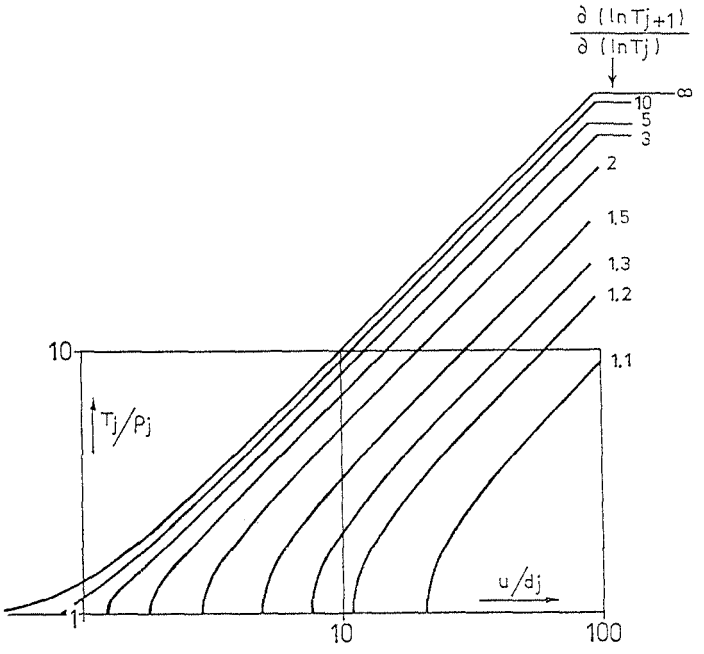

Fig.1. Graph showing the error magnification incurred in reduction to a lower boundary plane.

The effect of the errors in T_{j+1} upon the determination of d_{j+1} and ρ_{j+1} is illustrated on Fig.2. The full drawn curve on this figure is a four-layer transform curve. The vertical crosses represent points of the reduced transform curve. The ends of the vertical arms of these crosses are the reduced transform values that result when the values of the unreduced transform are taken two percent too high or two percent too low; these vertical arms thus represent the range of uncertainty in the reduced transform values.

The uncertainty in the values of the reduced transform leaves a considerable latitude in the manner in which a two-layer transform curve can be adapted, within the margin of error, to the early part of the reduced transform curve. On the figure the dashed lines marked A, B and C show three possible positions for such asymptotic two-layer curves; also shown on the figure are the "crosses" of these two-layer transform curves.

The coordinates of the crosses marked A and B, when used as parameters for the second layer, give four-layer transform curves that are just compatible, within the 2% error limit, with the correct transform curve. The coordinates of the cross marked C, however, when used as parameters for the second layer, give an impermissibly large error in the transform curve, although the two-layer transform curve C seems to fit the reduced transform curve. The cross and the two-layer curve marked B, on the other hand, indicate at the same time the ex-

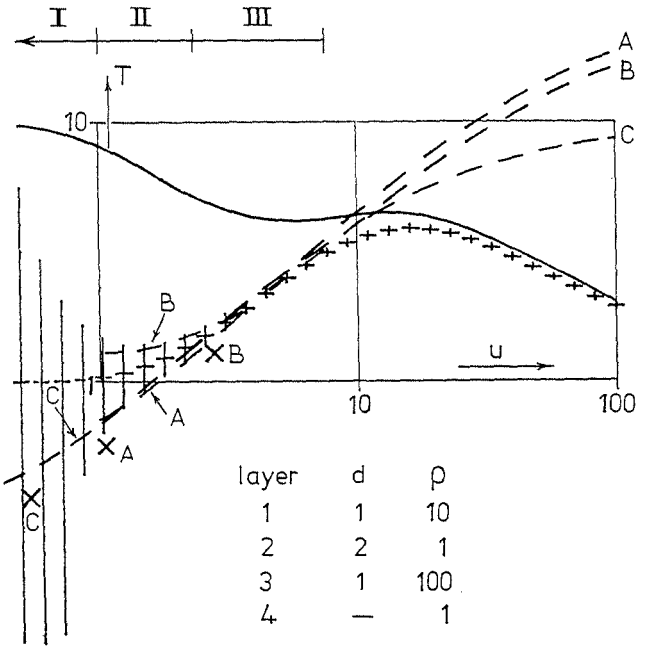

Fig. 2. Four-layer transform curve and result of reduction to a lower boundary plane with error limits.

treme possible values of the parameters of the second layer, and the extreme position to the right in which a two-layer curve can be fitted to the reduced transform curve. Thus it is possible to determine the parameters of the upper limit of the range of equivalence from the reduced transform curve taking the error limits in consideration.

With regard to the possible use of the reduced transform curve, the abscissa range in Fig.2 may be divided into three parts. In the part marked I on the figure the reduced transform, in view of its large error range, cannot give any contribution to the interpretation at all. Computation, or graphical determination, of the reduced transform in this part serves no useful purpose. In the part marked II on Fig.2 the reduced transform, together with its error limits, could be used to determine the upper limit of the range of equivalence. It is questionable, however, whether it would be useful in practice to do this. A computerized trial and error method would seem to be more indicated for this purpose. The part marked III on Fig.2, where the error margin of the reduced transform is small, is the really useful part of the reduced transform curve. By adaption of a two-layer transform curve to this part one can, with the well-known restrictions that are imposed by equivalence, determine the parameters of the second layer.

AN APPROXIMATE INTERPRETATION METHOD

A closer consideration of the last paragraph of the previous section shows that the parts of the curve that are actually used in the direct interpretation are essentially the same as those that are used in the approximate auxiliary points method, that is the ascending or descending flanks of the curve that mark the transition from the resistivity of one layer to that of the next. One is thus tempted to make a comparison between the direct interpretation method and the auxiliary point method, to analyze the differences between them, and to investigate whether a bridge between them can be laid.

The most conspicuous difference between the direct interpretation method and the auxiliary point method from the point of view of the final result is that in the direct interpretation method the coordinates of the cross of the asymptotic two-layer curve are equal to the parameters of the subsurface layer, whereas in the auxiliary point method they are not. In fact the auxiliary point method provides a graphical means of determining the layer parameters from the coordinates of the cross.

The above mentioned difference in the final result between the two methods is caused by three differences in their mode of application. The differences are:

(a) The direct interpretation method is applied to the resistivity transform curve whereas the auxiliary point method is applied to the apparent resistivity curve.

(b) The asymptotic two-layer curve is in the direct interpretation method a resistivity transform curve whereas in the auxiliary point method it is an apparent resistivity curve.

(c) In the direct interpretation method reduction to a lower boundary is applied between two successive stages of asymptotic approximation by a two-layer curve, whereas in the auxiliary point method no reductions to a lower boundary plane are applied.

It turns out that, at least in cases where layers with lower and higher resistivities alternate, the differences mentioned under (a) and (c) are the least important and moreover tend to cancel each other. The most important cause for the difference between the coordinates of the cross of the two-layer curve and the parameters of the subsurface layer in the auxiliary point method, is the fact that the asymptotic two-layer curve is an apparent resistivity curve rather than a resistivity transform curve.

The difficulty may thus be largely obviated by approximating to the original apparent resistivity curve by two-layer resistivity transform curves. The procedure is illustrated on Fig.3 for the layer distribution that was also used for Fig.2. The full drawn line in Fig.3 is the four-layer apparent resistivity curve; the dashed line is the two-layer *transform* curve which has the parameters of the second subsurface layer as coordinates of its cross. Figure 3 also emphasises the fact that the concept of "asymptotic approximation" by a two-layer curve, when applied to multi-layer cases, requires careful definition. In the above

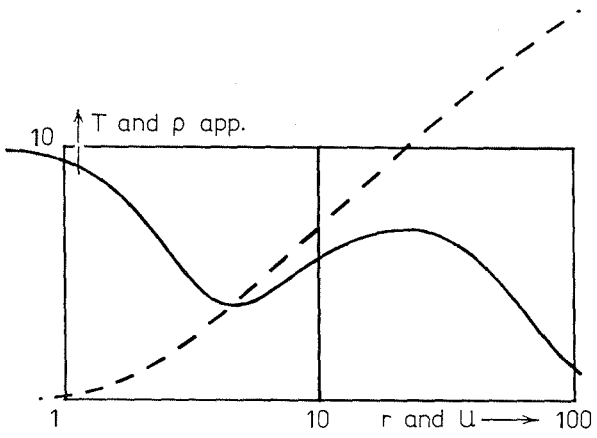

layer	d	ρ
1	1	10
2	2	1
3	1	100
4	—	1

Fig.3. Fout-layer apparent resistivity curve and approximation by a two-layer transform curve.

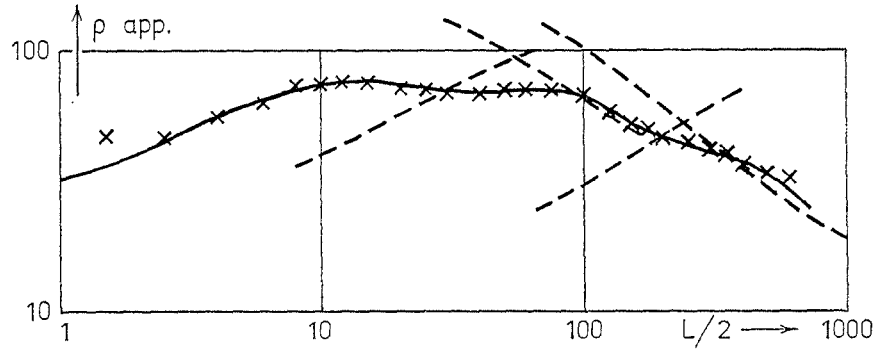

Fig.4. Field example of an apparent resistivity curve and approximate interpretation by means of two-layer transform curves.

mentioned case, where layers of lower and higher resistivity alternate, a useful definition appears to be (see Fig.3) that the two-layer transform curve should pass through the point of strongest curvature of the apparent resistivity curve.

Figure 4 illustrates the application of the method to field observations in a

diluvial area in the East of The Netherlands, where sand and clay layers alternate. The crosses in this figure are the observed apparent resistivity points. The full drawn line is the apparent resistivity curve for a layer model that was derived by trial and error. The dashed lines are the two-layer transform curves that were used for the approximate interpretation. Table II shows a comparison between the results obtained by the approximate method and those obtained by the exact trial and error method.

TABLE II

Layer parameters by the approximate and by the exact indirect method at the station illustrated on figure 4.

	Layer						
	1	2	3	4	5	6	7
App. thickness	1.0	12	8	32	70	80	—
App. resistivity	30	90	30	160	20	160	5
Exact thickness	1.1	11	8	24	70	65	—
Exact resistivity	30	90	30	160	20	160	8

Geoexploration, 14 (1976) 251—252

Abstracts

USE OF DIPOLE ARRAYS IN REGIONAL SURVEYS

L. ALFANO

Institute of Geophysics, Naples (Italy)

ABSTRACT

The role of the geoelectric methods using direct currents in hydrogeological researches is well known, particularly by means of the Schlumberger array. But this arrangement which generally gives good apparent resistivity diagrams, is convenient in the field only in relatively superficial explorations. When greater depths must be reached, very long cables and a cumbersome field organization are called for.

Other difficulties for the Schlumberger array may rise from the current leakages when long spreads lay on wet grounds and this disadvantage is present even if the cables are of good quality and new. So the field work in rainy periods may be difficult and dependent on a perfect condition of the electric insultation.

The depths of interest in water researches are often less than about 200 m, so the corresponding total length AB of a Schlumberger array may vary from 1200 m in the more favourable, to 6000 m in the more unfavourable cases. But since the water needs in the world are constantly increasing, in other cases much greater depths must be taken into consideration, especially when exploration of regional character are carried out.

Now, in a situation where the Schlumberger array presents the above disadvantages the dipole—dipole array, first proposed and experimented by some geophysicists in the Soviet Union, shows its favourable aspects and it may be useful or even necessary. But the substitution of the old by means of a new array may involve some difficulties of other types so that a more accurate analysis may be proper.

The problem presented by the dipole—dipole arrays is the great sensitivity to the lateral variations in the ground resistivities, which causes some difficulties in the interpretation of the apparent resistivity diagrams.

In effect it is known, and it is also demonstrable in a theoretical way, that the dipole—dipole diagrams may be noticeably scattered when the geology of the explored area presents complicated structures with sharp lateral variations, so that the interpretation by means of templates may be very difficult or impossible. A solution for this inconvenience may be reached if we transform the dipole—dipole into Schlumberger diagrams, whose sensitivity toward the lateral variations is noticeably less.

This procedure also allows us to interpret the diagrams with the aid of the

templates for the Schlumberger array, instead of the dipole—dipole templates, which are different for the different types of arrays.

But the transformation procedure must be seriously studied before stating practical rules for its execution: this is the subject of the following considerations. We note that:

(1) Theoretical formulae exist allowing to utilize the passage from a couple of dipole—dipole measurements carried out by two different arrays, to a corresponding Schlumberger measurement. In this way, if we have a dipole dipole apparent resistivity diagram for a set of measurements executed with different distances, we can transform the entire dipole—dipole curves obtained by means of different arrays into a Schlumberger diagram. But a serious difficulty exists nevertheless since such a formula is valid only in the case of plane-parallel stratification; the very possibility of existence for lateral influences may be sufficient to make the transformation useless and therefore the related interpretation. The practical use of these formulas is therefore problematic.

(2) The possible presence of scattering in the dipole—dipole diagram renders the knowledge of its shape defective, if the measurements are not carried out continuously, that is by making the successive dipole contiguous to each other.

The above considerations lead to the following conclusions:

(a) The only possible way to execute dipole—dipole vertical soundings valid in every geological situation, is to use the *continuous polar—dipole array*. Here the potential dipole MN is fixed and the successive current dipoles AB are contiguous. The length AB is approximately proportional to the distance between the dipoles so that they appear equal in the usual bilogarithmic scale;

(b) The transformation from a single polar—dipole diagram into the corresponding Schlumberger (half-spread) one, must be carried out by means of an integral formula which involves the whole field apparent resistivity diagram, both in its known, and in its unknown part. Therefore an unknown constant is required, and the transformed half-Schlumberger diagram is not uniquely determined. But, unfortunately, all possible derived Schlumberger diagrams have a common part, and some common interpretative results which may be referred to the dipole diagram obtained in the field (Alfano, 1974).

Another difficulty to overcome is the small magnitude of the voltages to be measured between the potentiometric electrodes M and N. A good solution is based on the use of commutated energizing current whose frequency is sufficiently low to avoid the skin effect. The voltages must be filtered by means of a band pass filter and, if necessary, they must be also processed by means of a mathematical filter.

The whole method has been tested in the field; exploration depths noticeably higher than necessary in water researches have been reached and only relatively small field crew were employed.

References

Alfano, L., 1974. A modified geoelectrical procedure using polar-dipole arrays — An example of application to deep exploration. Geophys. Prospect., XXII (3).

Geoexploration, 14 (1976) 253

TOTAL-FIELD RESISTIVITY MAPPING

ADEL A.R. ZOHDY

U.S. Department of the Interior Geological Survey, Denver, Colo, (U.S.A.)

ABSTRACT

The technique of total-field resistivity mapping consists of grounding a long current bipole (generally more than 2 km in length) and calculating the total electric field at various field stations from measurements of two components. The lengths of the measuring dipoles must be small (50—100 m) in comparison to the distance from the nearest current electrode. By using a 30 kV-A generator, carefully selected grounding points with low contact resistances, and potentiometric chart recorders, total-field measurements often can be made over an area of about 500 km^2. A general formula is given for the calculation of apparent resistivities along the primary field, total field, or any other direction. For horizontally stratified laterally homogeneous media, total-field and other types of bipole-dipole apparent resistivity maps can be calculated from the apparent resistivity values on a Schlumberger VES curve which is measured (or calculated) over that medium.

Conversely, the Schlumberger VES curve can be constructed from measurements of the total field at various stations, except for those stations that fall along the polar axis of the current bipole. Residual or percent-lateral-effect maps, which accentuate the effect of lateral changes in layer thickness or resistivities, are calculated by subtracting the total-field, apparent-resistivity values which are calculated for horizontal layering from those observed in the field. This technique was applied to data obtained in the geothermal area of Long Valley, California. The advantages and limitations of the total-field resistivity mapping technique are outlined.

Geoexploration, 14 (1976) 254—258

ELECTROMAGNETIC DEPTH SOUNDING FOR GROUND WATER WITH PARTICULAR REFERENCE TO CENTRAL FREQUENCY SOUNDING: PRINCIPLES, INTERPRETATION AND APPLICATIONS

H.P. PATRA

Department of Geology and Geophysics, Indian Institute of Technology, Kharagpur, West Bengal (India)

ABSTRACT

The planning of a ground-water exploration program at a reasonably low survey cost in hard and soft formations calls for electrical and electromagnetic methods of geophysical prospecting. It needs no emphasis that direct-current geoelectric sounding has a very limited application in resistive formations, e.g., in crystalline rocks and in loose dry sands. Hydrogeologically, these hard rocks are represented by resistive formations within which aquifer porosity is mainly secondary in nature due largely to joints, fissures and crevices. In crystaliine rocks, such as, granites, gneisses and schists, ground water is found at the zone of weathering. In limestone areas potential aquifers may be located in the zones of secondary porosity caused by caving. Under the situations noted herein, the problem to be tackled by geophysical methods is to locate comparatively conducting water bearing zones within highly resistive formations. The problem reduces, therefore, to detection of horizontal discontinuities and electromagnetic depth sounding appears to be the only correct approach for solving such problems rapidly and at a comparatively low cost as against equally preferred seismic methods.

Artificially energized alternating current methods of prospecting normally require a transmitter-receiver system for field operations, in the frequency range 20 Hz to 20 kHz. The primary field is established, in practice, by means of a linear cable, a dipole or a loop source of current. While the linear cable method is used mainly for profiling, dipole and loop methods may be conveniently adopted for electromagnetic depth sounding over a stratified earth and therefore in ground-water exploration. In electromagnetic depth sounding, either the frequency of the primary source current or the spacing between transmitter and receiver is changed to obtain different effective depths of penetration, referred respectively to frequency (parametric) and geometric soundings. Frequency sounding which, compared to geometric sounding, is particularly convenient from an operational point of view ensures a reasonably high depth of investigation and a better resolution at smaller and larger conductivity contrasts.

Frequency depth sounding may be carried out using a loop source or a dipolar source. Of the various combinations of dipolar transmitter—receiver systems, the horizontal coplanar one is most commonly used particularly with problems of horizontal stratification. In the system the source is a small vertical magnetic dipole and the vertical component of the magnetic field is measured at a fixed distance from the source by means of a pick-up coil. Since varied depth of penetration is achieved by changing frequency the sounding by horizontal coplanar dipolar system will simply be referred to as Dipole Frequency Sounding abbreviated as DFS. Another most convenient method of sounding using a comparatively larger loop introduced by the author, known as Central Frequency Sounding abbreviated as CFS, involves measurement of the vertical component of the magnetic field induced at the centre of a circular or a square loop.

Accordingly, theoretical backgrounds for CFS and DFS were developed for a horizontally stratified multi-layer earth under various simplified assumptions. These mathematically derived expressions were shown to form the basis for computation of theoretical master curves in forms suitable for interpretation of CFS and DFS field data. The expressions were put into computable forms with reference to actual practical problems. Various modes of presentation of master curves were outlined and the difficulties for the same discussed. Some representative two- and three-layer sets of theoretical master curves for CFS and DFS are reproduced in Figs.1—4. On these curves, the amplitude of the vertical component of the magnetic field (h_{OZ}) is plotted against the conductivity parameter with usual notations, R representing dipole separation for DFS

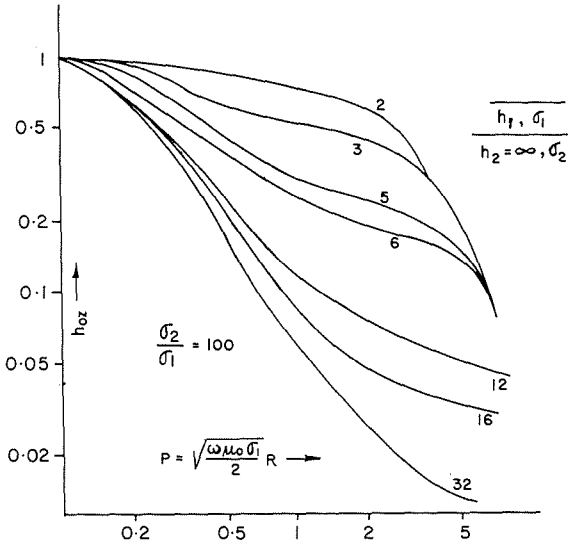

Fig.1. Theoretical two-layer curves (CFS). Curve parameter, R/h_1.

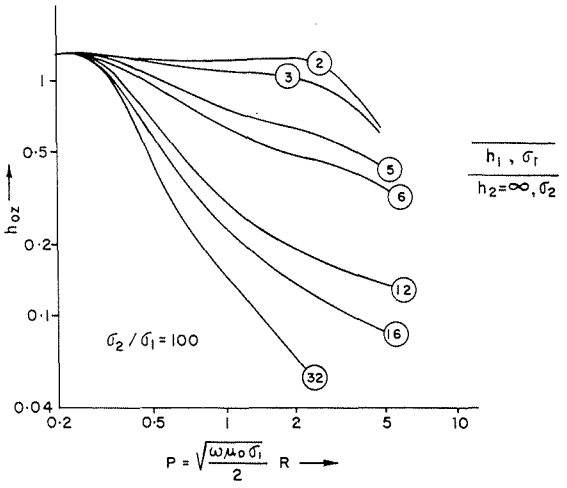

Fig. 2. Theoretical two-layer curves (DFS). Curve parameter, R/h_1 .

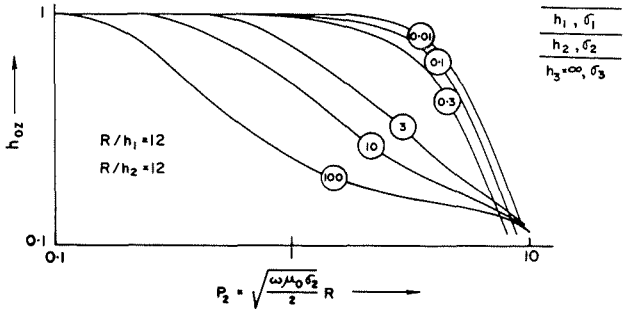

Fig. 3. Theoretical curves for three-layer earth (CFS). Top-layer highly resistive; curve parameter, σ_3/σ_2.

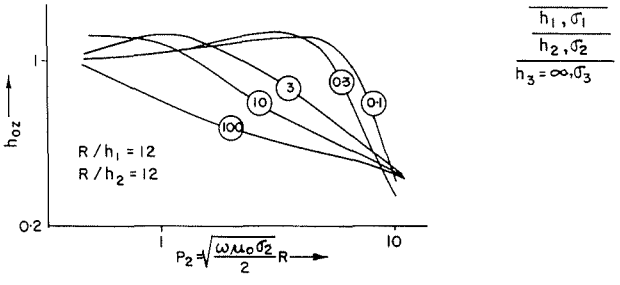

Fig. 4. Theoretical curves for three-layer earth (DFS). Top layer highly resistive; curve parameter, σ_3/σ_2.

and radius (a) of the loop for CFS. The procedure for interpretation of electromagnetic depth sounding data by way of the conventional forward approach of matching with album of curves was assessed. A simplified three-frequency method of interpretation for simpler cases was also discussed. The entire outlook was reviewed on the background of the present developments on the possibilities of direct interpretation of electromagnetic depth sounding data. Some examples on successful application of CFS system are given in Figs.5 6 where CFS is utilized to delineate water-bearing zones under a resistive surface layer.

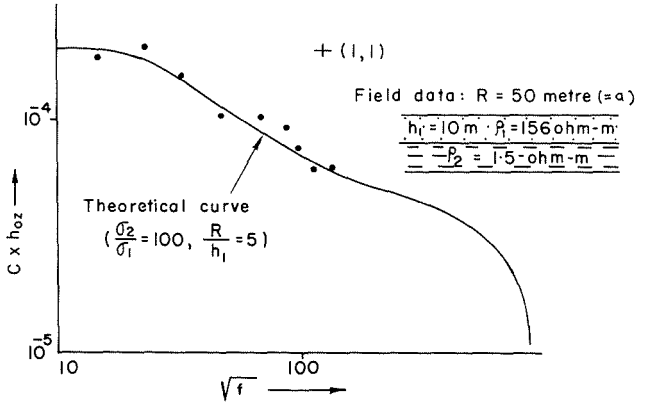

Fig.5. Field results (CFS).

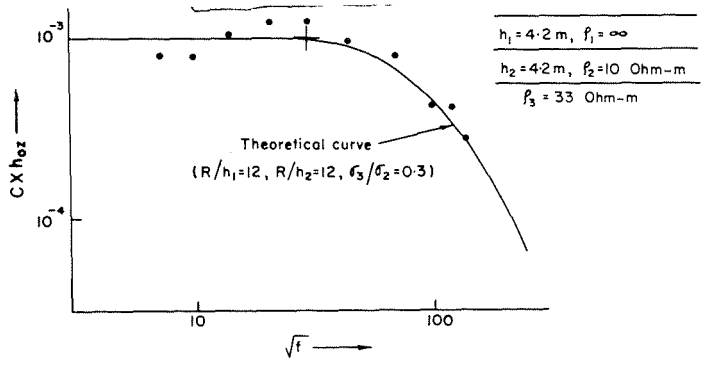

Fig.6. Field results (CFS, SA-1). $a = R = 50$ meters.

References

Patra, H.P., 1967. Some Studies on Geoelectric Sounding in Engineering and Hydrogeological Problems. Thesis, Indian Institute of Technology, Kharagpur, India (unpubl.)

Patra, H.P., 1970. Central Frequency Sounding in shallow engineering and hydrogeological problems. Geophys. Prospect., 18(2): 236—254.

Patra, H.P. and Sanyal, N., 1973. Electromagnetic depth sounding for ground water exploration in resistive formations, Proc. Int. Symp. on Development of Ground Water Resources, Madras, India, 1(Ib): 1—9.

Sanyal, N. and Patra, H.P., 1972. On the relative performances of Central Frequency Sounding (CFS) and Dipole Frequency Sounding (DFS). Pageoph, 99: 141—149.

Sanyal, N., 1975. Some Studies on Electromagnetic Depth Sounding for Shallow Ground Water Exploration Problems. Thesis, Indian Institute of Technology, Kharagpur, India. (unpubl.)

Geoexploration, 14 (1976) 259

INDUCED POLARIZATION IN THE FREQUENCY-DOMAIN: SOME CONSEQUENCES IN PARAMETRICAL INTERPRETATION

G. FINZI-CONTINI

Institute of Mineral Geophysics, Palermo (Italy)

ABSTRACT

A short review is done with the aim of recalling both the experimental and the theoretical backgrounds of the so-called membrane polarization of certain wet rocks; some features of a physical-and-mathematical model, formerly built up for the Time-Domain case, are briefly discussed for the Frequency-Domain and a simple, equivalent electrical circuit is examined for simulating conductivity and permittivity of a rock sample versus frequency.

With this basis, a more general aspect of the magnetotelluric response of the classical layered earth is considered, when frequency-dependent rock conductivities are introduced. Some foreseeable consequences connected with the prospecting of aquifers and thermalized waters are also discussed.

These results are used for illustrating some details of an interpretational procedure to be carried out by the computer. Schematized geophysical situations are proposed, which consider geological media characterized by physical quantities supposedly dependent on common parameters of interest for applied purposes: groups of results given by models are presented, these models being simultaneously studied by different methods, possibly based on independent geophysical assumptions.

Particular attention is paid to the possibility of evaluating the influence of IP-concerned quantities in the considered interpretational process, with reference to the water content.

Geoexploration, 14 (1976) 260

GEOPHYSICAL WELL LOGGING FOR HYDROGEOLOGICAL PURPOSES

P.G. VAN DONGEN

Groundwater Survey, TNO, Delft (The Netherlands)

ABSTRACT

To determine lithology, porosity and ground-water salinity of perforated strata in a rotary drilled borehole the following well logging methods have become standard procedure in The Netherlands:

(1) Electrical logging, being the recording of the spontaneous potential and "Normal" resistivity logging (at two electrode distances).

(2) Gamma-ray logging, by which the natural gamma radiation of rocks is recorded; normally combined with caliper logging.

A short description of the principles involved is given, after which an explanation is given of the interpretation procedure. A number of examples is shown.

Besides these standard logging procedures other useful logging techniques have come into use for hydrogeological investigations. Temperature, fluid conductivity and flowmeter logging are frequently applied; permanent electrode systems have been installed in many boreholes for water salinity control. Examples are shown and discussed.

Geoexploration, 14 (1976) 261

GRAVITY SURVEYS FOR UNDERGROUND WATER IN KARST AREAS: AN EXAMPLE OF APPLICATION ON THE ISLAND OF ØLAND (SWEDEN)

S. SAXOV

Laboratory of Geophysics, Aarhus University, Aarhus (Denmark)

ABSTRACT

The Swedish island of Øland is an oblong island about 135 km from north to south and only about 15 km from east to west. The island is situated east of Kalmarsund, which has a width of about 20 km.

The geology of the island is to some extent very simple, consisting of Cambrian and Ordovician rocks. It is a Karst area with a low annual precipitation. There may occur several months without precipitation at all.

In the fall of 1972 the Laboratory of Geophysics, Aarhus University, arranged a field course at Øland. However, that year rain had not fallen for about five months, and it turned out to be impossible to carry out electrical soundings. An attempt to apply hammer seismic was also without result. [In the fall of 1974 additional gravity profiles were conducted, and their results confirmed previous findings.]

The Geodetic Survey of Sweden has prior to our 1972 field course established the first gravimetric stations at Øland, and this reconnaissance survey looked so attractive that we decided to add additional gravimetric stations at the field course. As the trend of gravity deviated at the southernmost part of the island from the northernmost part, we concentrated in the first instance on the southernmost part, which accidentally was also the area where most detailed geological information was available. The gravimetric survey showed that the uniform geological structure, generally believed, does not exist in the southernmost part of the island. The gravimetric picture indicates a syncline which has been confirmed by drillings. The area is cut by fracture zones which are very often waterbearing. These zones are very clearly shown by small gravity minima.

Geoexploration, 14 (1976) 262—263

AN EXAMPLE OF THE USE OF GRAVITY IN GROUND-WATER EXPLORATION

R.G. VAN NOSTRAND

Teledyne Geotech, Alexandria Laboratories, Alexandria, Va. (U.S.A.)

ABSTRACT

A classic example of the utility of gravity exploration in the search for ground water was reported by Professor John Sumner at the 1974 Annual Meeting of the Society of Exploration Geophysicists in Dallas, Texas. The area is the Cave-Creek-Carefree area, an intermountain valley, 50 km northeast of Phoenix, Arizona, where a water supply evaluation was required. The area appeared to repose on shallow weathered granite and the potential water storage did not appear too favorable. However, shallow water well drilling encouraged a more detailed search using geophysics. Since gravity surveys have been successful in outlining sedimentary basin structures in the southwest, this technique was chosen first.

Using the regional gravity map to orient the survey a grid of stations was established with stations separated about 300 meters along both directions of the grid. Near field topographic corrections were based on station surveys and far field corrections were based on reading topographic maps. The field data were then reduced to regional and residual gravity maps using a digital computer. The residual gravity map is shown in Fig.1.

Structural interpretation was made on the basis of gravity profiles along lines shown in the Fig.1. The assumption was made that the gravity low was due to a Graben type structure filled with porous rock and that only two densities were represented, that of the underlying granite and that of the valley fill; it was further assumed that the gravity anomaly at any point on the profile was proportional to the depth to granite below datum. Starting with these assumptions, an iterative computation was performed to approximate the profile of the granite surface along the given profile. Several values of the density difference were also tried to get a most reasonable fit. The contours on the granite surface were determined from the assembled profiles (Fig.2).

As a result of the survey, there was found a lateral ridge which has dammed the filled valley forming an underground reservoir with about 40 km^2 surface and maximum depth of at least 1500 m. Water reserves can reasonably be estimated at about 10^9 tons of water.

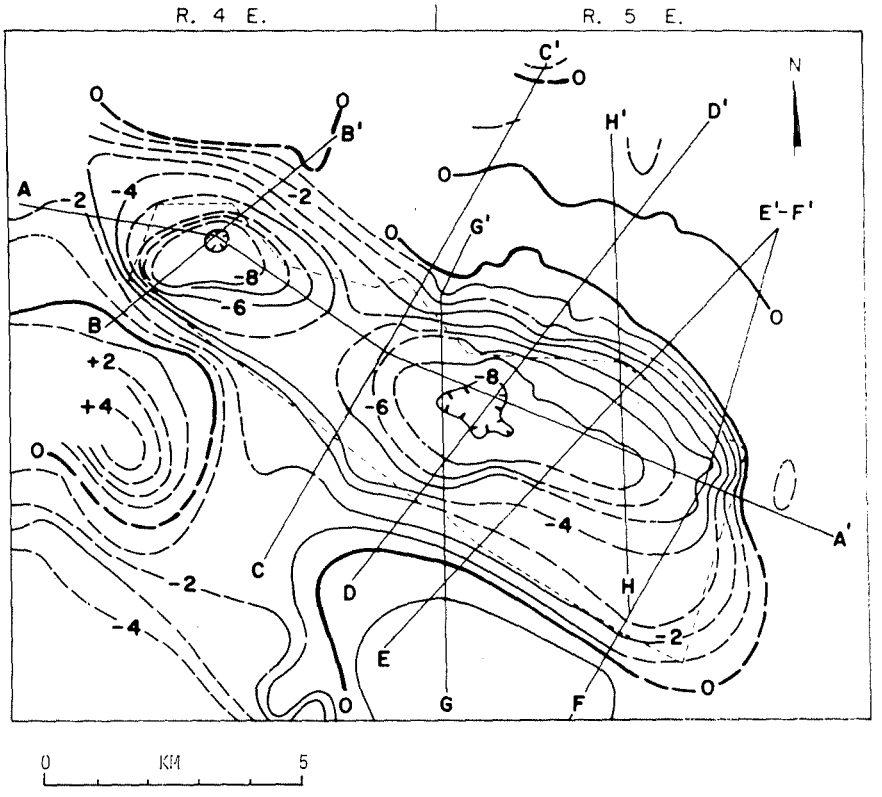

Fig.1. Residual Bouguer gravity map of the Cave Creek—Carefree Basin.

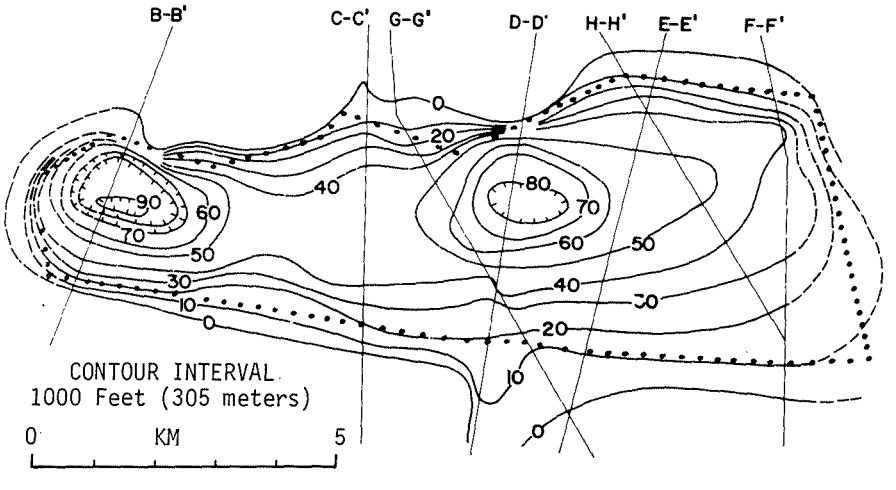

Fig. 2. Modeled basement contours, Cave Creek—Carefree Basin. $\Delta\sigma = -0.15$ g/cm^3. Basin outline.

Geoexploration, 14 (1976) 264

GEOTHERMAL MEASUREMENTS, THE SEARCH FOR HOT GROUNDWATER AND GEOTHERMAL POWER

D.S. PARASNIS

University of Luleå, Department of Applied Geophysics, Luleå (Sweden)

ABSTRACT

Geothermal measurements in drillholes can be made with a relative accuracy of 0.005°C or even better. Areas of anomalously high gradients can be delineated by direct temperature measurements but this requires access to sufficiently deep holes. Indirect methods of delineating the areas in crystalline rock areas include radioactivity assays and deep resistivity soundings. There is not much doubt about the feasibility of economic geothermal power production when gradients exceed, say, 70°C/km. However, large areas of the Earth's surface do not have gradients higher than 30—35°C/km while the Precambrian shields show gradients of only 10—20°C/km. If some reasonable assumptions are made about hole diameter, hole depth, fracturing, pumping rates, losses etc a pair of holes in a typical Precambrian area may be expected to yield a power of the order of 20 MW. However, the cost of this production must be viewed in relation to the cost of conventional energy production in which case it turns out that with present-day technology even gradients of the order of 30—35°C/km, may only be marginally interesting.

Geoexploration, 14 (1976) 265—266

CONTRIBUTION OF GEOPHYSICAL METHODS TO THE MANAGEMENT OF WATER RESOURCES

S. SCARASCIA

Institute for the Geophysics of the Lithosphere, National Research Council, Milan (Italy)

ABSTRACT

The management of underground-water resources may be faced adequately by the use of mathematical models of simulation.

The construction of a mathematical model needs the geometric description of the aquifers, their hydraulic characteristics and boundary conditions. Referring to aquifers in alluvial sediments, a proper geophysical method for such determinations is the electrical sounding, because a good electrical contrast between impervious and permeable beds can be generally expected.

The principle of an approximate method for the construction of the mathematical model, in the case of a free single-layer aquifer, is illustrated (inverse problem solution), by means of some hypothetical examples. The method may be based only on piezometric data and the exploitation conditions of the aquifer, that is only on hydrological parameters. In this case several sets of transmissivity values may be calculated, all satisfying input data, because of the indeterminateness of the problem. The method may be used as well if hydrodynamic characteristics of the aquifer in a few points are available; in this case a lower degree of indeterminateness can be reached.

In the determination of hydraulic parameters from resistivity measurements a reliable correlation between resistivity and permeability values (or between transversal resistance and transmissivity values) should be available. Toward this end Archie's formulas may be used, and also the use of tracers in the well may give some results. A more efficient way is to use pumping tests which give directly the transmissivity value of the aquifer, to be compared with transversal resistance of the electric sounding.

Some experiments carried out on aquifers in alluvial sediments, each one in a different region, show a linear correlation between electrical and hydraulic parameters, with nearly the same parametric constants; therefore it might be generalized and used at least as a first approximation in similar situations.

The probable linear correlation between resistivity and permeability values suggests another approach for the construction of a correct mathematical model. It should consist in the comparison of the maps of transversal re-

sistance with the different possible sets of transmissivity values, as calculated by the above mentioned mathematical method; among them, one will satisfy better the linearity conditions and will be a more probable model.
Some results obtained in the study of an aquifer in the Po valley are shown.

References

Beatrizzotti, G., Del Don, R. and Hansen, J., 1973. Determinazione della trasmissività nei terreni alluvionali mediante i sondaggi elettrici. Riv. Tecn., No. 794.

Cassinis, R., Giura, R., Ponzini, G.S. and Scarascia, S., 1973. Moderni metodi di indagine idrogeologica applicati all'acquifero di un territorio campione della Pianura Padana. Boll. Geofis. Teor. Appl., No. 59.

Duprat, A., Simpler, L. and Ungemach, P., 1970. Contribution de la prospection électrique a la recherche des caractéristiques hydrodynamiques d'un milieu aquifère. Terres et Eaux, No. 62.

Scarascia, S. and Ponzini, G.S., 1972. An approximate solution for the inverse problem in hydraulics. Energ. Elett., No. 8.

Geoexploration, 14 (1976) 267—268

INTRODUCTION TO THE ROUND TABLE ON REMOTE-SENSING APPLICATIONS IN WATER SURVEYS

R. CASSINIS

University of Milan (Italy)

"Remote Sensing" or better, "Remote Sensing for Earth Resources" is a new way to look at the surface of the Earth. It consists of a group of new methodologies that has enlarged, completely changing its philosophy, the field of application of aerial photography. The main factors characterizing remote sensing can be summarized as follows:

Multispectral approach: radiations emitted or reflected by the Earth's surface are gathered and analyzed in different bands, often very narrow, of the electromagnetic spectrum and combined in order to give the most valuable information. The radiations can be artificially generated by active sensors or can be natural (passive techniques).

Multiplicity of the scales: remote sensing can be carried out from platforms situated some meters above the surface, from aircrafts flying at different heights, or from artificial satellites (automated or manned). In particular, the satellites are very stable platforms, repeating many times the same orbit: these are the best conditions to observe relatively short-lived phenomena on the surface, by a synoptic view.

Multidisciplinary approach: the observation of the surface leads to applications in many fields; on the other hand, a correct evaluation of data requires the joint work of specialists in several disciplines, no matter what the objective of the investigation is. Namely, for geological applications, botanists and hydrologists must evaluate the effect of the vegetation blanket and of water content of rocks and soils before a correct interpretation of geology could be undertaken.

The main application of remote sensing in the field of geology and of exploration geophysics are:

— the *synthetic observation* of geologic features
— the analysis of *surface indicators* of deep phenomena or structures
— a better planning of geological and geophysical surveys.

In this Round Table the state of the art and the application (current and in the experimental stage) is outlined in the field of water-resources surveys, namely:

(1) Surveys on the open water bodies:
   — Inventory of water bodies
   — Study of currents

— Study of sediments pattern and deposition
— Study of the quality of water
— Flood forecasting

A particular application is described, the detection and the evaluation of submarine springs along Karst coasts.

(2) Contribution to the surveys for groundwater, through the evaluation of the following indicators:

— Soil moisture
— Vegetation
— Geologic structures
— Rock and soil type

Another application is illustrated, by detection of paleoriverbeds in alluvial plains, and its economical benefits discussed.

The requirements of data gathering and interpretation are also discussed considering the application to the water-resources surveys.

Geoexploration, 14 (1976) 269

DETECTION OF FRESH-WATER SUBMARINE SPRINGS BY MEANS OF REMOTE-SENSING TECHNIQUES: EXAMPLES OF APPLICATION IN ITALY

C.M. MARINO

Department of Geophysics, University of Milan (Italy)

Based on a wide spectrum of experiences the best way to detect such springs is to find at the sea surface the typical circular feature due to the fresh-water upwelling. The dimension of this circular feature varies and may reach tens of metres and changes its shape owing to winds and sea currents.

Fresh-water submarine springs are well known all over the world: they exist in the Persian Gulf, in U.S.A., in Bahamas, Chile and Hawaii. Along the shorelines of the Mediterranean Sea they are grouped in Lybia, Israel, Lebanon, Syria, Greece, Albania, Jugoslavia, Morocco, Italy etc.

In Italy Remote-Sensing techniques have been applied to two projects: the Cefalù area in Sicily and the shorelines of Puglia. Both these two areas are in south Italy.

The first project is a research which was conducted in July 1974 in the framework of the activity of Remote Sensing group of the National Research Council in Milano, the area surveyed with a Daedalus 1230 thermal scanner is only few square kilometres, but the results are outstanding.

Based on these experiences a team of public and private enterprises with the valuable aid of people coming from universities and research groups started one of the largest projects of Remote Sensing applied to the study of fresh water submarine springs ever done before: the Puglia Project.

The survey (more than 1000 km of flights) was performed at the end of Summer 1974 utilizing a dual channel thermal scanner and a cluster of four Hasselblad (EL/70) cameras.

The thermal contrast at the sea surface and changes in water penetration were recorded.

Normal and special play-backs were applied in order to enhance the IR thermal records.

These examples show the way of the operative application of Remote Sensing techniques to the study of fresh water submarine springs.

Geoexploration, 14 (1976) 270

METHODS AND PLATFORMS FOR INVESTIGATION ON WATER SURFACE AND HYDROGEOLOGICAL PROBLEMS

A.M. TONELLI

Laboratory for the Geophysics of the Lithosphere, National Research Council, Milan (Italy)

A short overview of the Remote Sensing techniques applied to hydrological and hydrogeological problems is presented.

Referring to the specific field of fresh-water spring detection along the shorelines the methods of multispectral photography and of thermal IR scanning are compared.

Thermal survey seems to be a very powerful system to map the distribution of fresh-water springs as well as for pollutants detection. While with thermal scanning especially using two channels, within the atmospheric windows, 3—5 and 9—11 μ, it is possible to approach the quantitative evaluation of the minimum available flow, the multispectral photography in green and blue bands seems to be an important tool to investigate the submarine behaviour of springs.

The study of sediment transport is also considered on the satellite scale: owing to the different water penetration of the four ERTS-1 bands, the Sele and Volturno plumes have been mapped for increasing depths.

Finally the problem of paleoriverbeds mapping is considered.

Two surveys were carried out in North Italy along the Adige valley in July '73 and July '74 with thermal IR to compare the thermal patterns in different soil moisture conditions. The map obtained by comparison of these thermograms shows a kind of stereogram of the paleoriverbed traces. On satellite scale, using Skylab red and orange bands, the paleoriverbeds as well as the fresh-water spring line have been successfully mapped in the Venetian Plain (North Italy), by the means of ratio performed in analog way.

Contents

Geoexploration, vol. 14, 1976